Great Britain Journals Press

Print ISSN: 2631-8490

Online ISSN: 2631-8504

DOI: 10.17406/LJRS

London Journal of Research In Science: Natural and Formal

Volume 26 | Issue 4 | Compilation 1.0

Possible Relationship between Sea Quarks...

Gravitational Waves and Black Holes: Beyond the...

Timber Management Costs in Acre, Brazilian Amazon

Chemical-Environmental Aspects of Measures to...

IN THIS ISSUE

COMPILED IN UNITED KINGDOM

MULTILINGUAL

GREAT BRITAIN JOURNALS PRESS

London Journal of Research In Science: Natural and Formal

General Catalogue

Volume 26 Issue 4 2026

EDITION

Digital Journal

Released digital issue assembled for the public journal archive.

REGISTER

LJRS / 26.4

PUBLICATION DOSSIER

LJRS - Section

Science: natural and formal register for physical, mathematical, chemical, earth, and life science scholarship.

PUBLISHER

Great Britain Journals Press
United States

ISSUE RECORD

LJRS Volume 26 Issue 4

CIRCULATION BASIS

This compiled issue file is distributed for archive, cataloguing, review, and citation continuity. Individual article records retain their own article-level rights and metadata.

Oversight and Review Route

Editorial review in LJRS prioritizes theoretical rigor, measurement traceability, symbol discipline, and the separation between result, inference, and conjecture.

PRIMARY ROUTE

Editorial Office, Great Britain Journals Press
journalspress.com

For the current handling chain, consult the issue registry and journal management records.

Issue Prospectus

This issue register in London Journal of Research In Science: Natural and Formal is assembled for theoretical, mathematical, experimental, and observational work across the natural and formal sciences.

Contributors should keep notation, derivations, measurement conditions, and model assumptions explicit enough for later verification, comparison, and reuse in the scientific record.

Issued on behalf of Great Britain Journals Press.

Issue Register

Great Britain Journals Press

RESEARCH FINGERPRINT

IDENTIFIER
LJRS-226226

PEER REVIEW
Double Blind

SIMILARITY CHECK
Perplexity AI and iThenticate

ACCESS
Open Access

LANGUAGE
English

PRINT ISSN
2631-8490

ONLINE ISSN
2631-8504

EDITION

ABBREVIATION
LJRS

VOLUME
26

ISSUE
4

YEAR
2026

KEY DATES

RECEIVED
2026-03-06

ACCEPTED
2026-03-12

ONLINE PUBLISHED
2026-05-11

PUBLISHED
2026-06-16

CATALOGING

CROSSMARK DOI
10.34257/LJRS226226UK

DDC CLASS
539.721

ACCESS ONLINE

London Journal of Research In Science: Natural and Formal
General Section

Article Record

Possible Relationship between Sea Quarks Distribution Functions and Valence Distribution Functions in Proton

CORRESPONDENCE

AUTHORS & AFFILIATIONS

Dr. Teruo Kurai ¶*

¶ Researcher, Tokyo

ABSTRACT

We attempt to show a possible relationship between sea quarks distribution functions and valence quark distribution functions in proton by considering Atlas experiment results, We obtain similar behavior of valence u quark and valence d quark distribution functions by considering that sea quarks is unbound state and by assuming that its distribution functions is described as a close state of our unbound pion distribution functions.

Index Terms: distribution amplitude • distribution functions • sea quarks • valence quark

FUNDING
No external funding was declared for this work.

CONFLICTS
The authors declare no conflict of interest.

AI USAGE
No generative AI was used for analysis or results.

HOW TO CITE
Kurai (2026). Possible Relationship between Sea Quarks Distribution Functions and Valence Distribution Functions in Proton. London Journal of Research In Science: Natural and Formal, 26(4), 1-16. DOI: 10.34257/LJRS226226UK

METADATA CONTINUATION

AUTHOR CONTACT QR LEDGER

Dr. Teruo Kurai¶*

Article ID LJRS-226226 · DOI 10.34257/LJRS226226UK

Print ISSN 2631-8490 · Online ISSN 2631-8504

RESEARCH ARTICLE

Possible Relationship between Sea Quarks Distribution Functions and Valence Distribution Functions in Proton

Dr. Teruo Kurai[¶*]

AFFILIATIONS

¶ Researcher, Tokyo

Abstract

We attempt to show a possible relationship between sea quarks distribution functions and valence quark distribution functions in proton by considering Atlas experiment results, We obtain similar behavior of valence u quark and valence d quark distribution functions by considering that sea quarks is unbound state and by assuming that its distribution functions is described as a close state of our unbound pion distribution functions.

Keywords: *distribution amplitude, distribution functions, sea quarks, valence quark*

Correspondence: Dr. Teruo Kurai

1 Introduction

After Gell-Mann succeeded to predict the existence of Ω^- by estimating its mass by his eight-fold way model [1], people had believed that baryons including nucleons are consisted by three quarks. However, New Muon Collaboration (NMC) [2], NA51 Collaboration [3] and E866 Collaboration [4] reported $\bar{d}-\bar{u}$ asymmetry in proton. These results has stimulated people's concern for the structure of proton. As results, H1 and Zeus (DESY) [5] and Atlas (CERN) [6] have reported sea quarks (quark-antiquark system) distribution functions, valence quark distribution functions and gluon distribution functions in proton. These results show that proton has more profound structure than that composed by simple three quarks. H1 and Zeus results are obtained by electron-proton collision, while Atlas results are obtained by proton-proton collision. Especially, Atlas results show the following very interesting properties. Besides they found $s\bar{s}$ sea quarks distribution functions denoted as $x\bar{s}$, $x\bar{d}$ value at $x = 1 \times 10^{-3}$ looks like equal to the peak value of $x\bar{d}$ and $x\bar{u}$ value at $x = 1 \times 10^{-3}$ looks like one half of the peak value of xu. In addition, $x\bar{d}$ value at $x = 1 \times 10^{-3}$ looks like equal to $x\bar{u}$ value at $x = 1 \times 10^{-3}$. Note that Atlas group denote each sea quarks distribution functions as xu, xd and xs, respectively, and also denote valence u quark and valence d quark distribution functions as xu and xd, respectively [6]. These properties indicate that it is possible or rather probable that there are some relationship between sea quarks distribution functions and valence quark distribution functions. In Atlas experiment, there is no valence s quark distribution functions. We try to explain the possibility of existence of sea quark distribution functions and valence u and d quark distribution functions. Pions are composed of $u\bar{d}$, $u\bar{u}$ and $d\bar{d}$ only. Thus, we use pion distribution functions as basis. In this paper, we attempt to show behavior of $\bar{u}$ and $\bar{d}$ sea quarks distribution functions and that of valence u quark and valence d quark distribution functions starting from our charged pion distribution amplitude and functions shown in ref. [7] and ref. [8], respectively. Even in Lattice QCD calculation, recently, Francis et al. shows asymptotic limit of charged pion distribution function is close to 1, ie, $(1-x)^{\beta}, \beta \approx 1$ [9]. This supports our asymptotic form of charged pion distribution functions.

2 Formulation

We proposed for description of baryons as composition of bound and unbound state of sea quarks [10]. By following those descriptions, proton is described as composition of a charged pion $\pi^+(u\bar{d})$ and a neutral pion π^0 (mix of $u\bar{u}$ and $d\bar{d}$ $((u\bar{u} - d\bar{d})/\sqrt{2})$) besides s unbound sea quarks. Important point is that π^+ and π^0 can take either bound state or unbound state repeatedly. For an example of numerical calculation, we showed proton and neutron electromagnetic form factors using pion pair consideration [11]. Note that we used π^+ wave function for π^0 wave function in proton case in that paper because we had not obtained π^0 wave function yet at that paper's publication date. In addition, we obtained a charged pion distribution amplitude [7] and its distribution function [8]. Using those arguments, we attempt to explain the behavior of Atlas experiment results [6].

Although we proposed that proton is composed as π^+ and π^0 besides $s\bar{s}$ in ref. [10], in reality, the distribution functions of $u\bar{d}$, uu and $d\bar{d}$ should be slightly different from those of π^+ and π^0 because there is no evidence that shows to exist exact π^+ and π^0 in proton. Thus, we use our distribution amplitude and functions of charged pion as basic forms but we deviate slightly to describe the distribution amplitude and functions of **u**$\bar{d}$, u$\bar{u}$ and d$\bar{d}$ in proton. Here, we use our approximate forms for distribution amplitude and functions of charged pion. Note that, as we mentioned in ref. [7], our approximate forms are sufficient to compare to other proposed distribution amplitude, thus, also to other proposed distribution functions from the definition as shown in later. Our approximate form of distribution amplitude of charged pion is described as [7]

$$F_3(x) = \frac{1-x}{x}\left(1 - e^{-\rho\frac{x}{1-x}}\left(sin\left(\rho\frac{x}{1-x}\right) + cos\left(\rho\frac{x}{1-x}\right)\right)\right) \tag{1}$$

where $\rho = \frac{u}{\sqrt{2|\alpha|}}, |\alpha| = \frac{g^2}{16}, \ x \in [0,1]$

Note that $F_3(x)$ is actually $|F_3(x)|$.

From Eq. (1), our approximate form of the charged pion distribution functions is described as [8]

$$\begin{aligned} f_3(x) &= \text{const } x|F_3(x)| \\ &= \text{const } (1-x)\left(1 - e^{-\rho\frac{x}{1-x}}\left(\sin\left(\rho\frac{x}{1-x}\right) + \cos\left(\rho\frac{x}{1-x}\right)\right)\right) \end{aligned} \tag{2}$$

We consider that sea quarks states correspond to unbound state. Here, we define unbound state as follows:

Definition:

Unbound state is a state corresponding to a distribution amplitude, that is, exponential $e^{-\rho\frac{x}{1-x}}$ becomes negligibly small because the coupling constant g^2 is sufficiently small.

Thus, Eq. (1) gives our distribution amplitude of sea quarks $\bar{d}$ that come from π^+ as

$$F_3^{sea\bar{d}}(x) = \frac{1-x}{x} \tag{3}$$

Thus, our distribution functions of $\bar{d}$ become

$$f_{\pi^+}^{sea\bar{d}}(x) = const x F_3^{sea\bar{d}}(x) = const(1-x) \tag{4}$$

Notation of $f_{\pi^+}^{sea\bar{d}}(x)$ means sea quarks $\bar{d}$ distribution functions come from π^+ .

The behavior of $f_{\pi^+}^{sea\bar{d}}(x)$ in Eq. (4) shows a little bit larger than that of sea quarks distribution functions xd shown in Atlas experiment results [6]. Therefore, we deviate distribution amplitude slightly from Eq. (1). For this point, we compare above sea quarks distribution functions to our view point of sea quarks distribution functions due to gluon splitting in Appendix A.

To achieve this purpose, we return to the exact form of our distribution amplitude shown in Eq. (40) in ref. [7] as:

$$\begin{aligned} F_3(|q|) = &\Gamma\left(1+\frac{i}{\pi}\right)e^{-i\frac{\pi}{4}}\frac{1}{\sqrt{|\alpha|}}\int_0^\infty dzexp\left(-\frac{|q|}{\sqrt{2|\alpha|}}z(1-i)\right)e^{\frac{1}{4}z^2}\left(\frac{1}{2}z\right)^{-\frac{1}{2}}W_{-\frac{1}{4}-\frac{i}{\pi},-\frac{1}{4}}\left(\frac{1}{2}z^2\right) \\ &-\Gamma\left(1-\frac{i}{\pi}\right)e^{-i\frac{\pi}{4}}\frac{1}{\sqrt{|\alpha|}}\int_0^\infty dzexp\left(-\frac{|q|}{\sqrt{2|\alpha|}}z(1+i)\right)e^{\frac{1}{4}z^2}\left(\frac{1}{2}z\right)^{\frac{1}{2}}W_{-\frac{1}{4}+\frac{i}{\pi},-\frac{1}{4}}\left(\frac{1}{2}z^2\right) \end{aligned} \tag{5}$$

To evaluate the integral in Eq. (5), we again divide the integral as $\int_0^\infty dz = \int_0^u dz + \int_u^\infty dz$ and use the argument for large |q| case shown in ref. [7]. Then, our distribution amplitude is represented by following equation.

$$\begin{aligned} F_3(|q|) = &\Gamma\left(1+\frac{i}{\pi}\right)e^{-i\frac{\pi}{4}}\frac{1}{\sqrt{|\alpha|}}\int_0^u dzexp\left(-\frac{|q|}{\sqrt{2|\alpha|}}z(1-i)\right)e^{\frac{1}{4}z^2}\left(\frac{1}{2}z\right)^{-\frac{1}{2}}W_{-\frac{1}{4}-\frac{i}{\pi},\frac{1}{4}}\left(\frac{1}{2}z^2\right) \\ &-\Gamma\left(1-\frac{i}{\pi}\right)e^{-i\frac{\pi}{4}}\frac{1}{\sqrt{|\alpha|}}\int_0^u dzexp\left(-\frac{|q|}{\sqrt{2|\alpha|}}z(1+i)\right)e^{\frac{1}{4}z^2}\left(\frac{1}{2}z\right)^{-\frac{1}{2}}W_{\frac{1}{4}+\frac{i}{\pi},-\frac{1}{4}}\left(\frac{1}{2}z^2\right) \end{aligned} \tag{6}$$

Recalling that we obtained our approximate form of pion distribution amplitude using only the first term of $M_{\kappa,\mu}(z)$ to evaluate the integral in the case of large $|q|$ and also recalling that $W_{\kappa,\mu}(z)$ is defined as $W_{\kappa,\mu}(z) = \frac{\Gamma(-2\mu)}{\Gamma\left(\frac{1}{2}-\mu-\kappa\right)}M_{\kappa,\mu}(z) + \frac{\Gamma(2\mu)}{\Gamma\left(\frac{1}{2}+\mu-\kappa\right)}M_{\kappa,-\mu}(z)$ [12], a slight deviation can be considered by adding the first term of $M_{\kappa,-\mu}(z)$ because actual form of $W_{\kappa,\mu}(z)$ in Eq. (6) is $W_{\kappa,\mu}\left(\frac{1}{2}z^2\right)$.

The definition of $M_{\kappa,\mu}(z)$ is described as [12]

$$M_{\kappa,\mu}(z) = z^{\mu+\frac{1}{2}}e^{-\frac{z}{2}}{}_1F_1\left(\mu-\kappa, 2\mu+1; z\right)$$

where ${}_1F_1$ is the confluent hypergeometric series defined as [12]

$$\begin{aligned} {}_1F_1\left(\eta,\zeta;z\right) &= \sum_{n=0}^{\infty}\frac{\eta(\eta+1)\cdots(\eta+n-1)\,z^n}{\zeta(\zeta+1)\cdots(\zeta+n-1)} \\ &= 1 + \sum_{n=1}^{\infty}\frac{\eta(\eta+1)\cdots(\eta+n-1)}{\zeta(\zeta+1)\cdots(\zeta+n-1)}\frac{z^n}{n!} \end{aligned}$$

Thus, the first term of $M_{\kappa,-\mu}\left(\frac{1}{2}z^2\right)$ in the case of $\kappa = -\frac{1}{4} \mp \frac{i}{\pi}$ and $\mu = -\frac{1}{4}$ becomes 1. Thus, Eq. (6) becomes

$$\begin{aligned} F_3(|q|) &= e^{-i\frac{\pi}{4}} 2^{\frac{1}{4}} \frac{1}{\sqrt{|\alpha|}} \int_0^u dz \exp\left(-\frac{|q|}{\sqrt{2|\alpha|}} z(1-i)\right)\left[\Gamma\left(\frac{1}{2}\right) + \frac{\Gamma\left(1+\frac{i}{\pi}\right)}{\Gamma\left(\frac{1}{2}+\frac{i}{\pi}\right)}\Gamma\left(-\frac{1}{2}\right)\left(\frac{1}{2}\right)^{\frac{3}{4}} z\right] \\ &- e^{-i\frac{\pi}{4}} 2^{\frac{1}{4}} \frac{1}{\sqrt{|\alpha|}} \int_0^u dz \exp\left(-\frac{|q|}{\sqrt{2|\alpha|}} z(1+i)\right)\left[\Gamma\left(\frac{1}{2}\right) + \frac{\Gamma\left(1-\frac{i}{\pi}\right)}{\Gamma\left(\frac{1}{2}-\frac{i}{\pi}\right)}\Gamma\left(-\frac{1}{2}\right)\left(\frac{1}{2}\right)^{\frac{3}{4}} z\right] \\ &= e^{-i\frac{\pi}{4}} 2^{\frac{1}{4}} \sqrt{\pi}\left[\frac{1}{\sqrt{|\alpha|}} \int_0^u dz \exp\left(-\frac{|q|}{\sqrt{2|\alpha|}} z(1-i)\right)\left[1 - \frac{2\cosh(1)}{\pi\sqrt{\sinh(1)}}\left(\frac{1}{2}\right)^{\frac{3}{4}} z\right]\right. \\ &\left. - \frac{1}{\sqrt{|\alpha|}} \int_0^u dz \exp\left(-\frac{|q|}{\sqrt{2|\alpha|}} z(1+i)\right)\left[1 - \frac{2\cosh(1)}{\pi\sqrt{\sinh(1)}}\left(\frac{1}{2}\right)^{\frac{3}{4}} z\right]\right] \end{aligned} \tag{7}$$

In Eq. (7), we use the facts that $\Gamma\left(1 \pm \frac{i}{\pi}\right) = \left[\pi\left(\frac{\pm 1}{\pi}\right)/\sinh\left(\pi\left(\frac{\pm 1}{\pi}\right)\right)\right]^{\frac{1}{2}} = \left(\frac{1}{\sinh(1)}\right)^{\frac{1}{2}}$ and $\Gamma\left(\frac{1}{2} \pm \frac{i}{\pi}\right) = \frac{\pi}{\cosh\left(\pi\left(\frac{\pm 1}{\pi}\right)\right)} = \frac{\pi}{\cosh(1)}, \Gamma\left(\frac{1}{2}\right) = \sqrt{\pi}, \Gamma\left(-\frac{1}{2}\right) = -2\sqrt{\pi}\left(\Gamma\left(-n+\frac{1}{2}\right) = \frac{(-1)^n 2^n}{(2n-1)!!}\sqrt{\pi}[11]\right)$ as shown in ref. [7].

Integral of $\int_0^u dz \exp(-\mu_{\mp} z) z$ becomes

$$\int_0^u dz e^{-\mu_{\mp} z} z = -\frac{e^{-\mu_{\mp} u}}{\mu_{\mp}} + \frac{1}{\mu_{\mp}^2}[1 - e^{-\mu_{\mp} u}] \tag{8}$$

where $\mu_{\mp} = \frac{|q|}{\sqrt{2|\alpha|}}(1 \mp i)$

By following our definition of unbound state, sea quarks states (unbound state), are defined as follows.

Definition: $\sqrt{|\alpha|} \propto \sqrt{g^2}$ is sufficiently small so that the exponential term becomes negligibly small in entire x domain.

Thus, this part gives $\frac{\sqrt{|\alpha|}}{|q|^2} \longrightarrow \sqrt{|\alpha|}\frac{(1-x)^2}{x^2}$ term.

Important point is that the first term of Eq. (8) is the same order of $|q|$ as the first terms of the first and the second terms of Eq. (7). However, including terms that come from this integral breaks the constraint condition of our distribution amplitude, such as $F_3(|q|) \longrightarrow x$ when $x \longrightarrow 0$ as shown in ref. [7] (We obtain this condition by using the integral representation of $W_{\kappa,\mu}(z)$) when coupling constant g^2 is not sufficiently small ($\sqrt{|\alpha|}$ is not smal) so that the exponential term remains. Breaking the constraint condition means that including only the first term of $M_{\kappa,-\mu}\left(\frac{1}{2}z^2\right)$ does not describe the exact pion state. This is plausible because there is no evidence which shows to exist the exact pion in proton.

Recalling that our pion distribution amplitude and functions correspond to the charged pion $\pi^{\pm}$, we also need those of neutral pion π^0 for further consideration. Looking at Eq. (7) and Eq. (8) in ref. [7] and recalling that we are considering the chiral limit case (massless quark case), our equation for χ_0 , which corresponds to π^0 , becomes

$$(P_0^2 - P_i^2)\chi_0 = 0 \tag{9}$$

In rest frame, that is $P_1 = 0$, P_0 becomes equal to W_0 so that Eq. (8) becomes

$$W_0^2 \chi_0 = 0 \tag{10}$$

Thus, for the pion case, that is $W_0 = 0$, χ_0 cannot be determined.

However, Dlamini et al. [13] shows, for the neutral pion π^0, that t dependence ($t = (q - q')^2$, q is virtual photon momenta and q' is π^0 momenta) usually parametrized by Regge-like functions is no longer valid when $(-t)$ is larger than 1 GeV^2 and that cross section is represented as $d\sigma = \text{const}Q^{-6}\exp(-Bt')$ ($t' = t_{min} - t$) when $Q^2 = 5.49$ and 8.31 GeV^2 shown in Fig. 3 of ref. [13].

The results of Dlamini et al. means that when Q^2 is smaller than those values and π^0 momenta is small, π^0 behaves as Regge-like function (cross section is described by omitting form of exponential term). In addition, Horn [14] shows, for the charged pion $\pi^{\pm}$, that cross section is represented as $d\sigma = \text{const}Q^{-6}$. Considering the results of Dlamini et al. together with the results of Horn leads to the fact that cross section of π^0 becomes same description of that of $\pi^{\pm}$ when Q^2 or π^0 momenta is small. Recalling that Q^2 of Atlas experiment is $Q^2 = 1.9$ GeV^2 and Q^2 of H1 and Zeus experiment is $Q^2 = 10$ GeV^2 and that main range of the distribution functions of sea quarks is less than $x = 0.4$, we can consider that π^0 (actually close state of π^0) behaves as Regge-like function in both experiment cases. Therefore, we assume that the distribution amplitude and functions of π^0 in Atlas experiment case are represented as the similar forms that described by our charged pion distribution amplitude and functions. From Eq. (7) and Eq. (8) and using our definition of sea quarks, distribution amplitude of sea quarks is described as:

$$|F_3^{sea}(x)| = const\left[\frac{1-x}{x} - \frac{2^{\frac{3}{4}}\cosh(1)}{\pi\sqrt{\sinh(1)}}\sqrt{|\alpha|}\frac{(1-x)^2}{x^2}\right] \tag{11}$$

Recalling that the distribution functions is proportional to **X** times the distribution amplitude. Thus, our sea quarks distribution functions $f^{sea}(x)$ are described as

$$f^{sea}(x) = const\left[(1-x) - \beta\sqrt{|\alpha|}\frac{(1-x)^2}{x}\right] \tag{12}$$

where $\beta = \frac{2^{\frac{3}{4}}\cosh(1)}{\pi\sqrt{\sinh(1)}}$

Recalling that our definition of sea quarks is that the coupling constant g^2 is sufficiently small so that the exponential term becomes negligibly small for entire **X** domain, $\sqrt{|\alpha|}$ is sufficiently small for entire x domain because $|\alpha|$ is proportional to g^2 as shown in Eq. (1). Here, we use the following ansatz to satisfy this condition.

Ansatz:

Coupling constant g^2 depends on momentum. The property of the coupling constant g^2 is that g^2 becomes smaller as momentum is larger and also g^2 becomes smaller when momentum is smaller.

The first part of property is not so peculiar but the second part is technical. However, the exponential term is multiplied by $(\sin\rho\frac{x}{1-x}+\cos\rho\frac{x}{1-x})$ when calculating integral in Eq. (7) (refer to ref. [7]). Thus, the second term of Eq. (8) becomes const when x goes to 0 so that, for the distribution functions, this term becomes const when x goes to 0. Therefore, in the case of using only the first part of property in the ansatz, the second term of Eq. (8) goes to 0 when x goes to 0 even though g^2 becomes constant when x goes to 0. Actually, we need only this property for the adding term (deviation term). In addition, the first term of Eq. (8) becomes constant for the distribution functions when x goes to 0 because of multiplication of x. Thus, the adding term changes only constant value when x goes to 0 because constant term in parenthesis of the integral in Eq. (7) becomes 0 when x goes to 0. In Sec. 4, we check the magnitude of the exponential in the case of using ansatz. According to the argument in Sec.4, the exponential is sufficiently small in most of all region of x except for the region that **X** is very close to 0 even though $\sqrt{|\alpha|}$ is constant. The previous paragraphs indicate that the behavior of sea quarks distribution functions would be different form, that is not uniquely decreasing, in the neighbor of x = 0 in spite of starting from constant value at · if we use only the first part of property in the ansatz. Recalling that x domain of Atlas experiment results is _ , it is possible that x domain of Atlas experiment results is outside of the region in which possible improper behavior occurs. Thus, it is meaningful to remove this possible improper behavior simply, by adding the second part of property in the ansatz. Thus, we use the ansatz here.

Using this ansatz, $\sqrt{|\alpha|}$ is represented as

$$\sqrt{|\alpha|} = \gamma x^{1+p_1}(1-x)^{p_2} \tag{13}$$

where γ , p_1 and p_2 are positive constant.

The reason we use this representation is as follows.

Exponent of exponential is, $-\frac{x}{1-x}\frac{u}{\sqrt{2|\alpha|}}$, thus, to satisfy the condition that this becomes $-\infty$ when x goes to 0, $\sqrt{|\alpha|}$ must be a function of x^{1+p_1} (p_1 is positive) and to satisfy the condition that $\sqrt{|\alpha|}$ becomes smaller when x goes to 1, $\sqrt{|\alpha|}$ must also be a function of $(1-x)^{p_2}$(p_2 is positive) and this keeps the condition that exponent becomes $-\infty$ when x goes to 1.

This representation satisfies the condition that the exponential term becomes negligibly small in the entire x domain because we later show that the value of the constant γ is less than 4 and $\bar{u}$ ($\bar{u} = \frac{u}{\sqrt{2}}$) value in ρ for π^+ case is larger than 10 because a pion (actually close state of pion) in the proton must be considered as a state after evolution. We define valence quark distribution functions of proton (valence u quark and valence d quark) as

$$f^{val}(x) = \text{upper value} - \text{our defined sea quarks}$$

where $x \in [0,1]$,

the upper value = 0.4 ($0 \le x \le x$ value of the first extrema of our sea quarks)

= our u or d quark distribution functions (one half of our pion distribution functions) of which the x value of peak is the same as the x value of the first extrema of our sea quarks (x value of the first extrema of our sea quarks $\le x \le 1$)

We consider that valence u quark distribution functions of proton are the sum of valence u quark distribution functions come from charged pion π^+ (close state of π^+)and that come from neutral pion π^0 (close state of π^0) and also consider that valence d quark distribution functions is the same as valence u quark distribution functions come from neutral pion π^0 (close state of π^0).

Following our definition and consideration, we show how to obtain valence u and d quark distribution functions denoted as $f^{valu}(x)$ and $f^{vald}(x)$, respectively, as follows.

From Eq. (11) and Eq. (12), and recalling that upper vale is 0.4 at **x**=0 , our sea quarks distribution functions is described as

$$f^{sea}(x) = 0.4\left[(1-x) - \bar{\gamma}x^{p_1}(1-x)^{2+p_2}\right] \tag{14}$$

For p_1 and p_2, we set $p_1 = 0.55, p_2 = 0.43$ for all our sea quarks distribution functions, i.e., $x\bar{d}$ come from π^+ denoted as $f^{sea\bar{d}}_{\pi^+}(x)$, $x\bar{d}$ come from π^0 denoted as $f^{sea\bar{d}}_{\pi^0}(x)$ and $x\bar{u}$ come from π^0 denoted as $f^{sea\bar{u}}_{\pi^0}(x)$. From now on, we call those as temporal sea quarks distribution functions.

First, we show the process to obtain valence u quark distribution functions come from π^+. As we recall sea quarks $f^{sea\bar{d}}_{\pi^+}(x)$ come from π^+. For this case, we set $\bar{\gamma} = 2.57$ in Eq. (14). The reason for choosing this $\bar{\gamma}$ value is as follows. We consider that temporal sea quarks distribution functions $x\bar{d}$ denoted as $f^{sea\bar{d}}(x)$ is mean value of temporal sea quarks distribution functions $f^{sea\bar{d}}_{\pi^+}(x)$ come from π^+ and neutral pion $f^{sea\bar{d}}_{\pi^0}(x)$ come from π^0 and also consider that temporal sea quarks distribution functions $f^{sea\bar{d}}_{\pi^0}(x)$ come from π^0 is same as temporal sea quarks distribution functions $f^{sea\bar{u}}_{\pi^0}(x)$ come from π^0. According to Atlas experiment results, the value of sea quarks distribution functions $x\bar{u}$ at $x = 0.1$ is a little bit larger than 0. Thus, $f^{sea\bar{u}}_{\pi^0}(x) = f^{sea\bar{d}}_{\pi^0}(x)$ at $x = 0.1$ must be around 0.1. Then, recalling that $f^{sea\bar{d}}(x)$ is the mean value of $f^{sea\bar{d}}_{\pi^+}(x)$ and $f^{sea\bar{d}}_{\pi^0}(x)$, $f^{sea\bar{d}}_{\pi^+}(x)$ at $x = 0.1$ must be around 0.13 because the value of sea quarks distribution functions $x\bar{d}$ at $x = 0.1$ of Atlas experiment results is around 0.12 and 0.13. To satisfy this condition, we choose $\bar{\gamma} = 2.57$.

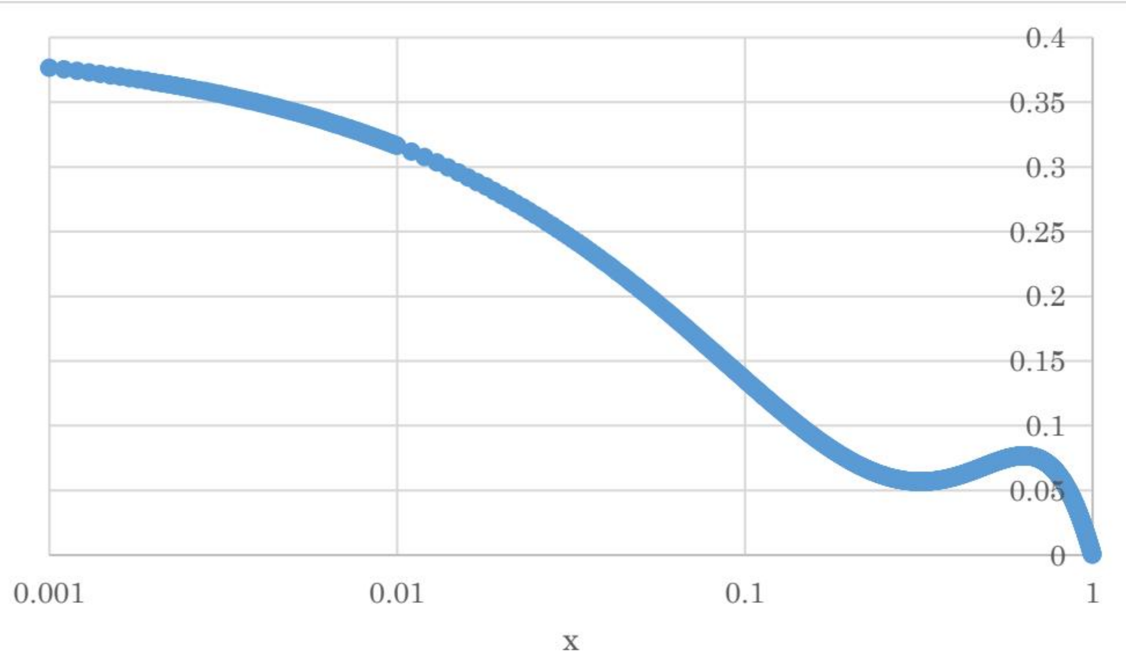

Figure 1. Temporal sea quarks distribution functions $f_{\pi^+}^{sea\bar{d}}(x)$.

Fig. 1 shows temporal sea quarks distribution functions $f_{\pi^+}^{sea\bar{d}}(x)$.

Note that $f_{\pi^+}^{sea\bar{d}}(x)$ has two extrema but that important one is extrema of which x value is smaller one. In this case, x=0.32 .

Our pion distribution functions of which the **x** value of the peak point is x=0.32 can be obtained by taking · value as $\rho = 5$ in Eq. (2). Fig. 2 shows our u quark distribution functions in the case of $\rho = 5$, that is one half of our pion distribution functions of which ρ value is $\rho = 5$.

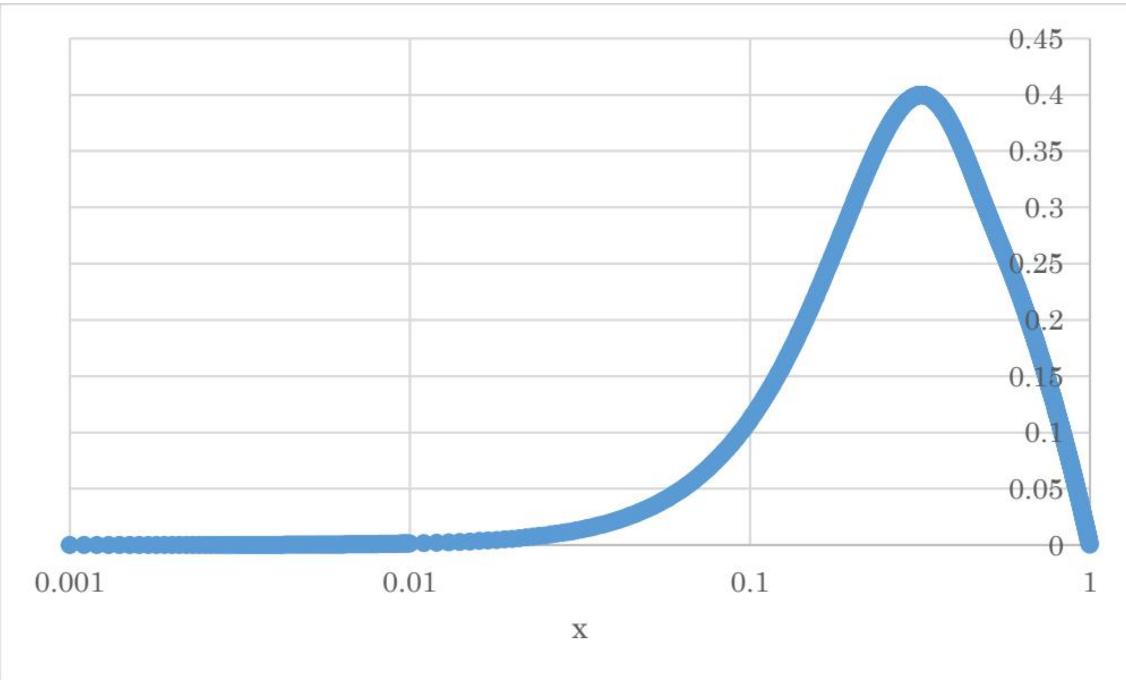

Figure 2. $u(d)$ quark distribution functions in the case of $\rho = 5$.

Note that we adjust the constant of Eq. (2) so that peak value becomes 0.4. Using the adjustment of the constant means removing the requirement of normalization condition that is necessary to obtain the distribution functions of pion as shown in ref. [8]. The fact that we need to remove the requirement of normalization condition may also reflect the situation that $u\bar{d}$ system in proton is not exact pion but only close state. However, this adjustment is not so large as shown in the following paragraph.

Actual peak value of pion distribution functions in the case of $\rho = 5$ is 0.6217 and peak value of pion distribution functions in the case of $\rho = 3$ is 0.7359 as shown in Fig. 1 of ref. [8]. Recalling that u quark distribution functions is obtained by multiplying $\frac{1}{2}$ to pion distribution functions as shown in ref. [8], actual peak value of u quark distribution functions in the case of $\rho = 5$ is 0.31085.

Recalling that our definition of valence quark distribution functions, for this case, upper value is 0.4 when range of **X** is $\mathbf{x} \in [0, 0.32]$, and upper value corresponds to down slope of u quark distribution functions in the case of $\rho = 5$ when range of x is · . Then, we obtain the following figure for valence u quark distribution functions fvl(come from π^+ .

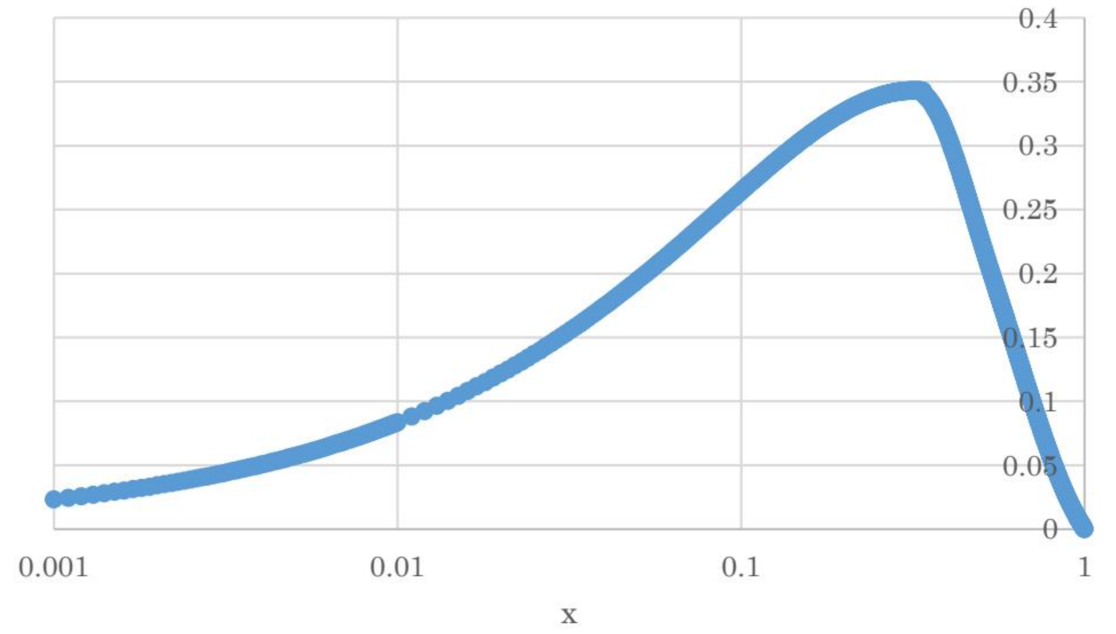

Figure 3. Valence quark distribution functions $f_{\pi^+}^{valu}(x)$ come from π^+.

Fig. 3 shows valence u quark distribution functions $f_{\pi^+}^{valu}(x)$ come from π^+. Note that the shape of down slope becomes similar to that of valence u quark distribution functions of Atlas experiment results. Comparing the shape of down slope of $f_{\pi^+}^{valu}(x)$ in Fig. 3 to that of u quark distribution functions in the case of $\rho = 5$ in Fig. 2, this point is very clear. Although we need to add up valence u quark distribution functions $f_{\pi^0}^{valu}(x)$ come from π^0 to obtain our final valence u quark distribution functions $f^{valu}(x)$, the shape of down slope changes only slightly. Thus, over all shape of $f^{valu}(x)$ becomes similar to that of Atlas experiment results using subtraction of the temporal sea quarks distribution functions in entire x domain. Therefore, the temporal sea quarks distribution functions must have some meaning which we have not figured out yet. Using the same procedure, we show valence quark distribution functions $f_{\pi^0}^{valu}(x)$ come from π^0 in Fig. 4. $f_{\pi^0}^{valu}(x)$ has peak at $x = 0.243$.

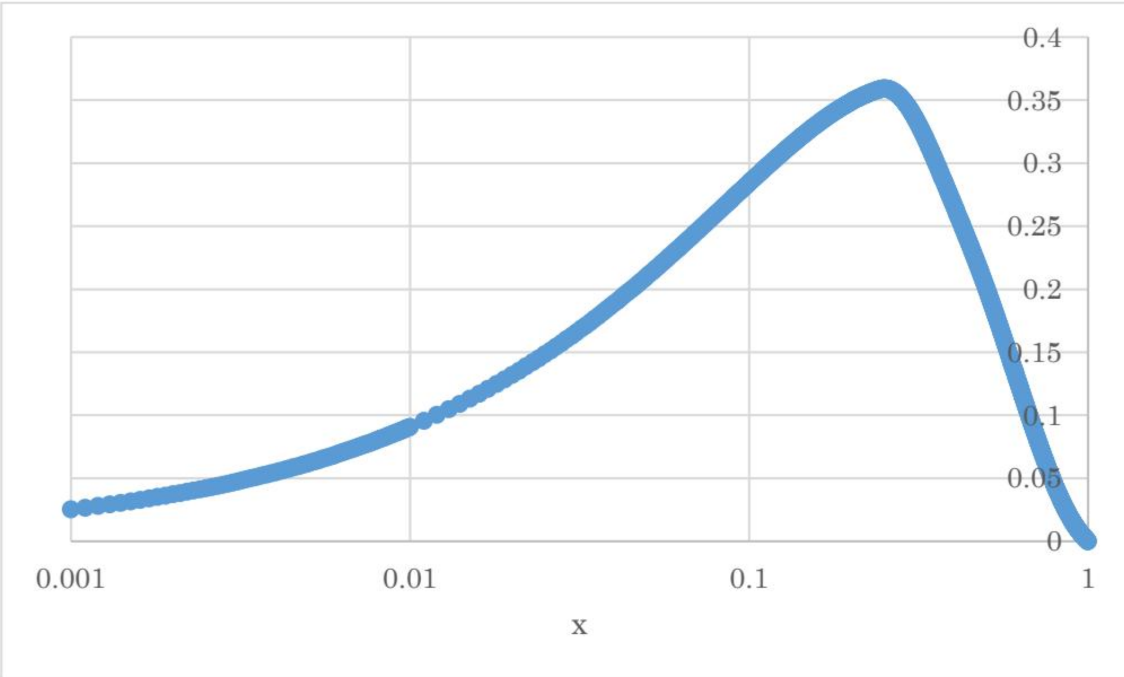

Figure 4. Valence quark distribution functions $f_{\pi^0}^{valu}(x)$ come from π^0.

Note that, in our consideration, valence d quark distribution functions $f^{vald}(x)$ is same as $f_{\pi^0}^{valu}(x)$ as mentioned before. Thus, Fig. 4 shows valence d quark distribution functions $f_{\pi^0}^{vald}(x)$.

To obtain $f_{\pi^0}^{valu}(x)$, we use temporal sea quarks distribution functions $f_{\pi^0}^{sea\bar{u}}(x)$ as shown in Fig. 5.

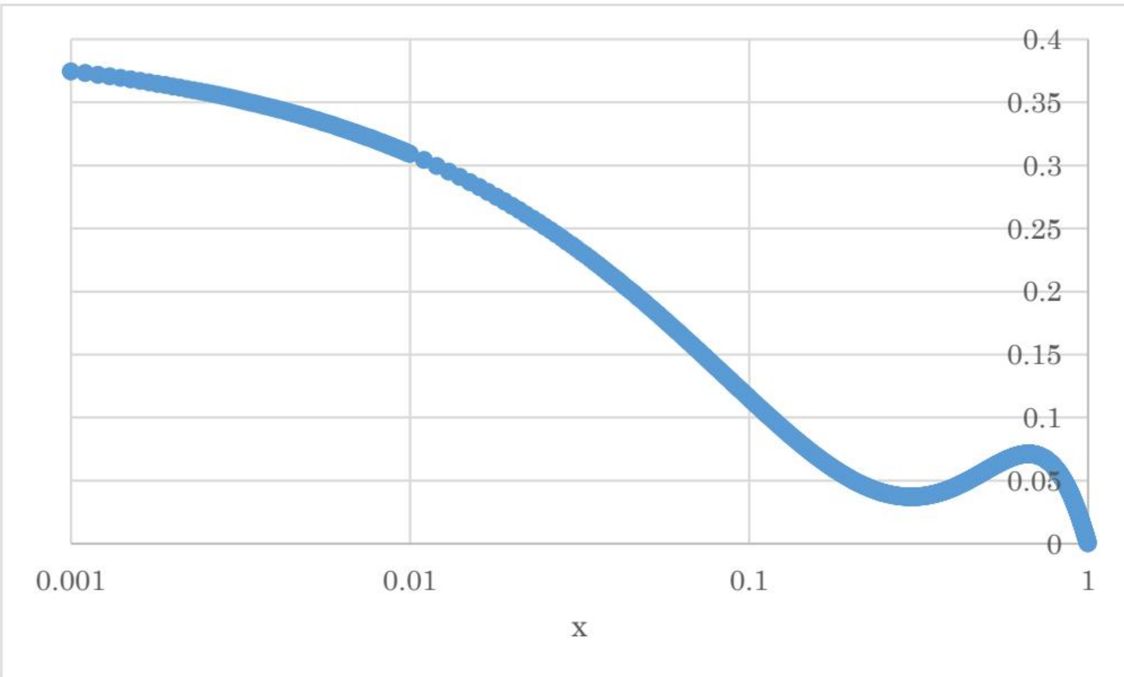

Figure 5. Temporal sea quarks distribution functions $f_{\pi^0}^{sea\bar{u}}(x)$.

Note again that, in our consideration, temporal sea quarks distribution functions $f_{\pi^0}^{sea\bar{d}}(x)$ is same as that of $f_{\pi^0}^{sea\bar{u}}(x)$.

To obtain $f_{\pi^0}^{sea\ :\overline{u}}(x)$,we take $\bar{\gamma}$ as $\bar{\gamma} = 2.8$ to satisfy the condition tht $f_{\pi^0}^{sea\ :\overline{u}}(x)$ at $\mathbf{X} = 0.1$ must be around 0.1. This $\bar{\gamma}$ value gives that $f_{\pi^0}^{sea\ :\overline{u}}(x)$ at x = 0.1 is 0.1156, actually little bit larger, and generates that the **X** value of the first extrema point is x = 0.243 . Thus, the **X** value of peak point of $f_{\pi^0}^{valu}(x)$ is x = 0.243 We do not show the figure of **u** quark distribution functions of which the **x** value of peak point is x = 0.243 here, however, corresponding u quark distribution functions is obtained by setting ρ value as $\rho = 7.8$.

Recalling that valence u quark distribution functions in proton, $f^{valu}(x)$, are the sum of $f_{\pi^+}^{valu}(x)$ and $f_{\pi^0}^{valu}(x)$, we show $f^{valu}(x)$ in Fig. 6.

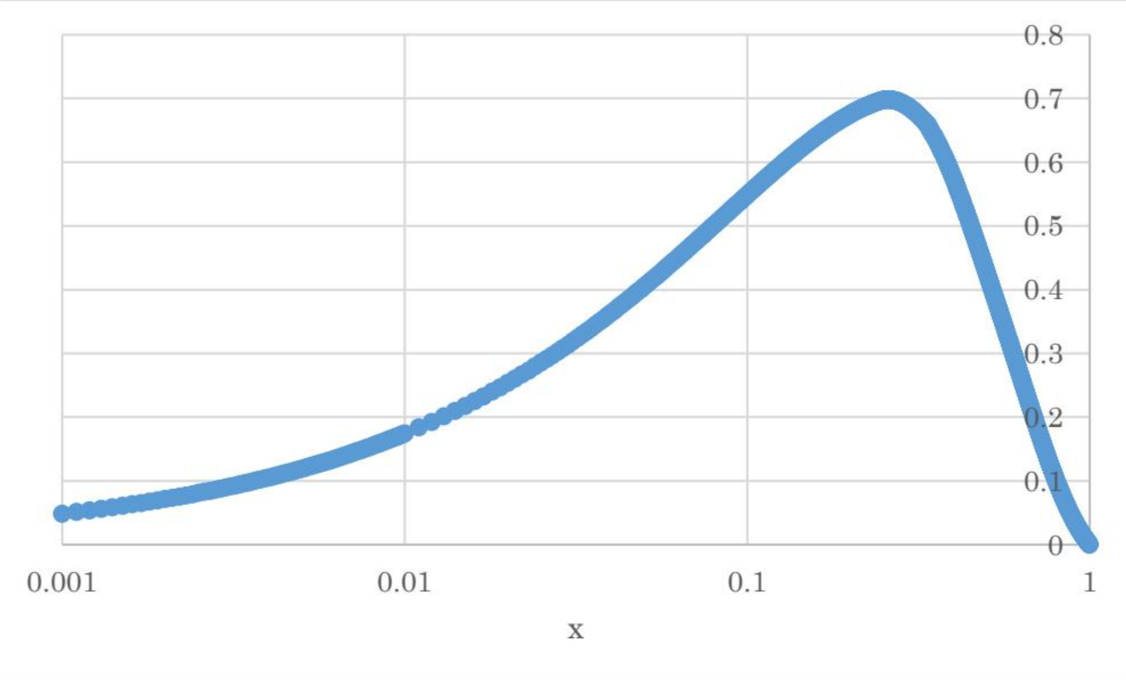

Figure 6. Valence u quark distribution functions $f^{valu}(x)$.

Note that the x value of peak point of $f^{valu}(x)$ is $x = 0.258$ This **X** value of peak point is a little bit larger than that of Atlas experiment results (x is around 0.24).

For actual sea quarks distribution functions corresponding to $x\bar{u}$ and $x\bar{d}$ denoted as $f^{sea\bar{u}}(x)$ and $f^{sea\bar{d}}(x)$, we simply use the shape of down slope of $f_{\pi^0}^{valu}(x)$ when x is larger than the x value of the first extrema of $f_{\pi^0}^{sea\bar{u}}(x)$ ($x = 0.243$) for $f^{sea\bar{u}}(x)$, and use the shape of down slope of $f_{\pi^0}^{valu}(x)$ for $f_{\pi^0}^{sea\bar{d}}(x)$ and $f_{\pi^+}^{valu}(x)$ for $f_{\pi^+}^{sea\bar{d}}(x)$ when x is larger than each x value that represents the first extrema point ($x = 0.243$ for $f_{\pi^0}^{sea\bar{d}}(x)$ and $x = 0.32$ for $f_{\pi^+}^{sea\bar{d}}(x)$), respectively. Then, Fig. 7 and Fig. 8 show our actual sea quarks distribution functions $f^{sea\bar{u}}(x)$ and $f^{sea\bar{d}}(x)$, respectively. Note that $f^{sea\bar{d}}(x)$ is the mean value of $f_{\pi^0}^{sea\bar{d}}(x)$ and $f_{\pi^+}^{sea\bar{d}}(x)$.

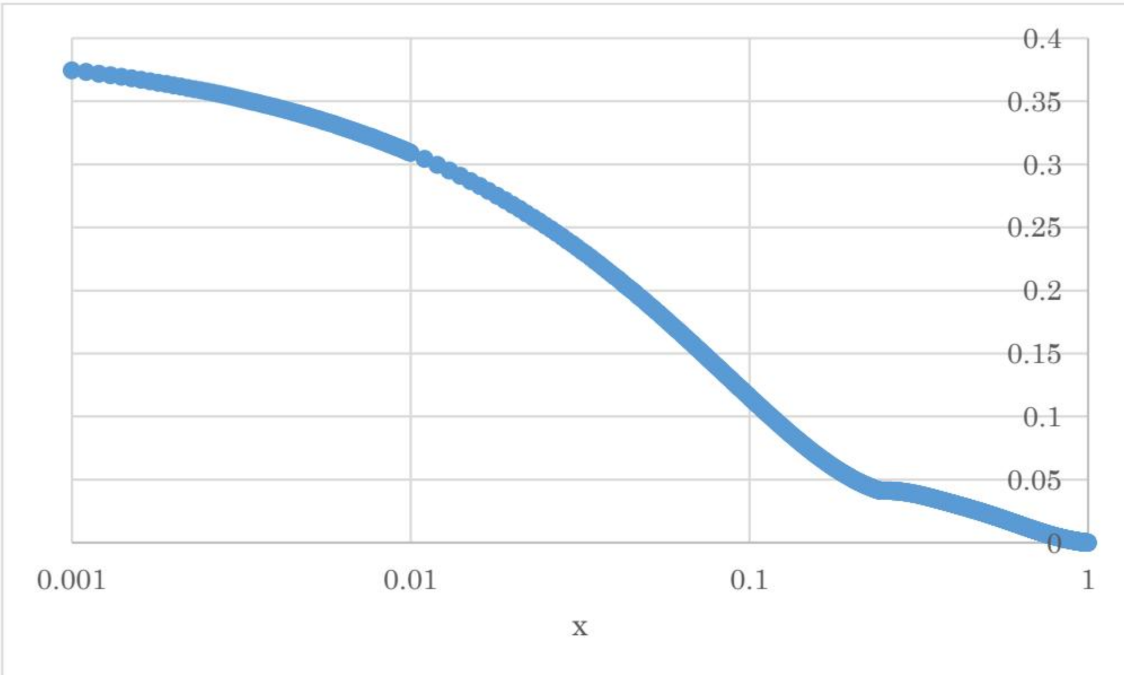

Figure 7. Sea quarks distribution functions $f^{sea\bar{u}}(x)$.

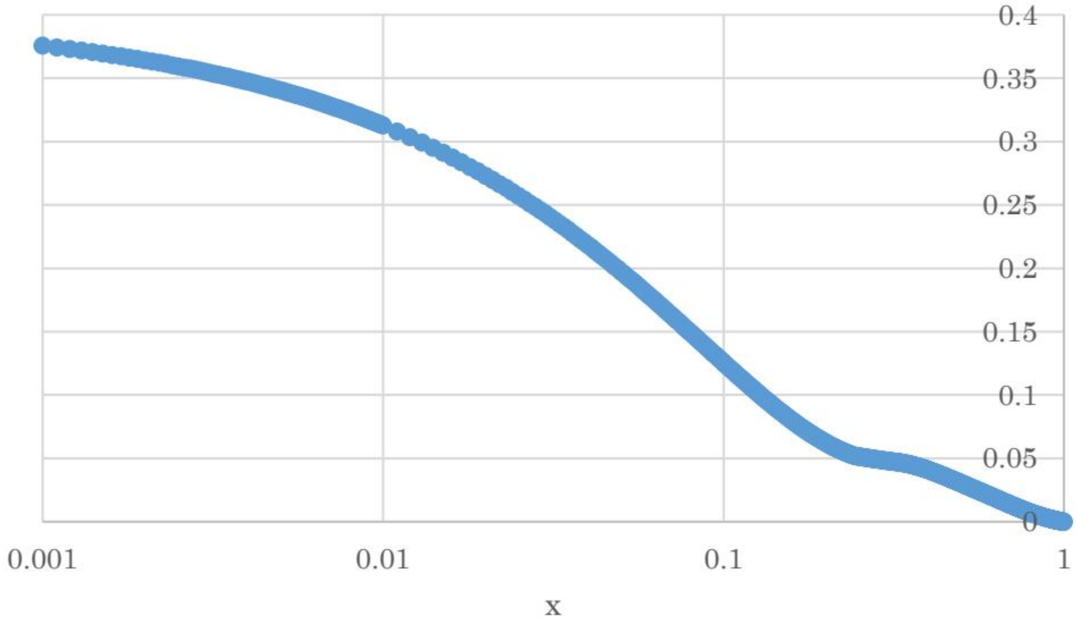

Figure 8. Sea quarks distribution functions $f^{sea\bar{d}}(x)$.

Because γ in Eq. (13) is represented as $\gamma = \hat{\gamma}/\beta$, $\gamma = 3.373$ for π^+ and $\gamma = 3.675$ for π^0 . Thus, we can use the form of $\sqrt{|\alpha|}$ as $\sqrt{|\alpha|} = 4x^{1.55}(1-x)^{0.43}$ for checking the magnitude of the exponential term. For the π^+ case, form of exponent becomes $-\frac{\bar{u}}{4x^{0.55}(1-x)^{1.43}}$ where $\bar{u} = u/\sqrt{2}$ when considering sea quark distribution functions.

Because $\rho = 5$ for π^+ distribution functions case, that is, 10 times larger than $\rho = 0.5$ corresponding to initial scale (rest frame) distribution functions as shown in ref. [8]. That the $\cdot$ value is 10 times larger means the $\bar{u}$ value in ρ is 10 times larger. Thus, for sea quarks distribution of π^+ we can take $\bar{u}$ as $\bar{u} = 10$ when we take $\bar{u} = 1$ for initial scale (rest frame) and for example $x = 1/2$. In this case, the exponential almost becomes maximum of about $\exp(-10) = 4.54 \times 10^{-5}$. Actually, even in rest frame (initial scale), proton has sea quarks state. The reason is as follows. The initial scale (rest frame) distribution functions corresponds to the distribution functions before evolution. The distribution functions before evolution must be non-zero, otherwise, sea quarks distribution functions become zero by considering evolution equation, for an example, DGLAP evolution equation [15]. Because we consider that sea quarks state is unbound state, the exponential must be sufficiently small even in rest frame because of our definition of unbound state so that the $\bar{u}$ value for initial scale (rest frame) is not 1 but much larger value. For the π^0 case, π^0 distribution functions corresponds to the distribution functions in the case of $\rho = 7.8$, that is, 15.6 times larger. Thus, we can confirm that the magnitude of exponential term, of which exponent is $-\frac{\bar{u}}{4x^{0.55}(1-x)^{1.43}}$,is negligibly small in entire x domain for both cases.

3 Results

We obtain valence u quark distribution functions and valence d quark distribution functions as follows.

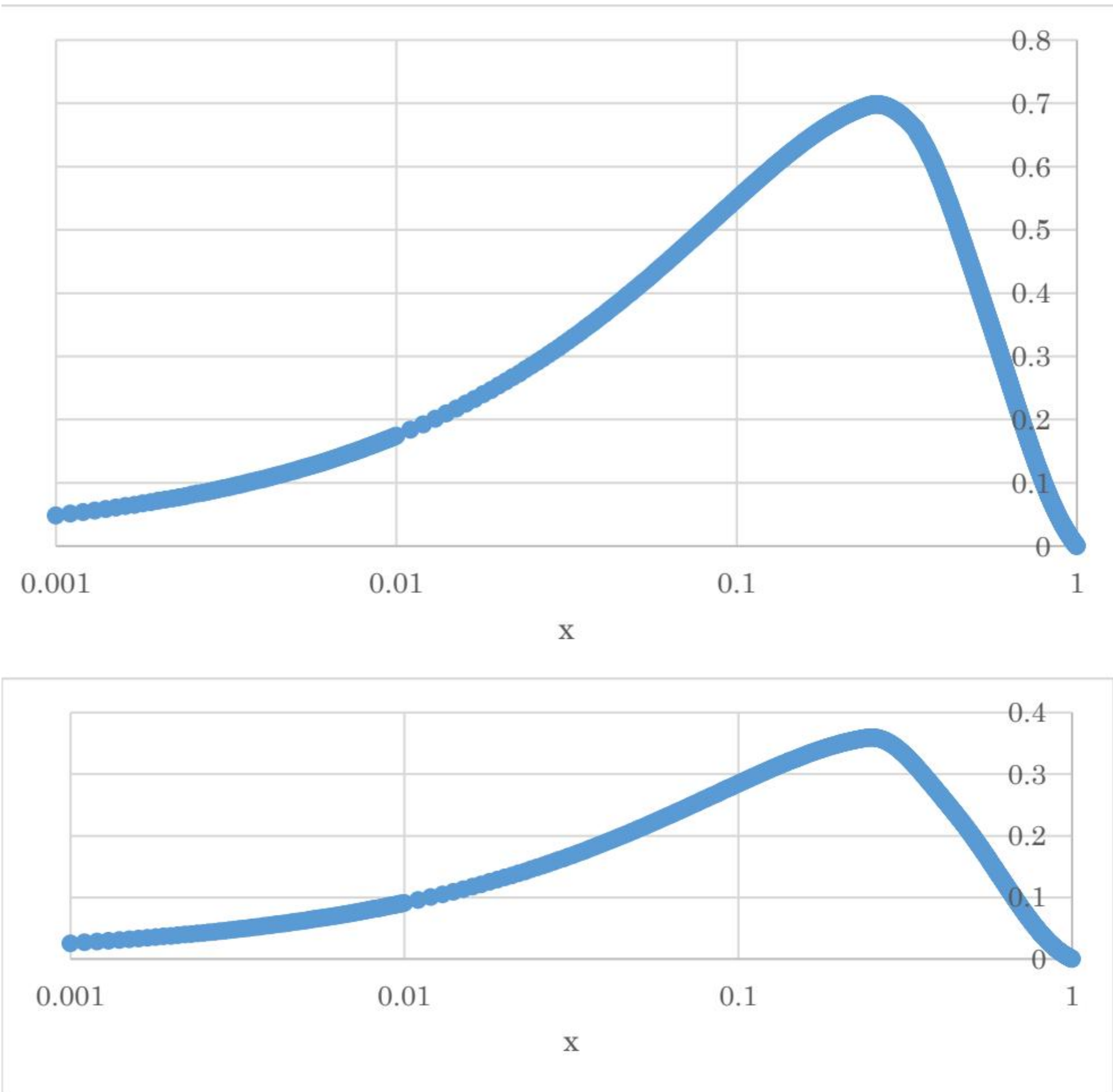

Figure 9. Comparison of valence u distribution functions $f^{valu}(x)$ and valence d distribution functions $f^{vald}(x)$; upper panel is $f^{valu}(x)$ of which the x value of the peak is $x = 0.258$ and lower panel is $f^{vald}(x)$ of which the x value of the peak is $x = 0.243$

We also obtain sea quarks distribution functions as follows.

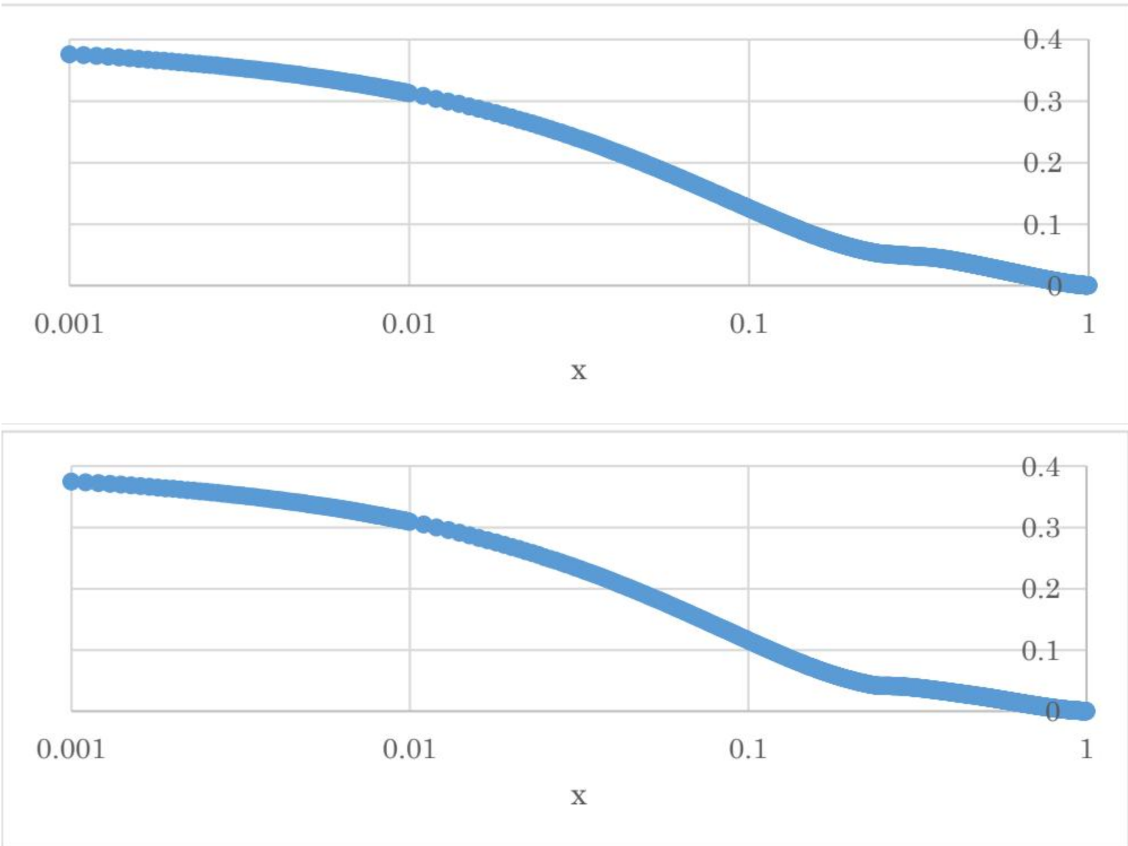

Figure 10. Comparison of sea quarks distribution functions of $f^{sea\bar{d}}(x)$ and $f^{sea\bar{u}}(x)$; upper panel is $f^{sea\bar{d}}(x)$, and lower panel is $f^{sea\bar{u}}(x)$

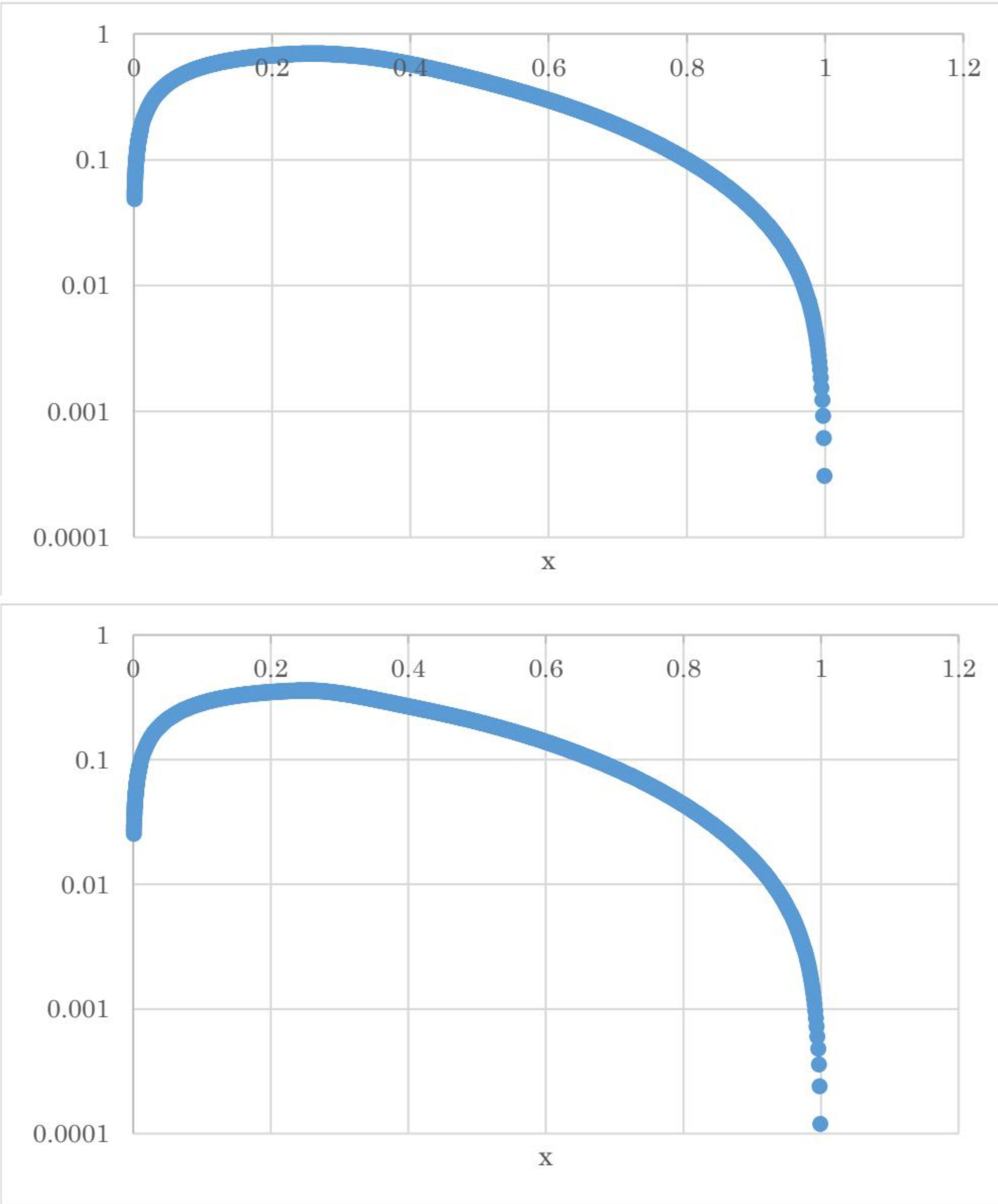

Figure 11. Comparison of valence u distribution functions $f^{valu}(x)$ and valence d distribution functions $f^{vald}(x)$ in logarithmic vertical axis (horizontal axis is linear); upper panel is $f^{valu}(x)$, lower panel is $f^{vald}(x)$

Comparing $f^{valu}(x)$ and $f^{vald}(x)$, described in Fig. 9 to Fig. 11, to those of Atlas experiment results, over all shape are similar for both cases and Fig. 11 shows that even value itself is close up to $x = 0.6$ for $f^{valu}(x)$ and up to $x = 0.7$ for $f^{vald}(x)$, respectively.

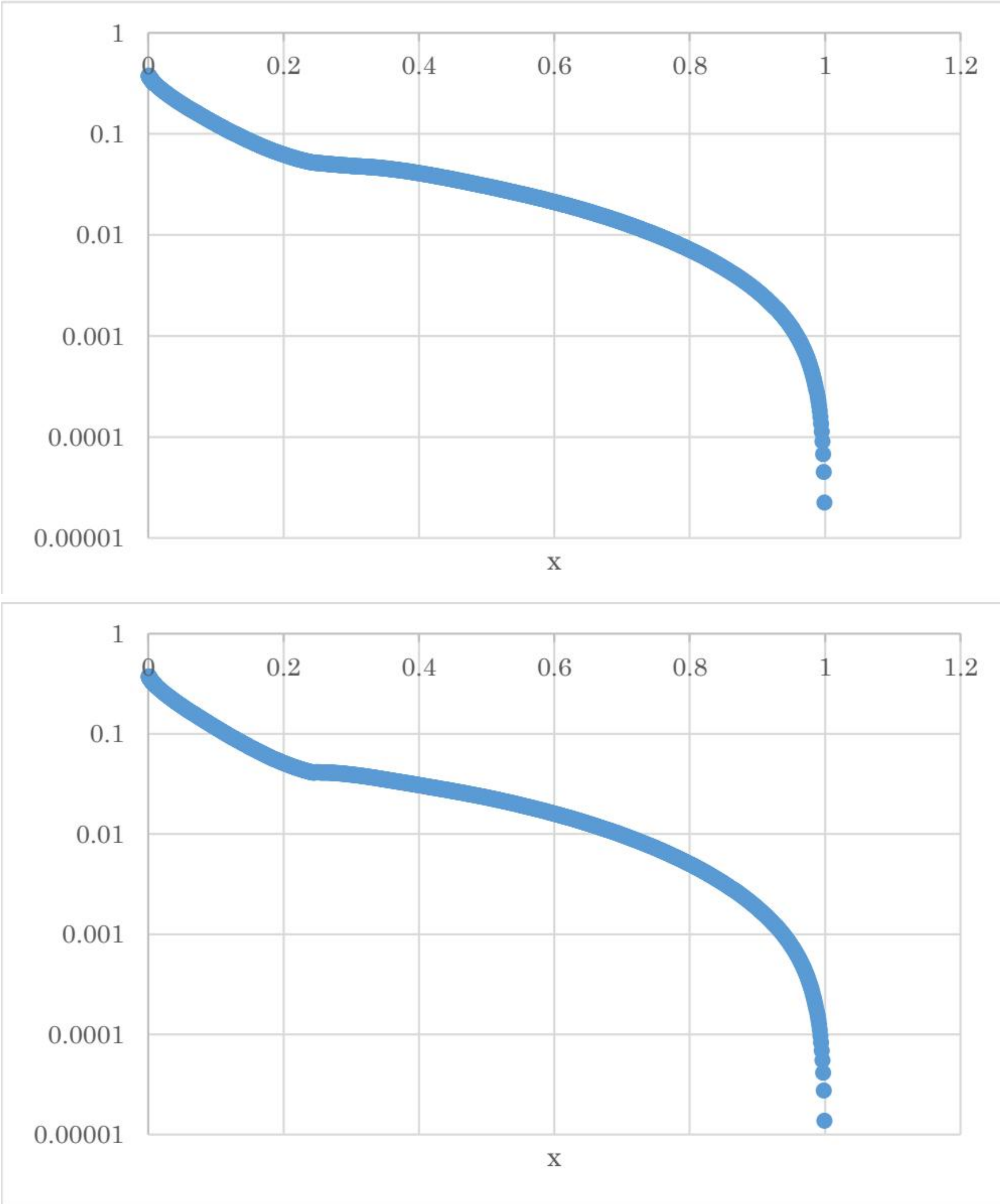

Figure 12. Comparison of sea quarks distribution functions of $f^{sea\bar{d}}(x)$ and $f^{sea\bar{u}}(x)$ in logarithmic vertical axis (horizontal axis is linear); upper panel is $f^{sea\bar{d}}(x)$, and lower panel is $f^{sea\bar{u}}(x)$

Comparing $f^{sea\bar{d}}(x)$ to that of Atlas experiment results, over all shape is similar and even value itself is close if we compare it to upper limit of that of Atlas experiment results. Comparing $f^{sea\bar{u}}(x)$ to that of Atlas experiment results, $f^{sea\bar{u}}(x)$ is similar only up to the x value of the first extrema point. In the range of larger than the x value of the first extrema point, Atlas experiment results decrease much faster than $f^{sea\bar{u}}(x)$. However, recalling that we adopt the shape of down slope of valence quark distribution functions corresponding to that in the range larger than the x value of the first extrema point, we can compare $f^{sea\bar{d}}(x)$ and $f^{sea\bar{u}}(x)$ to those of Atlas results only up to the x value of the first extrema.

4 Conclusion and Discussion

We obtain similar behaviors of valence u quark and valence d quark distribution functions to those of Atlas experiment results using the close states described by starting from our charged pion distribution functions with evolution and together with using the ansatz. Actually, this ansatz is technical, however, in reality, systems of $u\bar{u}$ and $d\bar{d}$ are not exact π^+ or π^0 but only close states of these. We think that this ansatz reflects this situation.In addition, this ansatz generates two extrema in each temporal sea quarks states. In addition, x value of the first extrema $f_{\pi^0}^{sea\bar{d}}(x)$ $(x = 0.243)$ is very close to x value of peak of valence d quark of Atlas experiment results (x is around 0.2) and for valence u quark distribution functions, x value of the first extrema of $f_{\pi^0}^{sea\bar{u}}(x)$ (same as $f_{\pi^0}^{sea\bar{d}}(x)$) $(x = 0.243)$ and x value of the first extrema of $f_{\pi^+}^{sea\bar{d}}(x)$ $(x = 0.32)$ which are same x values of peak points of $f_{\pi^0}^{valu}(x)$ and $f_{\pi^+}^{valu}(x)$, respectively, and x value of peak point of sum of these, i.e., $f^{valu}(x)$ $(x = 0.258)$ is also very close to valence u quark distribution functions of Atlas experiment results (x is around 0.24).Thus, this ansatz is meaningful. However, as mentioned in Sec. 2, we have not figured out its real meaning yet. Using the shape of down slope of valence u quark or that of d quark distribution functions to obtain sea quarks distribution functions is really technical because we do not know how to estimate this part. Except for this process, we think that our process is reasonable. As a final comment, we consider behavior of $u\bar{d}$, $u\bar{u}$ and $d\bar{d}$ inside proton as following way. Exact pions decay very quickly so that inside proton pions must be unbound state, however, when x is very small that corresponds to very surface of proton (r is large), by absorbing gluons, quark and antiquark pair becomes bound state so that confinement potential reappears. Thus, free quarks or antiquarks cannot be observed from proton.

Actually, gluon distribution functions becomes decreasing when x is smaller than 0.003. we think this behavior is reflection of above mentioned mechanism.

5 Appendix A

According to standard QCD, sea quarks appears by gluon splitting. In this case, quarks is described as $q\bar{q}$ state that corresponds to exactly coupling constant $g^2 = 0$ case of our definition of [7]. In our case, these are obtained from following two parts.

One is from our solution $\chi_3(r)$ (σ_1 component) [7] which gives to Eq. (1) and Eq. (2). The other one comes from vacuum expectation value $S(r) = \frac{1}{2\pi} Pr\frac{1}{r}(i\sigma_3$ component)[7]. To obtain wave function, we use NJR's Word Identity, especially, in our case, as shown in Appendix A in ref. [16]. This gives this part represents $\chi_0(r)$ (Unit component). For distribution amplitude, we use one dimensional Fourier transform that becomes

$$q\int_0^\infty drJ_{\frac{1}{2}}(qr) = q\left(\int_0^u drJ_{\frac{1}{2}}(qr) + \int_u^\infty drJ_{\frac{1}{2}}(qr)\right)$$

Again we consider only First term integral because of considering large q case [7]. Then the first term integral becomes [17]

$$q\int_0^u drJ_{\frac{1}{2}}(qr) = -\frac{1}{2}quJ_{\frac{1}{2}}(qu) + S_{-1,-\frac{1}{2}}(qu) - quJ_{-\frac{1}{2}}(qu)S_{0,\frac{1}{2}}(qu) + 1$$

where $S_{\mu,\nu}(z)$ denotes Lommel function defined as [18]

$$\begin{aligned} S_{\mu,\nu}(z) = & \frac{{}_1F_2\left(1; \frac{1}{2}(\mu-\nu+3), \frac{1}{2}(\mu+\nu+3); \frac{1}{4}z^2\right)}{(\mu+1)^2-\nu^2} z^{\mu+1} \\ & + \frac{2^{\mu-1}\pi^2\csc(\pi\nu)}{\Gamma\left(\frac{1}{2}(-\mu-\nu+1)\right)\Gamma\left(\frac{1}{2}(-\mu+\nu+1)\right)}\left(J_{-\nu}(z)\sec\left(\frac{1}{2}\pi(\mu+\nu)\right)\right. \\ & \left. -J_\nu(z)\sec\left(\frac{1}{2}\pi(\mu-\nu)\right)\right) \end{aligned}$$

Recalling that domain of above q is $[0, \infty]$, q becomes $\frac{x}{1-x}$, $x \in [0, 1]$. In addition, these terms are for distribution amplitude so that this part of distribution functions is obtained by multiplication of x. In our case, $\mu = 0, \nu = \frac{1}{2}$ explicit description of this term becomes for small x

$$f_{\text{gluon}}^{\text{sea2}}(x) \approx x\left(1 + a\sqrt{\frac{1-x}{x}} - b\right)$$

where $a = \frac{1}{\Gamma(\frac{5}{4})\Gamma(\frac{3}{4})}\frac{\pi^2}{2\sqrt{u}}$, $b = 4 + \frac{1}{\Gamma(\frac{1}{4})\Gamma(\frac{3}{4})}\frac{\pi^2}{\sqrt{2}}$.

Recalling that, chiral limit case, $m_\pi \to 0$ and that Renner relation such as $\frac{M}{m_\pi} \to \bar{\rho}$ constant, we can consider $\frac{\sqrt{2}}{f_\pi}\bar{\rho}$ as parameter $[C]$. Therefore, we can choose this parameter to cancel out $-x$ term of Eq. (2) obtained by considering $\chi_3(r)$. In addition, we can also use u as parameter. Thus, for small x case, sea quarks distribution functions by gluon splitting up to $x = 0.07$ is described as

$$f_{\text{gluon}}^{\text{sea}}(x) = 2\left(1 - \bar{a}\sqrt{x(1-x)} + bx\right)$$

$(0.001 \leq x \leq 0.07)$

For $0.07 \leq x \leq 1$, we use the shape of down slope of sum of valence u and valence d quark distribution functions. We choose the shape of down slope to satisfy the condition both curves are smoothly connected at $x = 0.07$.

This gives following figure for sea quarks distribution functions splitting by gluons (Fig. 1).

This is similar to gluon distribution functions of Atlas experiment except range $x = [0.001, 0.003]$. This is understood by considering that distribution functions of $q\bar{q}$ corresponds to that of gluons because we can consider that just after splitting momentum keeps that of just before splitting.

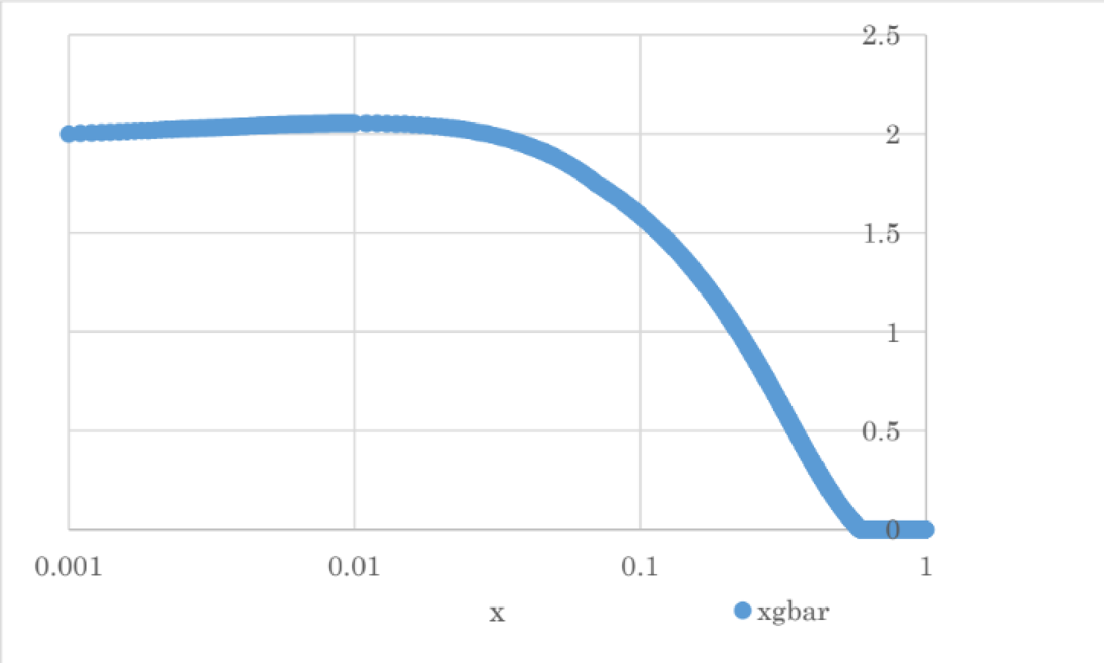

Figure 13. Gluon distribution functions of $x\bar{g}$

From this consideration, we think sea quarks described in Atlas experiment are not generated by gluon splitting. We cannot really clarify the boundary of coupling constant g^2 value, however, definitely not exactly zero. This also gives why we use our ansatz besides our argument in Sec. 2.

REFERENCES

[1] M. Gell-Mann; Eight-fold way, OSTI. Gov. Report No. TID-12608, CTSL-20 (1961)

[2] M. Areneodo et al. (NMC Collaboration); Reevaluation of the Gottfried sum, Phys. Rev. D50 R1 (1994)

[3] A. Baldit et al. (NA51 Collaboration); Study of the isospin symmetry breaking in the light quark sea of the nucleon from the Drell-Yan process, Phys. Lett. B332, 244 (1994)

[4] E.A. Hawker et al. (E866 Collaboration); Measurement of the Light Antiquark Flavor Asymmetry in the Nucleon Sea, Phys. Rev. Lett. 80, 3715 (1998)

[5] H. Abramowicz et al. (H1 and ZEUS Collaboration); Combination of Measurements ofInclusive Deep Inelastic $e^{\pm}\mathfrak{p}$ Scattering Cross Sections and QCD Analysis of HERA Data, Euro. Phys. Journal C75, 580

[6] G. Aad et al. (Atlas); Determination of the parton distribution functions of the proton using diverse ATLAS data from pp collisions at $\sqrt{s} = 7, 8$ and $13TeV$, Euro. Phys. Journal C82, 438

[7] T. Kurai; New Approach to Pion Distribution Amplitude, Journal of Modern Physics (JMP), Vol. 16, No. 6 (2025)

[8] T. Kurai; Pion Distribution Functions and Kaon Distribution Amplitude and Functions as a Bound System in $1 + 1$ Dimensional QCD, JMP, Vol. 17, No. 1 (2026)

[9] A. Francis, P. Fritzsch, R. Kaurur, J. Kim, G. Pederiva, D. A. Pefkou A. Rago, A. Shindler, A. Walker-Loud and S. Zafeiropoulos; Moment of parton distribution functions of the pion from lattice QCD using gradient flow, Phys. Rev. D113, 074520 (2026)

[10] T. Kurai; Describing a Baryon as a Composition of Bound Stated and Unbound Stated Sea-Quarks, JMP, Vol. 15, No.10 (2024)

[11] T. Kurai; Proton and Neutron Electromagnetic Form Factors Based on Bound System in $_{3+1}$ Dimensional QCD, JMP, Vol. 11, No.5 (2020)

[12] S. Moriguchi, K. Udagawa and S. HItitsumatsu; Table of Mathematica III (Special functions), Iwanami, 1975

[13] M. Dlamini et al. (Jefferson Lab Hall A Collaboration); Deep Exclusive Electroproduction of π^0 at High Q^2 in the Quark Valence Regime, Phys. Rev. Lett. 127 , 152301 (2021)

[14] T. Horn; Experimental Overview on Experiments for Pion/Kaon structure, CFNS Workshop on Elucidating the Structure of Nambu-Goldstone Bosons, New York, 24-28 June 2024 (2024)

[15] V. N. Gribov and L.N. Lipatov: Deep in elastic electron scattering in perturbation theory, Phys. Lett. B37 (1), 78, (1971)

[16] T. Kurai; Pion wave-function as a bound system in 3 + 1 dimensional QCD, Result in physics vol. 7, 2066, (2017)

[17] I. S. Gradshteyn and I. M. Ryzhic; Table of integrals, series and products (corrected and enlarged edition), Academic Press (1980)

[18] E. W. Weisstein; Lommel Function – from Wolfram MathWorld, Wolfran MathWorld (2003)

Great Britain Journals Press

RESEARCH FINGERPRINT

IDENTIFIER
LJRS-226244

PEER REVIEW
Double Blind

SIMILARITY CHECK
Perplexity AI and iThenticate

ACCESS
Open Access

LANGUAGE
English

PRINT ISSN
2631-8490

ONLINE ISSN
2631-8504

EDITION

ABBREVIATION
LJRS

VOLUME
26

ISSUE
4

YEAR
2026

KEY DATES

RECEIVED
2026-03-06

ACCEPTED
2026-03-13

ONLINE PUBLISHED
2026-05-15

PUBLISHED
2026-06-16

CATALOGING

CROSSMARK DOI
10.34257/LJRS226244UK

LCC CLASS
QC178

ACCESS ONLINE

London Journal of Research In Science: Natural and Formal

General Section

Article Record

Gravitational Waves and Black Holes: Beyond the Mirror

CORRESPONDENCE

AUTHORS & AFFILIATIONS

Dr. J.-F. Pommaret ¶*

ORCID 0000-0003-0907-2601

¶ CERMICS, Ecole des Ponts ParisTech, Paris, France (OA)

ABSTRACT

E. Beltrami introduced in 1892 the Beltrami operator acting on six stress functions in order to parametrize the Cauchy stress equations of elasticity theory in space, similarly to the single Airy stress function for plane elasticity, but this number has been then reduced to three by J.C. Maxwell and G. Morera. In 1915, A. Einstein introduced the Einstein operator for general relativity (GR) in space-time without any reference to Beltrami though the comparison needs no comment. In fact, both are using the same operator, ignoring it is self-adjoint and confusing therefore stress functions with the variation of the metric. I proved in 1995 that the Einstein equations in vacuum cannot be parametrized like the Maxwell equations. This purely mathematical result proves that the ten equations of the gravitational waves (GW) are described by the adjoint of the Ricci operator and GW cannot...

Full abstract continues on the metadata continuation sheet.

Index Terms: Differential sequence • Adjoint sequence • Spencer cohomology • Lie pseudogroups • Lie algebroids • Killing operator • Riemann operator • Bianchi identities • Minkowski metric • Schwarzschild metric

FUNDING
No external funding was declared for this work.

CONFLICTS
The authors declare no conflict of interest.

AI USAGE
No generative AI was used for analysis or results.

HOW TO CITE
Pommaret (2026). Gravitational Waves and Black Holes: Beyond the Mirror. London Journal of Research In Science: Natural and Formal, 26(4), 17-44. DOI: 10.34257/LJRS226244UK

METADATA CONTINUATION

AUTHOR CONTACT QR LEDGER

Dr. J.-F. Pommaret¶*

FULL ABSTRACT

E. Beltrami introduced in 1892 the Beltrami operator acting on six stress functions in order to parametrize the Cauchy stress equations of elasticity theory in space, similarly to the single Airy stress function for plane elasticity, but this number has been then reduced to three by J.C. Maxwell and G. Morera. In 1915, A. Einstein introduced the Einstein operator for general relativity (GR) in space-time without any reference to Beltrami though the comparison needs no comment. In fact, both are using the same operator, ignoring it is self-adjoint and confusing therefore stress functions with the variation of the metric. I proved in 1995 that the Einstein equations in vacuum cannot be parametrized like the Maxwell equations. This purely mathematical result proves that the ten equations of the gravitational waves (GW) are described by the adjoint of the Ricci operator and GW cannot thus exist, not because of a problem of detection but because of a more fundamental problem of equations that we shall point out. The second purpose of this paper is to prove also that black holes (BH) cannot exist, not for a problem of detection but because their existence should contradict the link existing between the Janet and Spencer differential sequences existing in differential geometry but never applied to GR. After recalling the way to construct these two sequences separately through explicit examples, we apply these results to Einstein equations, proving that the important object is not a metric but its group of invariance. Indeed, we shall explain why the Spencer sequence is isomorphic to the tensor product of the Poincar´e sequence for the exterior derivative by a Lie algebra of dimensions 10, 4 or 2 when dealing respectively with the Minkowski (M), the Schwarzschild (S) or the Kerr (K) metrics. Therefore, instead of shrinking down the dimension of this group, the idea is rather to enlarge the dimension of the group from 10 to 11 or 15 by using respectively the Poincar´e group of space-time, the Weyl group by adding 1 dilatation or the conformal group by adding 4 highly nonlinear elations along a way initiated by H. Weyl in 1918 for unifying electromagnetism with gravitation. Explicit motivating examples illustrate this paper at a student level, in order to introduce the new homological methods that are introduced for the first time in GR. Many among them are dealing with Lie pseudogroups that are groups of transformations solutions of systems of ordinary or partial differential equations.

ARCHIVAL RECORD

LJRS · Vol 26 · Issue 4 · 2026

Article ID LJRS-226244 · DOI 10.34257/LJRS226244UK

Print ISSN 2631-8490 · Online ISSN 2631-8504

RESEARCH ARTICLE

Gravitational Waves and Black Holes: Beyond the Mirror

Dr. J.-F. Pommaret¶* iD

AFFILIATIONS

¶ CERMICS, Ecole des Ponts ParisTech, Paris, France (**OA**)

Abstract

E. Beltrami introduced in 1892 the Beltrami operator acting on six stress functions in order to parametrize the Cauchy stress equations of elasticity theory in space, similarly to the single Airy stress function for plane elasticity, but this number has been then reduced to three by J.C. Maxwell and G. Morera. In 1915, A. Einstein introduced the Einstein operator for general relativity (GR) in space-time without any reference to Beltrami though the comparison needs no comment. In fact, both are using the same operator, ignoring it is self-adjoint and confusing therefore stress functions with the variation of the metric. I proved in 1995 that the Einstein equations in vacuum cannot be parametrized like the Maxwell equations. This purely mathematical result proves that the ten equations of the gravitational waves (GW) are described by the adjoint of the Ricci operator and GW cannot thus exist, not because of a problem of detection but because of a more fundamental problem of equations that we shall point out. The second purpose of this paper is to prove also that black holes (BH) cannot exist, not for a problem of detection but because their existence should contradict the link existing between the Janet and Spencer differential sequences existing in differential geometry but never applied to GR. After recalling the way to construct these two sequences separately through explicit examples, we apply these results to Einstein equations, proving that the important object is not a metric but its group of invariance. Indeed, we shall explain why the Spencer sequence is isomorphic to the tensor product of the Poincar´e sequence for the exterior derivative by a Lie algebra of dimensions 10, 4 or 2 when dealing respectively with the Minkowski (M), the Schwarzschild (S) or the Kerr (K) metrics. Therefore, instead of shrinking down the dimension of this group, the idea is rather to enlarge the dimension of the group from 10 to 11 or 15 by using respectively the Poincar´e group of space-time, the Weyl group by adding 1 dilatation or the conformal group by adding 4 highly nonlinear elations along a way initiated by H. Weyl in 1918 for unifying electromagnetism with gravitation. Explicit motivating examples illustrate this paper at a student level, in order to introduce the new homological methods that are introduced for the first time in GR. Many among them are dealing with Lie pseudogroups that are groups of transformations solutions of systems of ordinary or partial differential equations.

Keywords: *Differential sequence, Adjoint sequence, Spencer cohomology, Lie pseudogroups, Lie algebroids, Killing operator, Riemann operator, Bianchi identities, Minkowski metric, Schwarzschild metric, Kerr metric*

Correspondence: Dr. J.-F. Pommaret

1 INTRODUCTION

When M. Janet introduced in 1920 the first finite length differential sequence as a footnote of his paper [1], he surely did not know about the possibility to use such a sequence in elasticity theory along the way introduced by the brothers E. and F. Cosserat in 1909 [2]. Being a visiting student of D. C. Spencer (1912-2001) at Princeton University in 1970, I discovered that he was not even knowing the mathematical foundations of general relativity (GR) studied by his close friend J. A. Wheeler (1911-2008) who was offering 1000 dollars at that time to anybody finding a potential for Einstein equations in vacuum. This possibility is known to exist for Maxwell equations in electromagnetism (EM), usually defined by $dA = F$ while introducing the exterior derivative. I discovered in 1995 the negative solution of this challenge by using (formal) adjoint operators in a systematic way (See ideXlab on the net !), contrary to the general belief of the GR community. As a byproduct, such a result can only be found in books of control theory [3, 4]. In 1980, I met Janet who was still alive and he told me about the work of E. Vessiot and the resulting "affair" concerning the Differential Galois Theory [5, 6].

In 2015, a few meetings have been organized by the " Institut Henri Poincaré " (IHP) in Paris during three months about " Mathematical General relativity " . In particular, a Celebration of the 100th Anniversary was held on 16-20 November, largely dedicated to gravitational waves

(GW) and followed by two days in honor of A. Lichnerowicz on 19 + 20 December. As Lichnerowicz had been my main advisor during more than 20 years and died in 1998, I decided to participate to all these events. The atmosphere was very unpleasant because everybody knew that most sponsors should stop funding. One invited talk " Are Black Holes Real " given by S. Klainermann was so badly accepted that I could only answer to my neighbour, a young foreign student, that I was listening to it for the first time. The idea was to distinguish between three kinds of "Reality", namely "Virtual reality, Physical reality and Mathematical reality", the latter allowing to write a paper without any mathematical mistake but no comment was done on the mathematical assumptions used at the beginning [7, 8]. Less than 6 months later, LIGO announced to have detected GW produced by a couple of merging binary black holes (!) and this event, highly spread in newspapers, has been followed by the diffusion of pictures of black holes [9]. Since that time, I started to have doubts and, being specialist of control theory, I decided to use my knowledge for studying the origin of GW. In 2017, I discovered why GW cannot exist because Einstein, copying Beltrami, both ignoring that the Einstein operator, linearization of the Einstein tensor over the M metric, was surprisingly self-adjoint[10, 11]. I started to have doubts, not about the proper detection but mainly about the defining equations. Then, I started to have serious doubts when LIGO did stop for 3 years and I don't speak about the lack of any result for KAGRA after spending 250 millions of dollars. It is at this moment that I decided to care about black holes while taking into account a few recent papers I wrote about the comparison of the M,S and K metrics [12, 13] but also as a way to disagree with the approach used by L. Andersson and collaborators met while lecturing at the Albert Einstein Institute (AEI) of Potsdam (October 23-27, 2017) [14].

In the Special Relativity paper of Einstein (1905), only a footnote provides a reference to the conformal group of space-time, namely the group of transformations preserving the Minkowski metric ω up to a function factor, but there is no proof that the conformal factor should be equal to 1. Over a manifold of dimension $n \geq 3$, this group has n translations, $n(n-1)/2$ rotations, 1 dilatation and n non-linear elations introduced by E . Cartan in 1922, with a total number of $N = (n+1)(n+2)/2$ parameters that is $N = 15$ when $n = 4$ [15, 16]. However, it is also the number of the Cauchy stress equations (1823), the Cosserat couple-stress equations (1909), the only Clausius virial equation (1870), the Maxwell (1873) and Weyl (1918) equations which are among the most famous partial differential equations that can be found today in any textbook dealing with elasticity theory, continuum mechanics, thermodynamics or electromagnetism. The purpose of this paper is to prove that the form of these equations only depends on the structure of the conformal group for an arbitrary $n \geq 1$ because they are described as a whole by the (formal) adjoint of the first Spencer operator existing in the Spencer differential sequence. Such a group theoretical implication is obtained by applying totally new differential geometric methods in field theory. In particular, when $n = 4$, the main idea is to enlarge the group from 10 up to 11 or 15 parameters by using the Weyl or conformal group instead of the Poincaré group of space-time.

Contrary to the Einstein equations, these equations can be all parametrized by the adjoint of the second Spencer operator through $N = n(n-1)/2$ potentials. These results bring the need to revisit the mathematical foundations of both General Relativity (GR) and Gauge Theory (GT) according to a clever but rarely quoted paper of H. Poincaré (1901) [17]. They strengthen the comments we already made about the dual confusions made by Einstein (1915) while following Beltrami (1892), both using the same operator when $n = 3$ and $n = 4$ but ignoring it is self-adjoint in the framework of differential double duality. They also question the origin and existence of black holes.

With some more preliminary details provided in [18], we have successively:

When $n = 2$ in plane elasticity with Riemann operator $\Omega \to d_{22}\Omega_{11} + d_{11}\Omega_{22} - 2d_{12}\Omega_{12}$, G.B. Airy found in 1863 the possibility to parametrize the $Cauchy = ad(Killing)$ operator $\sigma \to$

$$\boxed{\begin{array}{lcl} d_1\sigma^{11} + d_2\sigma^{12} & = & 0 \\ d_1\sigma^{21} + d_2\sigma^{22} & = & 0 \end{array}}$$

$$\boxed{\begin{array}{ccccc} & & 1 & & \\ & \nearrow & & \searrow & \\ 2 & \xrightarrow{D} & 3 & \xrightarrow{D_1} & 1 \\ & & & & \\ 2 & \xleftarrow{ad(D)} & 3 & \xleftarrow{ad(D_1)} & 1 \end{array}}$$

with $\sigma^{12} = \sigma^{21}$ by a single stress function ϕ wearing his name through the $Airy = ad(Riemann)$ operator $\phi \to (d_{22}\phi, -d_{12}\phi, d_{11}\phi)$ as follows:

$$\boxed{\begin{array}{ccccccccc} & & 2 & \xrightarrow{D} & 3 & \xrightarrow{D_1} & 1 & \longrightarrow & 0 \\ & & & & & & & & \\ 0 & \longleftarrow & 2 & \xleftarrow{ad(D)} & 3 & \xleftarrow{ad(D_1)} & 1 & & \end{array}}$$

Multiplying the Riemann operator on the left by ϕ and "integrating by parts", we obtain:

$$\phi(d_{22}\Omega_{11}) = (d_{22}\phi)\Omega_{11} + d_2(\phi d_2\Omega_{11} - (d_2\phi)\Omega_{11})$$

As for the fact that the Cauchy operator is the adjoint of the Killing operator, this result can be found in any textbook of elasticity.

When $n = 3$ in space elasticity, E. Beltrami found in 1892 the possibility to parametrize the $Cauchy = ad(Killing)$ operator by means of six stress functions $\phi_{ij} = \phi_{ji}$ wearing his name through the self-adjoint $Beltrami = ad(Riemann)$ operator as follows:

$$\boxed{\begin{array}{ccccccccc} & & 3 & \underset{1}{\xrightarrow{Killing}} & 6 & \underset{2}{\xrightarrow{Riemann}} & 6 & \underset{1}{\xrightarrow{Bianchi}} & 3 & \rightarrow & 0 \\ 0 & \leftarrow & 3 & \underset{1}{\xleftarrow{Cauchy}} & 6 & \underset{2}{\xleftarrow{Beltrami}} & 6 & \underset{1}{\xleftarrow{Lanczos}} & 3 & & \end{array}}$$

As can be checked, the alternate sum of dimensions in each sequence, called Euler-Poincaré characteristic, does vanish indeed. More generally, studying the Lanczos problems in 2001 for a dimension $n \geq 3$, I discovered that the $Beltrami = ad(Riemann)$ operator can be parametrized by the

$Lanczos = ad(Bianchi)$ operator in the geometrical and physical adjoint sequences made by operators acting on tensors, giving order of operators and number of components as follows:

The geometrical and adjoint physical long exact differential sequences of operators acting on tensors, giving order of operators and number of components as follows:

$$\begin{array}{ccccccccccc} & n & \xrightarrow[1]{Killing} & \frac{n(n+1)}{2} & \xrightarrow[2]{Riemann} & \frac{n^2(n^2-1)}{12} & \xrightarrow[1]{Bianchi} & \frac{n^2(n^2-1)(n-2)}{24} & \rightarrow & 0 \\ 0 \leftarrow & n & \xleftarrow[1]{Cauchy} & \frac{n(n+1)}{2} & \xleftarrow[2]{Beltrami} & \frac{n^2(n^2-1)}{12} & \xleftarrow[1]{Lanczos} & \frac{n^2(n^2-1)(n-2)}{24} & & \end{array}$$

When $n = 4$ in space-time, Einstein, probably knowing the work of Beltrami because the comparison needs no comment ([18], Proposition 4.1, p 28), made a terrible confusion in 1915 between the $Cauchy = ad(Killing)$ operator and the div operator induced from the Bianchi operator because both have been using the same Einstein operator but ignoring that such an operator is self-adjoint in the framework of differential double duality when $n \geq 3$ (See [10] for more details).

Looking at [10] in order to understand the origin of GW or at section 4, the second order linearized Ricci operator $S_2T^* \rightarrow S_2T^* : (\Omega_{ij}) \rightarrow (R_{ij})$ with 4 terms is defined by the formula:

$$\boxed{2R_{ij} = \omega^{rs}(d_{rs}\Omega_{ij} + d_{ij}\Omega_{rs} - d_{ri}\Omega_{sj} - d_{sj}\Omega_{ri}) = 2R_{ji}}$$

Let us now introduce the linear map $C : S_2T^* \rightarrow S_2T^* : \Omega_{ij} \rightarrow \bar{\Omega}_{ij} = \Omega_{ij} - \frac{1}{2}\omega_{ij}\omega^{rs}\Omega_{rs}$ where Ω is a perturbation of the Minkowski metric ω , invertible if and only if $n \geq 3$. It is well known that the Einstein operator is defined by the same map $C : R_{ij} \rightarrow R_{ij} - \frac{1}{2}\omega_{ij}\omega^{rs}R_{rs} = E_{ij}$ not depending on any conformal factor. Comparing to [10] or to *any other textbook*, the GW are defined by the (strange!) composite operator $\mathcal{X} : \bar{\Omega} \xrightarrow{Einstein} E$ in such a way that $Einstein : \mathcal{X} \circ C$. Taking the respective adjoint operators, remembering that $Einstein = ad(Einstein)$ and that we have $ad(P \circ Q) = ad(Q) \circ ad(P)$ whenever P, Q are two operators, we obtain:

$$Einstein = ad(C) \circ ad(\mathcal{X}) = C \circ ad(\mathcal{X}) = C \circ Ricci$$
$$\Rightarrow ad(\mathcal{X}) = Ricci \Rightarrow \mathcal{X} = ad(Ricci)$$

Introducing the test functions $\lambda^{ij} = \lambda^{ji}$ and setting as usual $\Pi = \omega^{ij}d_{ij}$, we get:

$$\boxed{d_{ij}(\omega^{ij}\lambda^{rs} + \omega^{rs}\lambda^{ij} - \omega^{sj}\lambda^{ri} - \omega^{ri}\lambda^{sj}) = \sigma^{rs} \Rightarrow d_r(\sigma^{rs}) = 0}$$

which is exactly the generalized version of the Beltrami parametrization described in the preceding diagram with 10 instead of 20 stress functions when $n = 4$.

However, the above results are showing out the close links existing between group theory and differential sequences. For this reason, we briefly recall the historical framework leading to these new results and the reason for which we have not been able to quote many external references. This paper is also written as a smile to the famous English writer Lewis Carroll who used these words in the novel he wrote in 1871, six years after " Alice in Wonderland".

The concept of " group", introduced in mathematics for the first time by E. Galois (1830), slowly passed from algebra to geometry with the work of S. Lie on Lie groups (1880) and Lie pseudogroups (1890) of transformations. The concept of a finite length differential sequence, now called Janet sequence, has been described for the first time as a footnote by M. Janet (1920). Then, the work of D. C. Spencer (1970) has been the first attempt to use the formal theory of systems of partial differential equations in order to study the formal theory of Lie pseudogroups [20, 21].

However, the linear and nonlinear Spencer sequences for Lie pseudogroups, though never used in physics, largely supersede the " Cartan structure equations " (1905) and are quite different from the " Vessiot structure equations " (1903), introduced for the same purpose but still not known today because they have never been acknowledged by E. Cartan and successors [5, 6]. This diagram explains why it has never been possible to connect Gauge Theory (GT) using Maurer-Cartan (MC) equations with torsion $^+$ curvature with GR using (Riemann curvature alone:

$$\begin{array}{cccccc} & CARTAN & \longrightarrow & SPENCER & GT \\ \nearrow & & & & \\ LIE & \updownarrow & Cauchy, Cosserat, Maxwell & \updownarrow & \\ \searrow & & & & \\ & VESSIOT & \longrightarrow & JANET & GR \end{array}$$

Example 1.1: In order to explain the difference existing between a Lie group and a Lie pseudogroup of transformations, let us consider the Lie group of projective transformations of the real line and differentiate three times the local action law as follows with $a, b, c, d = cst$ with $d \neq 0$:

$$y = \frac{ax + b}{cx + d}$$
$$\Rightarrow \quad y_x = \frac{ad - bc}{(cx + d)^2}$$
$$\Rightarrow \quad y_{xx} = -2\frac{(ad - bc)c}{(cx + d)^3}$$
$$\Rightarrow \quad y_{xxx} = 6\frac{(ad - bc)c^2}{(cx + d)^4}$$

and get the single Schwarzian third order nonlinear OD equation $(y_{xxx}/y_x)-(3/2)(y_{xx}/y_x)^2=0$. Setting then $y=x+t\xi+...$ and linearizing at the identity $y=x$ when $t0$ we obtain the infinitesimal Lie equation $\xi_{xxx}=0 \Leftrightarrow \partial_{xxx}\xi=0$

$$\begin{array}{ccccccccccc} & & 0 & \rightarrow & \Theta & \stackrel{j_3}{\rightarrow} & 3 & \stackrel{d_1}{\rightarrow} & 3 & \rightarrow & 0 \\ & & & & & & \downarrow & & \| & & \\ & & 0 & \rightarrow & 1 & \stackrel{j_3}{\rightarrow} & 4 & \stackrel{d_1}{\rightarrow} & 3 & \rightarrow & 0 \\ & & & & \| & & \downarrow & & \downarrow & & \\ 0 & \rightarrow & \Theta & \rightarrow & 1 & \stackrel{D}{\rightarrow} & 1 & \longrightarrow & 0 & & \end{array}$$

with a basis of solutions $\{\theta_\tau\}=\{\partial_x, x\partial_x, \frac{1}{2}x^2\partial_x\}$ generating the space of solutions $\Theta\subset T$ over the constants with $[\Theta,\Theta]\subset\Theta$. We have the three abelian subgroups $y=ax, y=x+b, \frac{1}{y}=\frac{1}{x}+c$ $n=1$ with no rotation but $N=3$. However, the next examples will prove that no group theoretical technique may be applied when solutions cannot be known.

Example 1.2: With $m=n=2, q=1$ and $\omega=(\alpha\in T^*, \beta\in\wedge^2T^*,)$, let us consider the Lie operator $\mathcal{D}: T\rightarrow\Omega:\xi\rightarrow\mathcal{L}(\xi)\omega=(A=\mathcal{L}(\xi)\alpha, B=\mathcal{L}(\xi)\beta)$ and the first order involutive system:

The only Vessiot structure equation is $d\alpha=c\beta$ where now d is the exterior derivative and the only Vessiot structure constant is $c=cst$ [5]. We let the reader check that this system is formally integrable (FI), that is no new PD equation can be obtained by differentiating these three equations in any way, if and only if this condition is satisfied. We have the differential sequence:

$$0\rightarrow\Theta\rightarrow\xi\stackrel{\mathcal{D}}{\longrightarrow}\eta\stackrel{\mathcal{D}_1}{\longrightarrow}\zeta\rightarrow 0$$

with $\eta=(A_1,A_2,B)$ and $\zeta\in\wedge^2T^*$ and we may look for the adjoint differential sequence. Multiplying (A_1,A_2,B) respectively by (μ^1,μ^2,μ^3) and integrating by parts, we obtain the adjoint operator $ad(\mathcal{D})$ in the form:

$$-\alpha_1(\partial_1\mu^1+\partial_2\mu^2)-\beta(\partial_1\mu^3-c\mu^2)=\nu^1,\ -\alpha_2(\partial_1\mu^1+\partial_2\mu^2)-\beta(\partial_2\mu^3+c\mu^1)=\nu^2$$

Then, multiplying $\zeta=\dot{\partial}_1A_2-\dot{\partial}_2A_1-cB$ by λ , we obtain $ad(\mathcal{D}_1)$ as:

$$\partial_2\lambda=\mu^1,\ -\partial_1\lambda=\mu^2,\ -c\lambda=\mu^3$$

and obtain the adjoint differential sequence: $\nu\leftarrow\mu\leftarrow\lambda$.

in which $ad(\mathcal{D})$ may not generate the compatibility conditions (CC) of $ad(\mathcal{D}_1)$

We have therefore to consider the two cases [4]:

• $c=0$: With $\alpha=dx^1, \beta=dx^1\wedge dx^2$, we have $d\alpha=0$ and $ad(\mathcal{D}_1)$ is not injective with kernel $\lambda = cst$ but $ad(\mathcal{D})$ is surjective. The Lie pseudogroup Γ is made by transfomations $y^1=x^1+a, y^2=x^2+f(x^1)$ with $a=cst$ and $f(x^1)$ arbitrary.

• $c\neq 0$: Like Vessiot himself, we may choose $\alpha=x^2dx^1, \beta: dx^1\wedge dx^2$ and obtain $d\alpha+\beta=0$, that is $c=-1$. We check that $ad(\mathcal{D}_1)$ is now injective but that $ad(\mathcal{D})$ is still surjective. The Lie pseudogroup Γ is made by transformations $y^I=f(x^1), y'^2=x^2/(\partial f/\partial x^1)$ with f invertible.

We have thus discovered that the properties of the adjoint sequence largely depend on the Vessiot structure constant c . Finally, if $\alpha=x^2dx^1-x^1dx^2$, no explicit solution may be provided.

Example 1.3: (Contact transformations) With $m=n=3, q=1$ and ground differential field $K=\mathbb{Q}(x)$, we may introduce the 1-form $\alpha=dx^1-x^3dx^2\in T^*$ and consider the system of infinitesimal Lie equations defined by $\mathcal{L}(\xi)(\alpha)=\rho(x)\alpha$ after eliminating the factor ρ . However, we notice that α is not invariant by the contact Lie pseudogroup and cannot be considered as an invariant associated geometric object. In fact, it is known that the corresponding geometric object is a 1-form density ω leading to the system of infinitesimal Lie equations in Medolaghi form:

$$\boxed{\Omega_i\equiv(\mathcal{L}(\xi)\omega)_i\equiv\omega_r\partial_i\xi^r-\frac{1}{2}\omega_i\partial_r\xi^r+\xi^r\partial_r\omega_i=0}$$

and to the only Vessiot structure equation [6]:

$$\boxed{\omega_1(\partial_2\omega_3-\partial_3\omega_2)+\omega_2(\partial_3\omega_1-\partial_1\omega_3)+\omega_3(\partial_1\omega_2-\partial_2\omega_1)=c}$$

with the only structure constant c . We point out the fact that only the condition of constant Riemannian curvature is known today to be similar and we have explained why such a situation has been produced deliberately by the successors of Cartan. In the present contact situation, we may choose $\omega=(1,-x^3,0)$ and get $c=1$ but we may also choose $\omega=(1,0,0)$ and get $c=0$, these two choices both bringing an involutive system. Our problem will be now to construct the differential sequences: $\xi\stackrel{\mathcal{D}}{\longrightarrow}\Omega\stackrel{\mathcal{D}_1}{\longrightarrow}\zeta$ and its adjoint sequence: $\nu\stackrel{ad(\mathcal{D})}{\longleftarrow}\mu\stackrel{ad(\mathcal{D}_1)}{\longleftarrow}\lambda$

Linearizing the only Vessiot structure equation, we get the corresponding CC system $\mathcal{D}_1\Omega=0$

$$\begin{array}{c}\omega_1(\partial_2\Omega_3-\partial_3\Omega_2)+\omega_2(\partial_3\Omega_1-\partial_1\Omega_3)+\omega_3(\partial_1\Omega_2-\partial_2\Omega_1)\\ +(\partial_2\omega_3-\partial_3\omega_2)\Omega_1+(\partial_3\omega_1-\partial_1\omega_3)\Omega_2+(\partial_1\omega_2-\partial_2\omega_3)\Omega_3=0\end{array}$$

Multiplying on the left by a test function λ and integrating by parts, we get the operator $ad(\mathcal{D}_1)$ in the form:

$$\left\{\begin{array}{lll}\Omega_1\rightarrow & \omega_3\partial_2\lambda-\omega_2\partial_3\lambda+2(\partial_2\omega_3-\partial_3\omega_2)\lambda & =\mu^1\\ \Omega_2\rightarrow & \omega_1\partial_3\lambda-\omega_3\partial_1\lambda+2(\partial_3\omega_1-\partial_1\omega_3)\lambda & =\mu^2\\ \Omega_3\rightarrow & \omega_2\partial_1\lambda-\omega_1\partial_2\lambda+2(\partial_1\omega_2-\partial_2\omega_1)\lambda & =\mu^3\end{array}\right.$$

We obtain therefore the crucial formula $2c\lambda = \omega_i\mu^i$ showing how the previous sequences are essentially depending on the Vessiot structure constant c .

• Indeed, if $c \neq 0$, then $\mu = 0 \Rightarrow \lambda = 0$ and the operator $ad(\mathcal{D}_1)$ is injective. This is the case when $\omega = (1, -x^3, 0) \Rightarrow c = 1 \Rightarrow \lambda = 0$.

• On the contrary, if $c = 0$, then the operator $ad(\mathcal{D}_1)$ may not be injective as can be seen by choosing $\omega = (1, 0, 0)$. Indeed, in this case we get a kernel defined by $\partial_3\lambda = 0, \partial_2\lambda = 0$.

Finally, unimodular contact transformations are preserving the 1-form $\alpha = dx^1 - x^3dx^2$, thus also the 2-form $\beta = d\alpha = dx^2 \wedge dx^3$ and even the 3-form $\alpha \wedge \beta = dx^1 \wedge dx^2 \wedge dx^3$. The Vessiot structure equations for the geometric object $\omega = (\alpha, \beta)$ are now $d\alpha = c'\beta, d\beta = c''\alpha \wedge \beta$ with $0 = d^2\alpha = c'd\beta = c'c''\alpha \wedge \beta$ and the only Jacobi condition $c'c'' = 0$ because $\alpha \wedge \beta \neq 0$ [6].

Remark 1.4: When ω is a non-degenerate metric, that is $det(\omega) \neq 0$, it is well known since the work of L.P. Eisenhart on Riemannian geometry in 1926 that the first order Killing linear system defined by the $n(n+1)/2$ PD equations $\Omega_{ij} \equiv \omega_{rj}(x)\partial_i\xi^r + \omega_{ir}(x)\partial_j\xi^r + \xi^r\partial_r\omega_{ij}(x) = 0$ for a vector field $\xi = \xi^r\partial_r$, is formally integrable (FI), that is no new first order PD equation can be obtained iff the metric has a constant Riemannian curvature. We have proved in many books [20, 21] and papers that this is the only example of Vessiot equations known today and have explained in [4] that the reason for such a poor situation is related to a very unpleasant "Mathematical Affair" having to do with the differential Galois theory and involving the best french mathematicians of the beginning of the last century, namely H. Poincaré, E. Picard and G. Darboux (Original letters have been given directly to me by Janet because of the personal dedication of my first 1978 GB book and can be found in the library of ENS in Paris while a photocopy can be found in my 1988 GB book [6].

Meanwhile, mixing differential geometry with homological algebra, M. Kashiwara (1970) has created " differential homological algebra", in order to study differential modules by means of double duality and the corresponding extension modules (See [21] for references and Zbl 1079.93001). By chance, unexpected arguments have been introduced by the brothers E. and F. Cosserat (1909) in order to revisit elasticity and by H. Weyl (1918) in order to revisit electromagnetism through a unique differential sequence only depending on the structure of the conformal group. However, while the Cosserat brothers were only using (translations + rotations), Weyl has only been dealing with (dilatation $^+$ elations) as we shall explain [22, 23].

After recalling the negative answer we already provided in 1995 [19], the main purpose of this paper is to use new techniques of group theory in order to revisit the mathematical foundations of general relativity (GR) and gauge theory (GT) that are leading to gravitational waves. We point out the fact that all the diagrams presented can be obtained by means of computer algebra while using recent packages developed by my former PhD student A. Quadrat and his collaborators [24].

The solution of this striking but difficult problem has been announced, as we already said, is a series of lectures given at the Albert Einstein Institute (AEI, Potsdam, October, 23-27, 2017) "General Relativity and Gauge Theory: Beyond the Mirror" (hal-01632085, 09/11/2017). We shall prove in the next section that the study of the Killing operator done in [14] by means of purely technical relativistic tools has in fact nothing to do with GR and can be solved only counting with fingers. We also invite the reader to look at the more applied presentation (arXiv: 2302.06585) [25]. In this second approach, we advise the reader to have a special look at the photo-elastic beam experiment showing the link that may exist between high level mathematical mathematical tools and their phenomenological approach also done by J.C. Maxwell himself. We finally say that a rough sketch of the Spencer operator for systems with constant coefficients has been provided by F.S. Macaulay in 1916 through " Inverse Systems" in [26].

Before going ahead, let us prove that there may be only two types of differential sequences, the Janet sequence introduced by M. Janet in 1920 and the totally different Spencer sequence introduced by D. C. Spencer in 1970 though both only depend on the Spencer operator [27, 28]. Though the mathematical and physical communities still believe that a differential sequence must always be constructed " step by step", that is, starting with $\mathcal{D}\xi = \eta$ with generating CC $\mathcal{D}_1\eta = 0$, one may start anew with $\mathcal{D}_1\eta = \zeta$ with generating CC $\mathcal{D}_2\zeta = 0$ and so on. However, as we shall see, the Poincaré (also called de Rham out of France !) sequence for the exterior derivative may be defined "as a whole", a fact that led people to believe that the central operator for constructing differential sequences is the exterior derivative, a wrong way indeed (See [29] p 185 + 391).

For this, if E is a vector bundle over the base X , we introduce the q jet bundle $J_q(E)$ with sections $\xi_q : (x) \rightarrow (\xi^k(x), \xi^k_i(x), \xi^k_{ij}(x), ...)$ transforming like the sections $j_q(\xi) : (x) \rightarrow (\xi^k(x), \partial_i\xi^k(x), \partial_{ij}\xi^k_{ij}(x), ...)$. The Spencer operator $d : J_{q+1}(T) \rightarrow T^* \otimes J_q(T)$ allows to compare these sections by considering the differences $(\partial_i\xi^k(x) - \xi^k_i(x), \partial_i\xi^k_j(x) - \xi^k_{ij}(x), ...)$ and so on. For any system $R_q \subset J_q(E)$, differentiating once all the given OD or PD equations, we obtain the first prolongation $R_{q+1} \subset J_{q+1}(E)$ equations and the Spencer operator can be extended to an operator:

$$\boxed{d : \wedge^s T^* \otimes R_{q+1} \rightarrow \wedge^{s+1} T^* \otimes R_q : (\xi^k_{\mu,I}(x)\, dx^I) \rightarrow \left((\partial_i\xi^k_{\mu,I}(x) - \xi^k_{\mu+1_i,I}(x))\, dx^i \wedge dx^I\right)}$$

We use multi-indices $\mu = (\mu_1, ..., \mu_n)$ with $\mu + 1_i = (\mu_1, ..., \mu_i + 1, ..., \mu_n)$ and $\mid \mu \mid = \mu_1 + ... + \mu_n$ both with standard multi-index notation for exterior forms and one can check that $d \circ d = 0$. The Spencer operator and the exterior derivative are thus interlaced by the above formula. The restriction of d to the terms of upper order defining the symbols $g_{q+r} = R_{q+r} \cap S_{q+r}T^* \otimes E \subset J_{q+r}(E)$ is " minus" the Spencer map $\delta : \wedge^s T^* \otimes g_{q+1} \rightarrow \wedge^{s+1} T^* \otimes g_q$ with $\delta \circ \delta = 0$ through the formula $\xi^k_{\mu,I}dx^I \rightarrow \xi^k_{\mu+1_i,I}dx^i \wedge dx^I$ because $\xi^k_{\mu+1_i+1_j}dx^i \wedge dx^j = 0$ when $\mid \mu \mid = q, \mid \nu \mid = q+1$ The system R_q is said to be involutive if its symbol g_q is involutive, that is if all the δ sequences are exact, and the projection $\pi^{q+1}_q : R_{q+1} \rightarrow R_q$ is an epimorphism. For any system $R_q \subset J_q(E)$, we may define $R^{(s)}_{q+r} \subset R_{q+r} \subset J_{q+r}(E)$ by differentiating $r + s$ times and keeping only the equations of order $q + r$. When R_q is involutive, we may define the Janet bundles F_r, for $r = 0, 1, \dots, n$, by the short exact sequences [20, 29]:

$$\boxed{0 \rightarrow \wedge^r T^* \otimes R_q + \delta(\wedge^{r-1} T^* \otimes S_{q+1} T^* \otimes E) \rightarrow \wedge^r T^* \times J_q(E) \rightarrow F_r \rightarrow 0}$$

We may pick up a section of F_r , lift it up to a section of $\wedge^r T^* \otimes J_q(E)$ that we may lift up to a section of $\wedge^r T^* \otimes J_{q+1}(E)$ and apply d in order to get a section of $\wedge^{r+1} T^* \otimes J_q(E)$ that we may project onto a section of F_{r+1} in order to construct an operator $\mathcal{D}_{r+1} : F_r \rightarrow F_{r+1}$ generating the CC of $\mathcal{D}_r$ in the canonical linear Janet sequence:

$$0 \longrightarrow \Theta \longrightarrow E \xrightarrow{\mathcal{D}} F_0 \xrightarrow{\mathcal{D}_1} F_1 \xrightarrow{\mathcal{D}_2} \cdots \xrightarrow{\mathcal{D}_n} F_n \longrightarrow 0$$

If we have two involutive systems $R_q \subset \hat{R}_q \subset J_q(E)$, the Janet sequence for R_q projects onto the Janet sequence for $\hat{R}_q$ and we may define inductively canonical epimorphisms $F_r \to \hat{F}_r \to 0$ for $r = 0, 1, ..., n$ by comparing the previous sequences for R_q and $\hat{R}_q$.

A similar procedure can also be obtained if we define the Spencer bundles C_r for $r = 0, 1, ..., n$ by the short exact sequences [20, 29]:

$$0 \to \delta(\wedge^{r-1}T^* \otimes g_{q+1}) \to \wedge^r T^* \otimes R_q \to C_r \to 0$$

We may pick up a section of C_r , lift it to a section of $\wedge^r T^* \otimes R_q$, lift it up to a section of $\wedge^r T^* \otimes R_{q+1}$ and apply d in order to construct a section of $\wedge^{r+1} \otimes R_q$ that we may project to C_{r+1} in order to construct an operator $D_{r+1} : C_r \to C_{r+1}$ generating the CC of D_r in the canonical linear Spencer sequence which is another completely different resolution of the set Θ of (formal) solutions of R_q .

$$0 \longrightarrow \Theta \xrightarrow{j_q} C_0 \xrightarrow{D_1} C_1 \xrightarrow{D_2} C_2 \xrightarrow{D_3} \cdots \xrightarrow{D_n} C_n \longrightarrow 0$$

It can be proved that the Spencer sequence for $R_q \subset J_q(E)$ is the Janet sequence for $R_{q+1} \subset J_1(R_q)$ [22]. However, if we have two systems as above, the Spencer sequence for R_q is now contained

into the Spencer sequence for $\hat{R}_q$ and we may construct inductively canonical monomorphisms $0 \to C_r \to \hat{C}_r$ for $r = 0, 1, ..., n$ by comparing the previous sequences for R_q and $\hat{R}_q$.

Defining F_0 and $\Phi = \Phi_0$ by the short exact sequence $0 \to R_q \to J_q(E) \xrightarrow{\Phi} F_0 \longrightarrow 0$, all the previous results can be combined in the following essential commutative and exact diagram:

$$\begin{array}{ccccccc}
 & 0 & & 0 & & 0 & \\
 & \downarrow & & \downarrow & & \downarrow & \\
 & \wedge^{r-1}T^* \otimes g_{q+1} & \xrightarrow{\delta} & \wedge^r T^* \otimes R_q & \longrightarrow & C_r & \longrightarrow 0 \\
 & \downarrow & & \downarrow & & \downarrow & \\
 & \wedge^{r-1}T^* \otimes S_{q+1}T^* \otimes E & \xrightarrow{\delta} & \wedge^r T^* \otimes J_q(E) & \longrightarrow & C_r(E) & \longrightarrow 0 \\
 & \downarrow & & \downarrow \Phi_0 & & \downarrow \Phi_r & \\
 & \wedge^{r-1}T^* \otimes h_1 & \xrightarrow{\delta} & \wedge^r T^* \otimes F_0 & \longrightarrow & F_r & \longrightarrow 0 \\
 & \downarrow & & \downarrow & & \downarrow & \\
 & 0 & & 0 & & 0 &
\end{array}$$

in which $h_1 \subset T^* \otimes F_0$ is defined as the image of $\sigma_1(\Phi)$ in the exact symbol sequence:

$$0 \longrightarrow g_{q+1} \longrightarrow S_{q+1}T^* \otimes E \xrightarrow{\sigma_1(\Phi)} T^* \otimes F_0$$

It follows that the Janet bundles can be defined " as a whole" by the short exact sequences:

Considering the first order Killing system $\mathcal{L}(\xi)\omega = 0$, adding its first prolongation $\mathcal{L}(\xi)\gamma = 0$ while using ξ_2 instead of $j_2(\xi)$, we obtain a second order system $R_2 \subset J_2(T)$. When $n = 2$ and ω is the Euclidean or Minkowskian metric, we have a Lie group of isometries with the 3 infinitesimal generators $\{\partial_1, \partial_2, x^1\partial_2 - x^2\partial_1\}$. If we now consider the Weyl group defined by $\mathcal{L}(\xi)\omega = 2A\omega$ and $\mathcal{L}(\xi)\gamma = 0$, we have to add the only dilatation $x^1\partial_1 + x^2\partial_2$. As for the conformal system $\hat{R}_2 \subset J_2(T)$ defined by $(\mathcal{L}(\xi)\gamma)^k_{ij} = \delta^k_i A_j + \delta^k_j A_i - \omega_{ij}\omega^{kr}A_r$ according to [18], we have to add the two elations $\theta^1 = \frac{1}{2}((x^1)^2 + (x^2)^2)\partial_1 + x^1x^2\partial_2$ and $\theta^2 = \frac{1}{2}((x^1)^2 + (x^2)^2)\partial_2 + x^1x^2\partial_1$. As we have $g_3 = 0, \tilde{g}_3 = 0, \hat{g}_3 = 0$, we have the strict inclusions $R_3 \subset \tilde{R}_3 \subset \hat{R}_3 \subset J_3(T)$ of involutive systems with respective dimensions $3 < 4 < 6 < 20$. Collecting these results, we get the following commutative fundamental diagram I where the upper down arrows are monomorphisms while the lower down arrows are epimorphisms Φ_0, Φ_1, Φ_2 obtained by induction [20, 29]:

$$
\begin{array}{ccccccccccccc}
 & & & & & & 0 & & 0 & & 0 & & \\
 & & & & & & \downarrow & & \downarrow & & \downarrow & & \\
 & & 0 & \longrightarrow & \hat{\Theta} & \xrightarrow{j_3} & 6 & \xrightarrow{D_1} & 12 & \xrightarrow{D_2} & 6 & \longrightarrow 0 & \\
 & & & & & & \downarrow & & \downarrow & & \downarrow & & \\
 & & 0 & \longrightarrow & \Theta & \xrightarrow{j_3} & 3 & \xrightarrow{D_1} & 6 & \xrightarrow{D_2} & 3 & \longrightarrow 0 & Spencer \\
 & & & & & & \downarrow & & \downarrow & & \downarrow & & \\
 & & 0 & \longrightarrow & 2 & \xrightarrow{j_3} & 20 & \xrightarrow{D_1} & 30 & \xrightarrow{D_2} & 12 & \longrightarrow 0 & hybrid \\
 & & & & \parallel & & \downarrow \Phi_0 & & \downarrow \Phi_1 & & \downarrow \Phi_2 & & \\
0 & \longrightarrow & \Theta & \longrightarrow & 2 & \xrightarrow{D} & 17 & \xrightarrow{D_1} & 24 & \xrightarrow{D_2} & 9 & \longrightarrow 0 & Janet \\
 & & & & & & \downarrow & & \downarrow & & \downarrow & & \\
0 & \longrightarrow & \hat{\Theta} & \longrightarrow & 2 & \xrightarrow{\hat{D}} & 14 & \xrightarrow{\hat{D}_1} & 18 & \xrightarrow{\hat{D}_2} & 6 & \longrightarrow 0 & \\
 & & & & & & \downarrow & & \downarrow & & \downarrow & & \\
 & & & & & & 0 & & 0 & & 0 & &
\end{array}
$$

It follows that "Spencer and Janet play at see-saw", the dimension of each Janet bundle being decreased by the same amount as the dimension of the corresponding Spencer bundle is increased. The Poincaré sequence for the exterior derivative d is $\wedge^0 T^* \xrightarrow{d} \wedge^1 T^* \xrightarrow{d} \wedge^2 T^* \longrightarrow 0$ but it is only at the end of the paper that we shall understand the link with Maxwell equations when $n = 4$. In Special relativity, though surprising it may look like, the above example with $n = 2$ fits with Lorentz transformations if one is using the " hyperbolic" notations $s(h(\phi), ch(\phi), th(\phi) = sh(\phi)/ch(\phi)$ with $x^1 = x, x^2 = ct$ and $ds^2 = (dx^1)^2 - (dx^2)^2$. Indeed, setting $th(\phi) = u/c$ and $th(\psi) = v$ among dimensionless quantities, the Lorentz transformation is now described by the formulas: $\bar{x}^1 = ch(\phi)x^1 - sh(\phi)x^2, \bar{x}^2 = -sh(\phi)x^1 + ch(\phi)x^2$. We obtain thus for the composition of speeds $th(\phi + \psi) = ((u/c) + (v/c))/(1 + (u/c)(v/c))$ without the need of any " gedanken experiment" on light signals. A similar result can be obtained with the ordinary " tangent" for the composition of rotations when using the Euclidean metric $(ds)^2 = (dx^1)^2 + (dx^2)^2$ for the plane (x^1, x^2) .

2 MOTIVATING EXAMPLES

In all the following examples we shall study linear systems of ordinary differential (OD) or partial differential (PD) equations with m dependent variables, n independent variables, order q , Lie groups of dimension p , Lie groups of transformations of a manifold X with tangent bundle T , cotangent bundle T^* , made by a Lie group G acting on X with a graph $X \times G \rightarrow X \times X : (x, a) \rightarrow (x, y = f(x, a))$ or Lie pseudogroups with $m = n$ and geometric objects $(\omega, \gamma, \rho, ...)$ with perturbations $(\Omega, \Gamma, R, ...)$. Vector bundles over X will be denoted by $(E, F, ...)$ and their sections will be denoted by $(\xi, \eta, \zeta, ...)$. Symmetric covariant tensors will be denoted by $S_q T^*$ while r -forms will be sections of $\wedge^r T^*$. Whenever needed, we shall introduce the adjoint vector bundle $ad(E) = \wedge^n T^* \otimes E^*$ in which E^* is obtained from E by inverting the local transition maps, exactly like T^* is obtained from T . The jet bundle of E will be denoted by $J_q(E)$ as usual with an q injective operator $j_q : E \rightarrow J_q(E) : \xi \rightarrow j_q(\xi) = (\xi, \partial_i \xi, \partial_{ij}\xi, ...)$. Finally, if K is differential field with derivations ∂_i and d_i are commuting formal derivations with $d_i \mid K = \partial_i$, we shall introduce the non-commutative ring $D = K[d_1, ..., d_n]$ of linear differential operators with coefficients in K and we have $d_i a = a d_i + \partial_i a$ in the operator sense.

Example 2.1: With $m = 1, n = 2, q = 2$, let us consider the second order system $R_2 \subset J_2(E)$ written $d_{22}\xi - bx^2 d_1 \xi = \eta^2$, $d_{12}\xi - a d_{11}\xi = \eta^1$ or $\mathcal{D}\xi = \eta$ with two constant parameter (a, b) and ground differential field $K = \mathbb{Q}(a, b)(x)$. Three different situations may exist:

• If $a = 0, b = 0$, the reader will check at once the existence of the single first order CC $d_2\eta^1 - d_1\eta_2 = 0$ as an operator $\mathcal{D}_1\eta = 0$ but the second order operator $ad(\mathcal{D})$ does not generate the CC of $ad(\mathcal{D}_1)$ which are generated by a single first order CC.

• If $a = 1, b = 0$, the reader will check at once the existence of the single second order CC $d_{22}\eta^1 - (d_{12} - d_{11})\eta^2 = 0$ and that $ad(\mathcal{D})$ does now generate the CC of $ad(\mathcal{D}_1)$.

• It remains to study the case $a = 1, b = 1$ that will bring surprises. Indeed, differentiating once, we obtain the third order system $R_3 \subset J_3(E)$ with corresponding Janet tabular:

$$
\begin{array}{lcl}
d_{222}\xi - x^2 d_{12}\xi - d_1\xi & = & d_2\eta^2 \\
d_{122}\xi - x^2 d_{11}\xi & = & d_1\eta^2 \\
d_{112}\xi - x^2 d_{11}\xi & = & d_1\eta^2 - d_2\eta^1 \\
d_{111}\xi - x^2 d_{11}\xi & = & d_1\eta^2 - d_2\eta^1 - d_1\eta^1 \\
d_{22}\xi - x^2 d_1\xi & = & \eta^2 \\
d_{12}\xi - d_{11}\xi & = & \eta^1
\end{array}
$$

Though the symbol $g_3 = 0$ defined by $\xi_{222} = 0, \xi_{122} = 0, \xi_{112} = 0, \xi_{111} = 0)$ is trivially involutive, this system is not even formally integrable (FI). Indeed, trying all the usual crossed derivatives, we verac $R_2^{(2)} \subset R_2^{(1)} = R_2 \subset J_2(E)$ with respective dimension $3 < 4 = 4 < 6$. After a few tricky substitutions and eliminations, we obtain the totally new second order PD equation:

$$
A \equiv d_{11}\xi = d_{22}\eta^1 - d_{12}\eta^2 + d_{11}\eta^2 - x^2 d_1\eta^1 \in j_2(\eta)
$$

The hard step is to look for generating CC in the form of an operator $\mathcal{D}_1\eta = \zeta$. We obtain the commutative and exact diagram with $dim(R_3) = 4, dim(R_4) = 3$:

$$
\begin{array}{ccccccccccc}
 & & & & 0 & & 0 & & & & \\
 & & & & \downarrow & & \downarrow & & & & \\
 & & 0 & \longrightarrow & S_4T^*\otimes E & \longrightarrow & S_2T^*\otimes F_0 & \rightarrow & h_2 & \rightarrow & 0 \\
 & & \downarrow & & \downarrow & & \downarrow & & \downarrow & & \\
0 & \longrightarrow & R_4 & \longrightarrow & J_4(E) & \longrightarrow & J_2(F_0) & \rightarrow & Q_2 & \rightarrow & 0 \\
 & & \downarrow & & \downarrow & & \downarrow & & \downarrow & & \\
0 & \rightarrow & R_3 & \rightarrow & J_3(E) & \rightarrow & J_1(F_0) & \rightarrow & Q_1 & \rightarrow & 0 \\
 & & & & \downarrow & & \downarrow & & \downarrow & & \\
 & & & & 0 & & 0 & & 0 & &
\end{array}
$$

and the long exact connecting sequence: $0 \longrightarrow R_4 \longrightarrow R_3 \longrightarrow h_2 \longrightarrow Q_2 \longrightarrow Q_1 \longrightarrow 0$. It follows that $Q_1 \simeq Q_2 = 0$ because $dim(h_2) = 1$ and there cannot exist any first or second order CC. We may start afresh with the new system $R'_2 = R_2^{(2)} \subset R_2 \subset J_2(E)$ which is involutive with symbol $g'_2 = 0$.

$$
\left\{
\begin{array}{rcl}
d_{22}\xi - x^2 d_1\xi & = & \eta^2 \\
d_{12}\xi & = & A + \eta^1 \\
d_{11}\xi & = & A
\end{array}
\right.
\qquad
\begin{array}{|cc|}
\hline
1 & 2 \\
1 & \bullet \\
1 & \bullet \\
\hline
\end{array}
$$

We obtain therefore at once the Fundamental Diagram I for R'_2 :

$$
\begin{array}{|cccccccccccc|}
\hline
 & & & & & 0 & & 0 & & 0 & & \\
 & & & & & \downarrow & & \downarrow & & \downarrow & & \\
 & & 0 & \rightarrow & \Theta & \overset{j_2}{\rightarrow} & 3 & \overset{d_1}{\rightarrow} & 6 & \overset{d_2}{\rightarrow} & 3 & \rightarrow & 0 \\
 & & & & & & \downarrow & & \downarrow & & \| & & \\
 & & 0 & \rightarrow & 1 & \overset{j_2}{\rightarrow} & 6 & \overset{d_1}{\rightarrow} & 8 & \overset{d_2}{\rightarrow} & 3 & \rightarrow & 0 \\
 & & & & \| & & \downarrow & & \downarrow & & \downarrow & & \\
0 & \rightarrow & \Theta & \rightarrow & 1 & \overset{D}{\rightarrow} & 3 & \overset{D_1}{\rightarrow} & 2 & \rightarrow & 0 & & \\
 & & & & & & \downarrow & & \downarrow & & & & \\
 & & & & & & 0 & & 0 & & & & \\
\hline
\end{array}
$$

It finally remains to find out the generating CC for the initial second order operator $\mathcal{D}\xi = \eta$ which is neither FI nor involutive. Checking the two dots separately we have the two third order (!) CC:

$$B_1 \equiv d_1A - x^2A - d_1\eta^2 + d_2\eta^1 + d_1\eta^1 = 0, \qquad B_2 \equiv d_2A - x^2A - d_1\eta^2 + d_2\eta^1 = 0$$

$$
\begin{array}{r}
d_2A - d_1A - d_1\eta^1 \equiv d_{222}\eta^1 - d_{122}\eta^2 - d_{122}\eta^1 + 2d_{112}\eta^2 \\
- d_{111}\eta^2 - x^2 d_{12}\eta^1 - x^2 d_{11}\eta^1 = 0
\end{array}
\tag{1}
$$

Exactly like in [13], we now provide the link existing between these two third order CC and the Spencer operator. Indeed, using R_3 we obtain at once:

$$
\begin{array}{rclcl}
d_1\xi_{11} - \xi_{111} & = & d_1A - x^2A - d_1\eta^2 + d_2\eta^1 + d_1\eta^2 & = & B_1 \\
d_2\xi_{11} - \xi_{112} & = & d_2A - x^2A - d_1\eta^2 + d_2\eta^1 & = & B_2
\end{array}
$$

a result that we shall obtain after one more prolongation by the long exact sequence:

$$0 \rightarrow R_5 \rightarrow J_5(E) \rightarrow J_3(F_0) \rightarrow Q_3 \rightarrow 0 \qquad 0 \rightarrow 3 \rightarrow 21 \rightarrow 20 \rightarrow 2 \rightarrow 0$$

We may thus define $F_1 = Q_3$ with $dim(F_1) = 2$ and define similarly F_2 with $dim(F_2) = 1$ by the long exact sequence:

$$0 \to R_6 \to J_6(E) \to J_4(F_0) \to J_1(F_1) \to F_2 \to 0$$
$$0 \to 3 \to 28 \to 30 \to 6 \to 1 \to 0$$

We have indeed $d_1B_2 - d_2B_1 = 0$ and the exact differential sequence which is not a Janet sequence:

$$\boxed{0 \longrightarrow \Theta \to 1 \underset{2}{\overset{D}{\longrightarrow}} 2 \underset{3}{\overset{D_1}{\longrightarrow}} 2 \underset{1}{\overset{D_2}{\longrightarrow}} 1 \longrightarrow 0}$$

More generally, we have the long exact sequences $\forall r \geq 0$.

$$0 \to 3 \to J_{r+6}(E) \to J_{r+4}(F_0) \to J_{r+1}(F_1) \to J_r(F_2) \to 0 \qquad (2)$$

Using finally the basis $\{\theta_\tau(x) \mid 1 \leq \tau \leq 3\} = \{1, x^2, x^1 + \frac{1}{6}(x^2)^3\}$ for the vector space ν over the constants, the Spencer sequence of the Fundamental Diagram I is the tensor product by ν of the Poincaré sequence $\wedge^0 T^* \overset{d}{\to} \wedge^1 T^* \overset{d}{\to} \wedge^2 T^* \longrightarrow 0$ for the exterior derivative when $n = 2$. We shall discover later on that the sitution of the present example with two parameters (a, b) and three different cases is exactly similar to the one that will be provided by the M, S and K metrics with 2 parameters (m, a) and has thus nothing to do with any GR framework.

Example 2.2: With again $m = 1, n = 2, q = 2, K = \mathbb{Q}(x^2)$, the system $R_2 \subset J_2(E)$ defined by $d_{22}\xi - x^2 d_1\xi = 0, d_{12}\xi - \xi = 0$ has the only solution $\xi = 0$ because $R_2^{(3)} = 0$ with $r = 0, s = 3$ and only the central hybrid sequence for j_2 is left:

$$0 \longrightarrow 1 \overset{j_2}{\longrightarrow} 6 \overset{D_1}{\longrightarrow} 8 \overset{D_2}{\longrightarrow} 3 \longrightarrow 0$$

Example 2.3: (Macaulay) With $m = 1, n = 3, q = 2$ and $P, Q, R \in D = \mathbb{Q}[d_1, d_2, d_3]$, let us consider the linear homogeneous second order system of PD equations $R_2 \subset J_2(E)$ defined by:

$$P\xi \equiv d_{33}\xi = 0, \; Q\xi \equiv d_{23}\xi - d_{11}\xi = 0, \; R\xi \equiv d_{22}\xi = 0$$

but the reader may treat as well the system $(d_{33}\xi - d_{11}\xi = 0, d_{23}\xi = 0, d_{22}\xi - d_{11}\xi = 0)$. Of course, this system is FI because it is homogeneous but we let the reader check through the Janet tabular that g_2 is not involutive though the coordinate system is surely δ -regular because be have full class 3 and full class 2. All the third order jets vanish but $y_{123} - y_{111} = 0$ leading to $dim(g_3) = 1 \Rightarrow dim(R_3) = 8$. Finally $g_4 = 0 \Rightarrow dim(R_4) = 8$ and we could believe that we do not need any PP procedure as R_4 is an ivolutive system because $g_4 = 0$ is trivially involutive and R_2 is finite type like the Killing system. It is important to notice that the knowledge of the first second order operator does not provide any way to obtain the third without passing through the second, contrary to the situation existing in the Janet sequence. Such a procedure is rather "experimental" and must be coherent with a theorem saying that the order of generating CC is one plus the number of prolongations needed to reach a 2-acyclic symbol, that is g_3 must be 2-acyclic [20]. Equivalently the δ -sequence:

$$0 \to \bigwedge^2 T^* \otimes g_3 \overset{\delta}{\to} \bigwedge^3 T^* \otimes g_2 \to 0$$

must be exact. We let the reader prove that the corresponding 3×3 matrix has maximum rank. We recall the dimensions of the following jet bundles:

q	$\to$	0	1	2	3	4	5	6	7
S_qT^*	$\to$	1	3	6	10	15	21	28	36
$J_q(E)$	$\to$	1	4	10	20	35	56	84	120

and the commutative and exact diagram allowing to construct the Spencer bundles $C_r \subset C_r(E)$ and the Janet bundles F_r for $r = 0, 1, ..., n$ with $F_0 = J_q(E)/R_q$, showing that we have indeed with $q = 4$:

$$C_r = \wedge^r T^* \otimes R_q$$

$$C_r(E) = \wedge^r T^* \otimes J_q(E)/\delta(\wedge^{r-1} T^* \otimes S_{q+1} T^* \otimes E$$

$$F_r = \wedge^r T^* \otimes J_q(E)/(\wedge^r T^* \otimes R_q + \delta(\wedge^{r-1} T^* \otimes S_{q+1} T^{\otimes} E))$$

When $R_q \subset J_q(E)$ is involutive, that is formally integrable (FI) with an involutive symbol g_q , then these three differential sequences are formally exact on the jet level and, in the Spencer sequence:

$$0 \longrightarrow \Theta \overset{j_q}{\longrightarrow} C_0 \overset{D_1}{\longrightarrow} C_1 \overset{D_2}{\longrightarrow} ... \overset{D_n}{\longrightarrow} C_n \longrightarrow 0$$

the first order involutive operators $D_1, D_2, ..., D_n$ are induced by the Spencer operator $d : R_{q+1} \to T^* \otimes R_q$ already considered that can be extended to $d : \wedge^r T^* \otimes R_{q+1} \to \wedge^{r+1} \otimes R_q$. A similar condition is also valid for the Janet sequence:

$$0 \longrightarrow \Theta \longrightarrow E \overset{\mathcal{D}}{\longrightarrow} F_0 \overset{\mathcal{D}_1}{\longrightarrow} F_1 \overset{\mathcal{D}_2}{\longrightarrow} ... \overset{\mathcal{D}_n}{\longrightarrow} F_n \longrightarrow 0$$

which can be thus constructed "as a whole" from the previous extension of the Spencer operator (See [29], p 185 and 391 for diagrams missing in [14, 15] !). However, this result is still not known and not even acknowledged today in mathematicl physics, particularly in general relativity which is never using the Spencer δ -cohomology in order to define the Riemann or Bianchi operators. The study of the present Macaulay example will be sufficient in order to justify our comment. First of all, as g_2 is not 2-acyclic and the coeficients are constant, the second order CC are $Qw - Rv = 0,\ Ru - Pw = 0,\ Pv - Qu = 0$ and the simplest resolution is thus:

$$0 \longrightarrow \Theta \longrightarrow 1 \underset{2}{\overset{\mathcal{D}}{\longrightarrow}} 3 \underset{2}{\overset{\mathcal{D}_1}{\longrightarrow}} 3 \underset{2}{\overset{\mathcal{D}_2}{\longrightarrow}} 1 \longrightarrow 0$$

Secondly, as the first prolongation of R_2 becoming involutive is R_4 because $g_4 = 0$, an idea could be to start with the system $R_3 \subset J_3(E)$ but we have proved in ([32], Example 3.14, p 119 to 126) that the simplest formally exact sequence that could be formally exact is quite far from being a Janet sequence as it is:

$$0 \longrightarrow \Theta \longrightarrow 1 \underset{3}{\longrightarrow} 12 \underset{1}{\longrightarrow} 21 \underset{2}{\longrightarrow} 46 \underset{1}{\longrightarrow} 72 \underset{1}{\longrightarrow} 48 \underset{1}{\longrightarrow} 12 \longrightarrow 0$$

Indeed, the Euler-Poincaré characteristic is $1 - 12 + 21 - 46 + 72 - 48 + 12 = 0$ but we notice that the orders of the successive operators may vary up and down.

It remains to work out the Janet and Spencer sequences in the fundamental diagram I :

$$\begin{array}{cccccccccccccc}
 & & & & & 0 & & 0 & & 0 & & 0 & & \\
 & & & & & \downarrow & & \downarrow & & \downarrow & & \downarrow & & \\
 & 0 & \rightarrow & \Theta & \overset{j_4}{\longrightarrow} & 8 & \overset{d_1}{\longrightarrow} & 24 & \overset{d_2}{\longrightarrow} & 24 & \overset{d_3}{\longrightarrow} & 8 & \rightarrow & 0 \\
 & & & & & \downarrow & & \downarrow & & \downarrow & & \downarrow & & \\
 & 0 & \rightarrow & 1 & \overset{j_4}{\longrightarrow} & 35 & \overset{d_1}{\longrightarrow} & 84 & \overset{d_2}{\longrightarrow} & 70 & \overset{d_3}{\longrightarrow} & 20 & \rightarrow & 0 \\
 & & & \| & & \downarrow \Phi_0 & & \downarrow \Phi_1 & & \downarrow \Phi_2 & & \downarrow \Phi_3 & & \\
0 \rightarrow & \Theta & \rightarrow & 1 & \overset{D}{\longrightarrow} & 27 & \overset{D_1}{\longrightarrow} & 60 & \overset{D_2}{\longrightarrow} & 46 & \overset{D_3}{\longrightarrow} & 12 & \rightarrow & 0 \\
 & & & & & \downarrow & & \downarrow & & \downarrow & & \downarrow & & \\
 & & & & & 0 & & 0 & & 0 & & 0 & &
\end{array}$$

As there is no group background, it is nevertheless not evident that the above Spencer sequence is isomorphic to the tensor product of the Poincaré sequence for the exterior derivative by a vector space ν of dimension 8. For this, we notice that each solution is a linear combination of polynomials of degree 3 at most in $\mathbb{Q}[x^1, x^2, x^3]$. After tricky substitutions, we just need to choose the basis:

$$\theta_\tau \mid 1 \leq \tau \leq 8 = \{1, x^1, x^2, x^3, x^1x^2, x^1x^3, \frac{1}{2}(x^1)^2 + x^2x^3, \frac{1}{6}(x^1)^3 + x^1x^2x^3\}$$

All the operators are of order 1 but j_4 and $\mathcal{D}$ which are of order 4.

Example 2.4:(Contact transformations revisited) Whith $m = 3, n = 3$, let $\alpha = dx^1 - x^3dx^2 \in T^*$ be the so-called contact 1-form. The Lie pseudogroup of contact transformations $\Gamma = \{y = f(x) \mid dy^1 - y^3dy^2 = a(x)(dx^1 - x^3dx^2)\}$ preserves α up to a factor $a(x)$. Eliminating this factor among the three infinitesimal Lie equations, we obtain two PD equations but this system is neither involutive nor even FI. The system of infinitesimal Lie equations defining the infinitesimal contact transformations $\Theta \subset T$ is obtained by eliminating the factor $\rho(x)$ in the equations $\mathcal{L}(\xi)\alpha = \rho\alpha$ where $\mathcal{L}$ is the standard Lie derivative [26]. This system is thus only generated by η^1 and η^2 below but is not involutive and one has to introduce η^3 in order to obtain the following involutive system $R_1 \subset J_1(T)$ with two equations of class 3 and one equation of class 2, a result leading to

$dim(g_1) = 6$, $dim(g_2) = 10$ and $dim(g_3) = 15$.

$$\begin{array}{rcl|ccc|}
d_3\xi^3 + d_2\xi^2 + 2x^3d_1\xi^2 - d_1\xi^1 & = & \eta^3 & & & \\
 & & & 1 & 2 & 3 \\
d_3\xi^1 - x^3d_3\xi^2 & = & \eta^2 & 1 & 2 & 3 \\
 & & & 1 & 2 & \bullet \\
d_2\xi^1 - x^3d_2\xi^2 + x^3d_1\xi^1 - (x^3)^2d_1\xi^2 - \xi^3 & = & \eta^1 & & &
\end{array}$$

We have one first order CC:

$$d_3\eta^1 - d_2\eta^2 - x^3d_1\eta^2 + \eta^3 = \zeta$$

showing the origin of η^3 and finally get the Janet sequence:

$$\left|\ 0 \rightarrow \Theta \rightarrow 3 \overset{\mathcal{D}}{\longrightarrow} 3 \overset{\mathcal{D}_1}{\longrightarrow} 1 \rightarrow 0\ \right|$$

Let us now consider the new pseudogroup $\{\Gamma' \subset \Gamma \mid dy^1 - y^3dy^2 = dx^1 - x^3dx^1\}$ preserving the contact form α , thus also $\beta = d\alpha = dx^2 \wedge dx^3$ and $\gamma = \alpha \wedge \beta = dx^1 \wedge dx^2 \wedge dx^3$ which is the so-called volume form. The corresponding infinitesimal Lie equations are successively:

$$d_1\xi^1 - x^3 d_1\xi^2 0,\ d_2\xi^1 - x^3 d_2\xi^2 - \xi^3 = 0,\ d_3\xi^1 - x^3 d_3\xi^2 = 0$$

$$d_1\xi^2 = 0,\ d_1\xi^3 = 0,\ d_2\xi^2 + d_3\xi^3 = 0$$

$$d_1\xi^1 + d_2\xi^2 + d_3\xi^3 = 0$$

Doing the permutation (123)(312) , we obtain the first order system $R_1' \subset J_1(T)$:

$$\left\{\begin{array}{rcl} d_3\xi^3 & = & 0 \\ d_3\xi^2 & = & 0 \\ d_3\xi^1 & = & 0 \\ d_2\xi^3 + d_1\xi^2 & = & 0 \\ d_2\xi^1 - x^2 d_2\xi^2 & = & 0 \\ d_1\xi^1 - x^2 d_1\xi^2 - \xi^3 & = & 0 \end{array}\right. \quad \left|\begin{array}{ccc} 1 & 2 & 3 \\ 1 & 2 & 3 \\ 1 & 2 & 3 \\ 1 & 2 & \bullet \\ 1 & \bullet & \bullet \end{array}\right|$$

and we have the strict inclusions $R_1' \subset R_1 \subset J_1(T)$ with $6 < 9 < 12$. We have the new Janet sequence with $3 - 6 + 4 - 1 = 0$:

$$0 \rightarrow \Theta' \rightarrow 3 \xrightarrow{\mathcal{D}'} 6 \xrightarrow{\mathcal{D}_1'} 4 \xrightarrow{\mathcal{D}_2'} 1 \rightarrow 0$$

Contrary to other examples, in the present situation it is easy to work out the Janet sequences but much more difficult to work out the corresponding Spencer sequences. In fact, we obtain the following Fundamental diagram I in which the central hybrid sequence, which is at the same time a Janet sequence for $j_1 i$ and a Spencer sequence for $J_2(T) \subset J_1(J_1(T))$, is the same for $\Theta' \subset \Theta$ and all the operators involved are first order:

$$\begin{array}{ccccccccccccccc}
 & & & & & & 0 & & 0 & & 0 & & 0 & & \\
 & & & & & & \downarrow & & \downarrow & & \downarrow & & \downarrow & & \\
 & & 0 & \longrightarrow & \Theta' & \xrightarrow{j_1} & 6 & \xrightarrow{d_1} & 14 & \xrightarrow{d_2} & 11 & \xrightarrow{d_3} & 3 & \longrightarrow & 0 \\
 & & & & & & \downarrow & & \downarrow & & \downarrow & & \| & & \\
 & & 0 & \longrightarrow & 3 & \xrightarrow{j_1} & 12 & \xrightarrow{d_1} & 18 & \xrightarrow{d_2} & 12 & \xrightarrow{d_3} & 3 & \rightarrow & 0 \\
 & & & & \| & & \downarrow & & \downarrow & & \downarrow & & \downarrow & & \\
0 & \longrightarrow & \Theta' & \longrightarrow & 3 & \xrightarrow{D'} & 6 & \xrightarrow{D_1'} & 4 & \xrightarrow{D_2'} & 1 & \rightarrow & 0 & & \\
 & & & & & & \downarrow & & \downarrow & & \downarrow & & & & \\
 & & & & & & 0 & & 0 & & 0 & & & &
\end{array}$$

In actual practice, when g_q is involutive, its knowledge allows to determines the Hilbert function $dim(g_{q+r})$ and finally $dim(R_{q+r})$. Then $dim(C_r)$ may be computed by induction on r . In this example with $q = 1$, one has the commutative and exact diagram with $dim(C_0) = dim(R_1) = 9 \Rightarrow$

$dim(C_1) = 17 \Rightarrow dim(C_2) = 12$ and so on:

$$\begin{array}{ccccccccccc}
0 & \rightarrow & R_{q+2} & \rightarrow & J_2(R_q) & \rightarrow & J_1(C_1) & \rightarrow & C_2 & \rightarrow & 0 \\
 & & \downarrow & & \downarrow & & \downarrow & & \downarrow & & \\
0 & \rightarrow & R_{q+1} & \rightarrow & J_1(R_q) & \rightarrow & C_1 & \rightarrow & 0 & &
\end{array}$$

Unhappily, Spencer and collaborators, being unaware on one side of the computer algebra works of Janet and Gröbner or of the work of Vessiot on geometric objects, were unable to compute explicit examples. In particular, anybody can check that the examples presented in the introduction of [27] have no relation at all with the remaining of the book.

It is thus sometimes easier to exhibit the Janet sequences than the Spencer sequences. By chance the situation will be opposite when we shall deal with general relativity and black holes.

Example 2.5: (Bose conjecture) Last but not least, the following example is the most difficult of this paper as it is exhibiting a mixture of second and third order CC [4]. With $m = n = 3$, the trivial differential field $K = \mathbb{Q}$ and the ring $D = K[d_1, d_2, d_3]$ of differential operators, let us consider the D module M defined by the second order operator:

$$\mathcal{D} : (\xi^1, \xi^2, \xi^3) \rightarrow (\xi^3_{33} - \xi^1_1 = \eta^1, \xi^3_{23} - \xi^2_1 - \xi^3 = \eta^2)$$

A first question is to determine its torsion submodule $t(M)$ or, equivalently, to know whether $\mathcal{D}$ can be parametrized by a certain operator $\mathcal{D}_{-1}$ through a certain number of arbitrary potential functions ϕ . Using double duality, we may construct the adjoint operator $ad(\mathcal{D})$ by multiplying these equations respectively by (λ^1, λ^2) , adding and integrating by parts in order to get successively:

$$ad(\mathcal{D}) : (\lambda^1, \lambda^2) \to (d_1\lambda^1 = \mu^1, d_1\lambda^2 = \mu^2, d_{33}\lambda^1 + d_{23}\lambda^2 - \lambda^2 = \mu^3)$$
$$ad(\mathcal{D}_{-1}) : (\mu^1, \mu^2, \mu^3) \to d_{33}\mu^1 + d_{23}\mu^2 - d_1\mu^3 - \mu^2 = \nu$$
$$\mathcal{D}_{-1} : \phi \to (d_{33}\phi = \xi^1, d_{23}\phi - \phi = \xi^2, d_1\phi = \xi^3)$$

There is a new second order CC for $\mathcal{D}_{-1}$, namely $\eta^3 \equiv d_{33}\xi^2 - (d_{23} - 1)\xi^1 = 0$ and we check at once that $d_1\eta^3 = 0$, that is $t(M)$ is generated by η^3 because we have:

$$(d_{23} - 1)\eta^1 - d_{33}\eta^2 = (\xi^2_{133} + \xi^3_{33} - \xi^1_{123}) - (\xi^3_{33} - \xi^1_1) = \xi^2_{133} - \xi^1_{123} + \xi^1_1 = d_1\eta^3$$

It follows that $M' = M/t(M) \simeq D$ is a free, thus torsion-free and even projective module defined by $\mathcal{D}'$ which is parametrized by the injective operator $\mathcal{D}_{-1}$:

$$\mathcal{D}' : (\xi^1, \xi^2, \xi^3)(\xi^3_{33} - \xi^1_1 = \eta^1, \xi^3_{23} - \xi^2_1 - \xi^3 = \eta^2, \xi^2_{33} - \xi^1_{23} + \xi^1 = \eta^3)$$

Indeed, we have an isomorphism $M \simeq t(M) \oplus M'$ because the following splitting :

$$d_{33}\phi = \xi^1,\ d_{23}\phi - \phi = \xi^2 \ \Rightarrow\ d_3\phi = d_2\,\xi^1 - d_3\xi^2 \ \Rightarrow\ \phi = d_{22}\xi^1 - d_{23}\xi^2 - \xi^2$$

It is not at all evident that M' can be defined by only two differentially independent PD equations, the first one for (ξ^1, ξ^2) while the second is providing ξ^3 :

$$\xi^2_{33} - \xi^1_{23} + \xi^1 = 0, \xi^2_{123} - \xi^1_{122} + \xi^2_1 + \xi^3 = 0$$

a result showing that the CC operator $\mathcal{D}''$ of the parametrizing operator $\mathcal{D}_{-1}$ may be generated by one second order CC and one third order CC, a striking result providing the short exact sequence:

$$0 \longrightarrow 1 \xrightarrow{\mathcal{D}_{-1}} 3 \xrightarrow{\mathcal{D}''} 2 \longrightarrow 0$$

Now, we may consider the new system:

$$\left\{\begin{array}{rcl} \xi^3_{33} - \xi^1_1 & = & \eta^1 \\ \xi^2_{33} - \xi^1_{23} + \xi^1 & = & \eta^3 \\ \xi^3_{23} - \xi^2_1 - \xi^3 & = & \eta^2 \\ \xi^2_{13} - \xi^1_{12} + \xi^3_3 & = & d_2\eta^1 - d_3\eta^2 \end{array}\right. \quad \left|\begin{array}{ccc} 1 & 2 & 3 \\ 1 & 2 & 3 \\ 1 & 2 & \bullet \\ 1 & \times & \bullet \end{array}\right|$$

The lack of involutivity provides $d_{22}\eta^1 - d_{23}\eta^2 - \eta^2 = \xi^2_{123} - \xi^1_{122} + \xi^2_1 + \xi^3$.

Conversely,tiv $\xi^2_{13} - \xi^1_{12} + \xi^3_3 = 0$ and thus $\xi^2_{133} - \xi^1_{123} + \xi^3_{33} = 0$ However, we have $d_1\eta^3 = \xi^2_{133} - \xi^1_{123} + \xi^1_1 = 0$ d $\eta^1 = \xi^3_{33} - \xi^1_1 = 0$. Similarly, we obtain $\xi^2_{123} - \xi^1_{122} + \xi^3_{23} = 0$ and obtain by subtraction $\eta^2 = \xi^3_{23} - \xi^2_1 - \xi^3 = 0$.

Remark 2.6: Coming back to the previous motivating examples depending on parameters, we notice that the order of the generating CC may highly depend on the parameters. Such a situation, having nothing to do with physics, is nevertheless quite similar to that of the first order Killing system $R_1 \subset J_1(T)$ allowing to define the first order Killing operator $\mathcal{D} : T \to S_2T^* : \xi \to \mathcal{L}(\xi)\omega = \Omega$ through the Lie derivative of a non-degenerate metric ω , for example in the case of the M, S, K metrics where a prolongation $R^{(s)}_{q+r} = \pi^{q+r+s}_{q+r}(R_{q+r+s}) \subset R_{q+r}$ must be done. Using the Lie algebra $\vec{\mathcal{G}}$ with dimension 10 for M , 4 for S and 2 for K instead of n , the Spencer sequence is always isomorphic to the tensor product of the Poincaré sequence for the exterior derivative by a Lie algebra that may have a very small dimension as we shall see. Accordingly, we claim:

THE IMPORTANT OBJECT IS NOT THE METRIC BUT ITS GROUP OF INVARIANCE

In particular, the FACT that third order generating CC for the Killing operator may exist has no physical meaning as nobody is knowing a way to select a best candidate among the possible explicit solutions of Einstein equations in vacuum, a mathematical result questioning the origin and existence of black holes as we shall see !. We also notice the fact that the PP procedure is highly depending on the various parameters involved, namely the only parameter m for the S metric which is reduced to the M metric when $m = 0$ while the K metric depends on the two parameters (m, a) and is reduced to the S metric when $a = 0$. We study now this comment.

3 DIFFERENTIAL TOOLS

3.1 From Group Theory to Differential Sequences

Let G be a Lie group with coordinates $(a^\rho) = (a^1, ..., a^p)$ acting on a manifold X with a local action map $y = f(x, a)$. According to the second fundamental theorem of Lie, if $\theta_1, ..., \theta_p$ are the infinitesimal generators of the effective action of a lie group G on X , then $[\theta_\rho, \theta_\sigma] = c^\tau_{\rho\sigma}\theta_\tau$ where the $c = (c^\tau_{\rho\sigma} = -c^\tau_{\sigma\rho})$ are the structure constants of a Lie algebra of vector felds which can be identified with $\mathcal{G} = T_e(G)$ the tangent space to $\mathcal{G}$ at the identity $e \in G$ by using the action.

More generally, if X is a manifold and G is a lie group (not acting necessarily on X), let us consider gauging maps $a : X \to G : (x) \to (a(x))$. If $x + dx$ is a point of X close to x , then the tangent mapping $T(a) : T = T(X) \to T(G) : dx \to da = (\partial a/\partial x)dx$ will provide a point $a + da$ close to

a on G . We may bring a back to e on G by acting on a with a^{-1} on the left, that is $b \rightarrow a^{-1}b, \forall b \in G$. We get therefore a 1-form $a^{-1}da = A \in T^* \otimes \mathcal{G}$ and the curvature 2-form $F = (\partial_i A^\tau_j(x) - \partial_j A^\tau_i(x) - c^\tau_{\rho\sigma}A^\rho_i(x)A^\sigma_j(x) = F^\tau_{ij}(x)) \in \wedge^2 T^* \otimes \mathcal{G}$ in the nonlinear gauge sequence:

$$\begin{array}{ccccc} X \times G & \longrightarrow & T^* \otimes G & \longrightarrow & \wedge^2 T^* \otimes G \\ a & \longrightarrow & a^{-1}da = A & \longrightarrow & dA - [A,A] = F \end{array}$$

In 1956, at the birth of gauge theory (GT), the above notations were coming from the EM potential A and EM field $dA = F$ of relativistic Maxwell theory. Accordingly, $G = U(1)$ (unit circle in the complex plane) $\longrightarrow \dim(\mathcal{G}) = 1$ was the only possibility to get a 1-form A and a 2-form F with vanishing structure constants $c = 0$.

Choosing now a "close" to e , that is $a(x) = e + t\lambda(x) + ...$ and linearizing as usual, we obtain the linear operator $d : \wedge^0 T^* \otimes \mathcal{G} \rightarrow \wedge^1 T^* \otimes \mathcal{G}$: $(\lambda^\tau(x)) \rightarrow (\partial_i \lambda^\tau(x))$ and the linear gauge sequence:

$$\wedge^0 T^* \otimes \mathcal{G} \xrightarrow{d} \wedge^1 T^* \otimes \mathcal{G} \xrightarrow{d} \wedge^2 T^* \otimes \mathcal{G} \xrightarrow{d} ... \xrightarrow{d} \wedge^n T^* \otimes \mathcal{G} \longrightarrow 0$$

which is the tensor product by $\mathcal{G}$ of the Poincaré sequence for the exterior derivative.

Considering now a Lagrangian on $T^* \otimes \mathcal{G}$, that is an action $W = \int w(A)dx$ where $dx = dx^1 \wedge ... \wedge dx^n$, we may vary it. With $A = a^{-1}da$ we may introduce $\lambda = a^{-1}\delta a \in \mathcal{G} = \wedge^{\cup} T^* \otimes \mathcal{G}$ and get $\delta A^\tau_i = \partial_i \lambda^\tau - c^\tau_{\rho\sigma}A^\rho_i \lambda^\sigma$ ([20], p 180-185). Setting $\partial w/\partial A = \mathcal{A} = (\mathcal{A}^i_\tau) \in \wedge^{n-1} T^* \otimes \mathcal{G}^*$, we obtain the Poincaré equations $\partial_i \mathcal{A}^i_\tau + c^\sigma_{\rho\tau}\mathcal{A}^\rho_i \mathcal{A}^i_\sigma = 0$ as the adjoint of the previous operator (up to sign). Setting now $(\delta a)a^{-1} = \mu \in \mathcal{G}$,we get the adjoint representation $\lambda = a^{-1}((\delta a)a^{-1})a = Ad(a)\mu$ while, introducing B such that $B\mu = A\lambda$, we get the divergence-like equations $\partial_i B^i_\sigma = 0$.

In a different setting, if G acts on X , let $\{\theta_\tau \mid 1 \leq \tau \leq p = dim(G)\}$ be a basis of infinitesimal generators of the action. If $\mu = (\mu_1, ..., \mu_n)$ is a multi-index of length $\mid \mu \mid = \mu_1 + ... + \mu_n$ and $\mu + 1_i = (\mu_1, .., \mu_{i-1}, \mu_i + 1, \mu_{i+1}, ..., \mu_n)$, we may introduce the Lie algebroid $R_q \subset J_q(T)$ with sections defined by $\xi^k_\mu(x) = \lambda^\tau(x)\partial_\mu \theta^k_\tau(x)$ for an arbitrary section $\lambda \in \wedge^0 T^* \otimes \mathcal{G}$ and the trivially involutive operator $j_q : T \rightarrow J_q(T) : \theta \rightarrow (\partial_\mu \theta, 0 \leq |\mu| \leq q)$ of order q . We finally obtain the Spencer operator $d : R_{q+1} \rightarrow T^* \otimes R_q$ through the chain rule for derivatives [17]:

$$(d\xi_{q+1})^k_{\mu,i}(x) = \partial_i \xi^k_\mu(x) - \xi^k_{\mu+1_i}(x) = \partial_i \lambda^\tau(x)\partial_\mu \theta^k_\tau(x)$$

When q is large enough to have an isomorphism $R_{q+1} \simeq R_q \simeq \Lambda^0 T^* \otimes \mathcal{G}$ and the following linear Spencer sequence in which the operators D_r are induced by d as above:

$$0 \longrightarrow \Theta \xrightarrow{j_q} R_q \xrightarrow{D_1} T^* \otimes R_q \xrightarrow{D_2} \wedge^2 T^* \otimes R_q \xrightarrow{D_3} ... \xrightarrow{D_n} \wedge^n T^* \otimes R_q \longrightarrow 0$$

is isomorphic to the linear gauge sequence but with a completely different meaning because G is now acting on X and $\Theta \subset T$ is such that $[\Theta, \Theta] \subset \Theta$. Surprisingly, these results have NEVER been used in the study of the M, S and K metrics [13].

It is not evident, as we already saw, that the projective transformation $y = (ax + b)/(cx + d)$ of the real line with (a, b, c, d) constants is the generic solution of the third order OD equation $(y_{xxx}/y_x) - (3/2)(y_{xx}/y_x)^2 = 0$ and has three infinitesimal generators $(\partial_x, x\partial_x, \frac{1}{2}x^2\partial_x)$ providing the generic solution of the linearized OD equation $\xi_{xxx} = 0$. The situation of contact transformations met in Section 2 and of Lie pseudogroups in general needs new differential geometric tools as follows, not known by physicists because they necessarily involve the Spencer operator [20].

3.2 LIE ALGEBROIDS

If $R_q \subset J_q(E)$ is a system of order q on E , then $R_{q+r} = \rho_r(R_q) = J_r(R_q) \cap J_{q+r}(E) \subset J_r(J_q(E))$ is called the r -prolongation of R_q and is thus the system obtained after differentiating r times. In actual practice, if the system is defined by PDE $\Phi^\tau \equiv a^{\tau\mu}_k(x)\xi^k_\mu = 0$ the first prolongation is defined by adddng the PDE $d_i\Phi^\tau \equiv a^{\tau\mu}_k(x)\xi^k_{\mu+1_i} + \partial_i a^{\tau\mu}_k(x)\xi^k_\mu = 0$ .A Ccordingly, $\xi_q \in R_q \Leftrightarrow a^{\tau\mu}_k(x)\xi^k_\mu(x) = 0$ and $\xi_{q+1} \in R_{q+1} \Leftrightarrow a^{\tau\mu}_k(x)\xi^k_{\mu+1_i}(x) + \partial_i a^{\tau\mu}_k(x)\xi^k_\mu(x) = 0$ as identitties on X or at least over an open subset $U \subset X$. We finally obtain:

$$\partial_i \Phi^\tau - d_i \Phi^\tau \equiv a^{\tau\mu}_k(x)\big(\partial_i \xi^k_\mu(x) - \xi^k_{\mu+1_i}(x)\big) = 0 \Rightarrow d\xi_{q+1} \in T^* \otimes R_q$$

and the Spencer operator restricts to $d : R_{q+1} \rightarrow T^* \otimes R_q$.

Definition 3.B.1: We set $R^{(s)}_{q+r} = \pi^{q+r+s}_{q+r}(R_{q+r+s})$ and this system is called the s-prolonged system of order $q + r$. For Example, if we consider the second order Killing system $R_1 \subset J_1(T)$ defined by $x^2\xi^1_1 + \xi^2 = 0, \xi^1_2 = 0$ then $R^{(1)}_1 \subset R_1$ is defined by adding $\xi^1_1 + \xi^2_2 = 0$, even though both systems have the same " solutions".

Definition 3.B.2: The symbol of R_q is the family $g_q = R_q \cap S_q T^* \otimes E$ of vector spaces over X . The symbol g_{q+r} of $\mathcal{R}_{q+r}$ only depends on g_q by a direct prolongation procedure. We may define the vector bundle F_0 over $\mathcal{R}_q$ by the short exact sequence $0 \rightarrow R_q \rightarrow J_q(E) \rightarrow F_0 \rightarrow 0$ and we have the exact induced sequence $0 \rightarrow g_q \rightarrow S_q T^* \otimes E \rightarrow F_0$.

When $\mid \mu \mid = q$, we obtain:

$$g_q = \{v^k_\mu \in S_q T^* \otimes E \mid a^{\tau\mu}_k(x)v^k_\mu = 0\}, \mid \mu \mid = q$$

$$\Rightarrow g_{q+r} = \rho_r(g_q) = \{v^k_{\mu+\nu} \in S_{q+r} T^* \otimes E \mid a^{\tau\mu}_k(x)v^k_{\mu+\nu} = 0\},$$

$$\mid \mu \mid = q, \mid \nu \mid = r$$

In general, neither g_q nor g_{q+r} are vector bundles over X as can be seen in the simple example $xy_x - y = 0 \Rightarrow xy_{xx} = 0$.

On $\wedge^s T^*$ we may introduce the usual bases $\{dx^I = dx^{i_1} \wedge ... \wedge dx^{i_s}\}$ where we have set $I = (i_1 < ... < i_s)$. In a purely algebraic setting, one has:

Proposition 3.B.3: There exists a map $\delta : \wedge^s T^* \otimes S_{q+1}T^* \otimes E \rightarrow \wedge^{s+1}T^* \otimes S_q T^* \otimes E$ which restricts to $\delta : \wedge^s T^* \otimes g_{q+1} \rightarrow \wedge^{s+1}T^* \otimes g_q$ and $\delta^2 = \delta \circ \delta = 0$.

Proof: Let us introduce the map: $\omega = \{\omega^k_\mu = v^k_{\mu,I} dx^I\} (\delta\omega)^k_\mu = dx^i \wedge \omega^k_{\mu+1_i} (\delta^2\omega)^k_\mu = dx^i \wedge dx^j \wedge \omega^k_{\mu+1_i+1_j} = 0 \; a^{\tau\mu}_k (\delta\omega)^k_\mu = dx^i \wedge (a^{\tau\mu}_k \omega^k_{\mu+1_i}) = 0$

The kernel of each δ in the first case is equal to the image of the preceding δ but this may no longer be true in the restricted case and we set:

Definition 3.B.4: Let $B^s_{q+r}(g_q) \subseteq Z^s_{q+r}(g_q)$ and $H^s_{q+r}(g_q) = Z^s_{q+r}(g_q)/B^s_{q+r}(g_q)$ with $H^s(g_q) = H^s_q(g_q)$ be the coboundary space $im(\delta)$, cocycle space $ker(\delta)$ and cohomology space at $\wedge^s T^* \otimes g_{q+r}$ of the restricted g_q is said to be s-acyclic if $H^1_{q+r} = ... = H^s_{q+r} = 0, \forall r \geq 0$. The symbol g_q is said to be of finite type if $g_{q+r} = 0$ for r large enough. In particular, if g_q is involutive and finite type, then $g_q = 0$. Finally, $S_q T^* \otimes E$ is involutive for any $q \geq 0$ if we set $S_0 T^* \otimes E = E$.

A first point is provided by the following useful but technical results. As we do not want to provide details about groupoids, we shall introduce a " copy" Y (target) of X (source) and define simply a Lie pseudogroup $\Gamma \subseteq aut(X)$ as a group of transformations solutions of a (in general nonlinear) system $\mathcal{R}_q$, such that, whenever $y = f(x), z = g(y) \in \Gamma$ can be composed, then $z = g \circ f(x) \in \Gamma$, $x = f^{-1}(y) \in \Gamma$ and $y = id(x) = x \in \Gamma$. Setting $y = x + t\xi(x) + ...$ and passing to the limit when $t \rightarrow 0$, we may linearize the later system and obtain a (linear) system $R_q \subset J_q(T)$ such that $[\Theta, \Theta] \subset \Theta$. We may use the Frobenius theorem in order to find a generating fundamental set of differential invariants $\{\Phi^\tau(y_q)\}$ up to order q which are such that $\Phi^\tau(\bar{y}_q) = \Phi^\tau(y_q)$ whenever $\bar{y} = g(y) \in \Gamma$. We obtain the Lie form $\Phi^\tau(y_q) = \Phi_\tau(id_q(x)) = \Phi^\tau(j_q(id)(x)) = \omega^\tau(x)$ of $\mathcal{R}_q$.

Of course, in actual practice one must use sections of R_q instead of solutions and we now prove why the use of the Spencer operator becomes crucial for such a purpose. Indeed, we may define:

$$\{j_{q+1}(\xi), j_{q+1}(\eta)\} = j_q([\xi, \eta]), \forall \xi, \eta \in T \qquad (algebraic\ bracket)$$

We may obtain by bilinearity a bracket on $J_q(T)$ extending the bracket on T .

$$[\xi_q, \eta_q] = \{\xi_{q+1}, \eta_{q+1}\} + i(\xi)d\eta_{q+1} - i(\eta)d\xi_{q+1}, \forall \xi_q, \eta_q \in J_q(T) \qquad (differential\ bracket)$$

which does not depend on the respective lifts ξ_{q+1} and η_{q+1} of ξ_q and η_q in $J_{q+1}(T)$. This bracket on sections satisfies the Jacobi identity:

$$[[\xi_q, \eta_q], \zeta_q] + [[\eta_q, \zeta_q], \xi_q] + [[\zeta_q, \xi_q], \eta_q] = 0, \ \forall \xi_q, \eta_q, \zeta_q \in J_q(T) \qquad (Jacobs).$$

and we set [20]:

Definition 3.B.5: We say that a vector subbundle $R_q \subset J_q(T)$ is a system of infinitesimal Lie equations or a Lie algebroid if $[R_q, R_q] \subset R_q$, that is to say $[\xi_q, \eta_q] \in R_q, \forall \xi_q, \eta_q \in R_q$. Such a definition can be tested by means of computer algebra. We shall also say that R_q is transitive if we have the short exact sequence $0 \rightarrow R^0_q \rightarrow R_q \overset{\pi^q_0}{\rightarrow} T \rightarrow 0$.

Theorem 3.B.6: The bracket is compatible with prolongations:

$$[R_q, R_q] \subset R_q \quad \Rightarrow \quad [R_{q+r}, R_{q+r}] \subset R_{q+r}, \forall r \geq 0$$

Proof: When $r = 1$, we have $\rho_1(R_q) = R_{q+1} = \{\xi_{q+1} \in J_{q+1}(T) \mid \xi_q \in R_q, d\xi_{q+1} \in T^* \otimes R_q\}$ and we just need to use the following formulas showing how d acts on the various brackets if we set $L(\xi_1)\zeta = [\xi, \zeta] + i(\zeta)d\xi_1$ (See [22] and [26] or [32] for more details):

$$\begin{aligned} i(\zeta)d\{\xi_{q+1}, \eta_{q+1}\} &= \{i(\zeta)d\xi_{q+1}, \eta_q\} + \{\xi_q, i(\zeta)d\eta_{q+1}\}, \quad \forall \zeta \in T \\ i(\zeta)d[\xi_{q+1}, \eta_{q+1}] &= [i(\zeta)d\xi_{q+1}, \eta_q] + [\xi_q, i(\zeta)d\eta_{q+1}] \\ &\quad + i(L(\eta_1)\zeta)d\xi_{q+1} - i(L(\xi_1)\zeta)d\eta_{q+1} \end{aligned}$$

The right member of the second formula is a section of R_q whenever $\xi_{q+1}, \eta_{q+1} \in R_{q+1}$. The first formula may be used when R_q is formally integrable.

Corollary 3.B.7: The bracket is compatible with the PP procedure:

$$[R_q, R_q] \subset R_q \quad \Rightarrow \quad [R^{(s)}_{q+r}, R^{(s)}_{q+r}] \subset R^{(s)}_{q+r}, \forall r, s \geq 0$$

Example 3.B.8: When $n = 1$, one has the unusual successive formulas:

$$[\xi, \eta] = \xi\partial_x\eta - \eta\partial_x\xi$$

$$([\xi_1, \eta_1])_x = \xi\partial_x\eta_x - \eta\partial_x\xi_x$$

$$([\xi_2, \eta_2])_{xx} = \xi_x\eta_{xx} - \eta_x\xi_{xx} + \xi\partial_x\eta_{xx} - \eta\partial_x\xi_{xx}$$

$$([\xi_3, \eta_3])_{xxx} = 2\xi_x\eta_{xxx} - 2\eta_x\xi_{xxx} + \xi\partial_x\eta_{xxx} - \eta\partial_x\xi_{xxx}$$

They can be used for linear ($\xi_x = 0$), affine ($\xi_{xx} = 0$) or projective $\xi_{xxx} = 0$)transformations.

Example 3.B.9: With $n = m = 2$ and $q = 1$, let us consider the Lie pseudogroup $\Gamma \subset aut(X)$ of finite transformations $y = f(x)$ such that $y^2dy^1 = x^2dx^1 = \alpha$. Setting $y = x + t\xi(x) + ...$ and linearizing, we get the Lie operator $\mathcal{D}\xi = \mathcal{L}(\xi)\alpha$ where $\mathcal{L}$ is the Lie derivative and the system $R_1 \subset J_1(T)$ of linear infinitesimal Lie equations already met in Definition 3.B.1. Let us choose the two sections $\xi_1, \eta_1 \in J_1(T)$:

$$\xi_1 = \{\xi^1 = 0, \xi^2 = -x^2, \xi^1_1 = 1, \xi^1_2 = 0, \xi^2_1 = 0, \xi^2_2 = 0\} \in R_1$$
$$\eta_1 = \{\eta^1 = x^2, \eta^2 = 0, \eta^1_1 = 0, \eta^1_2 = -x2, \eta^2_1 = 0, \eta^2_2 = 1\} \in R_1$$

The reader may check that $[\xi_1, \eta_1] \in R_1$. However, we have the strict inclusion $R_1^{(1)} \subset R_1$ defined by the additional equation $\xi^1_1 + \xi^2_2 = 0$ and thus $\xi_1, \eta_1 \notin R_1^{(1)}$ though we have $[R_1^{(1)}, R_1^{(1)}] \subset R_1^{(1)}$, a result not evident and lacking in [14] because ξ_1 and η_1 have nothing to do with solutions.

3.3 JANET VERSUS SPENCER

When $R_q \subset J_q(E)$ is an involutive system on E , there is a Fundamental Diagram I with exact columns, where each operator is induced by the extension $d : \wedge^r T^* \otimes J_{q+1}(E) \wedge^{r+1} T^* \otimes J_q(E) : \alpha \otimes \xi_{q+1} \rightarrow d\alpha \otimes \xi_q + (-1)^r \alpha \wedge d\xi_{q+1}$ of the Spencer operator $d : J_{q+1}(E) \rightarrow T^* \otimes J_q(E) : \xi_{q+1} \rightarrow j_1(\xi_q) - \xi_{q+1}$. The upper sequence is the Spencer sequence while the lower sequence is the Janet sequence and the sum $dim(C_r) + dim(F_r) = dim(C_r(E))$ does not depend on the system while the epimorphisms Φ_r are induced inductively by $\Phi = \Phi_0$ [20, 29]:

$$\begin{array}{ccccccccccccc}
 & & & & & & 0 & & 0 & & & 0 & \\
 & & & & & & \downarrow & & \downarrow & & & \downarrow & \\
 & & 0 & \rightarrow & \Theta & \xrightarrow{j_q} & C_0 & \xrightarrow{d_1} & C_1 & \xrightarrow{d_2} ... \xrightarrow{d_n} & & C_n & \rightarrow 0 \\
 & & & & & & \downarrow & & \downarrow & & & \downarrow & \\
 & & 0 & \rightarrow & E & \xrightarrow{j_q} & C_0(E) & \xrightarrow{d_1} & C_1(E) & \xrightarrow{d_2} ... \xrightarrow{d_n} & & C_n(E) & \rightarrow 0 \\
 & & & & \| & & \downarrow \Phi_0 & & \downarrow \Phi_1 & & & \downarrow \Phi_n & \\
0 & \rightarrow & \Theta & \rightarrow & E & \xrightarrow{D} & F_0 & \xrightarrow{D_1} & F_1 & \xrightarrow{D_2} ... \xrightarrow{D_n} & & F_n & \rightarrow 0 \\
 & & & & & & \downarrow & & \downarrow & & & \downarrow & \\
 & & & & & & 0 & & 0 & & & 0 &
\end{array}$$

For later computations, the sequence $J_{q+1}(E) \xrightarrow{d} T^* \otimes J_q(E) \xrightarrow{d} \wedge^2 T^* \otimes J_{q-1}(E)$ can be described by the images $\partial_i \xi^k_\mu - \xi^k_{\mu+1_i} = X^k_{\mu,i}$ leading to the identities:

$$\partial_i X^k_{\mu,j} - \partial_j X^k_{\mu,i} + X^k_{\mu+1_j,i} - X^k_{\mu+1_i,j} = 0$$

We also recall that the linear Spencer sequence for a Lie group of transformations $G \times X \rightarrow X$, which essentially depends on the action because infinitesimal generators are needed, is locally isomorphic to the linear gauge sequence which does not depend on the action any longer as it is the tensor product of the Poincaré sequence by the Lie algebra $\mathcal{G}$ of G .

The main idea will be to introduce and compare the three Lie groups of transformations: The Poincaré group of transformations with 10 parameters leading to the Killing system R_2 :

$$\Omega_{ij} \equiv (L(\xi_1)\omega)_{ij} \equiv \omega_{rj}(x)\xi^r_i + \omega_{ir}(x)\xi^r_j + \xi^r \partial_r \omega_{ij}(x) = 0$$

$$\Gamma^k_{ij} \equiv (L(\xi_2)\gamma)^k_{ij} \equiv \xi^k_{ij} + \gamma^k_{rj}(x)\xi^r_i + \gamma^k_{ir}(x)\xi^r_j - \gamma^r_{ij}(x)\xi^k_r + \xi^r \partial_r \gamma^k_{ij}(x) = 0$$

The Weyl group of transformations with 11 parameters leading to the Weyl system $\tilde{R}_2$.

$$\Omega_{ij} \equiv \omega_{rj}(x)\xi^r_i + \omega_{ir}(x)\xi^r_j + \xi^r \partial_r \omega_{ij}(x) = 2\Lambda(x)\omega_{ij}(x)$$

$$\begin{aligned}\Gamma^k_{ij} &\equiv \xi^k_{ij} + \gamma^k_{rj}(x)\xi^r_i + \gamma^k_{ir}(x)\xi^r_j - \gamma^r_{ij}(x)\xi^k_r + \xi^r \partial_r \gamma^k_{ij}(x) \\ &= 0\end{aligned}$$

The conformal group of transformations with 15 parameters (4 translations $^{+6}$ rotations + 1 dilatation $^{+4}$ elations) leading to the conformal Killing system $\hat{R}_2$:

$$\Omega_{ij} \equiv \omega_{rj}(x)\xi^r_i + \omega_{ir}(x)\xi^r_j + \xi^r \partial_r \omega_{ij}(x) = 2\Lambda(x)\omega_{ij}(x)$$

$$\begin{aligned}\Gamma^k_{ij} &\equiv \xi^k_{ij} + \gamma^k_{rj}(x)\xi^r_i + \gamma^k_{ir}(x)\xi^r_j - \gamma^r_{ij}(x)\xi^k_r + \xi^r \partial_r \gamma^k_{ij}(x) \\ &= \delta^k_i \Lambda_j(x) + \delta^k_j \Lambda_i(x) - \omega_{ij}(x)\omega^{kr}(x)\Lambda_r(x)\end{aligned}$$

where one has to eliminate the arbitrary function $\Lambda(x)$ and 1-form $\Lambda_i(x)dx^i$ for finding sections, replacing the ordinary Lie derivative $\mathcal{L}(\xi)$ by the formal Lie derivative $L(\xi_q)$, that is replacing $j_q(\xi)$ by ξ_q when needed. When $n=4$, $\hat{R}_2$ is FI but $\hat{g}_2$ is only 2-acyclic while $\hat{g}_3=0$ and we have for the involutive $\hat{R}_3 \simeq \hat{R}_2$ (See [26] for details and counterexamples):

$$
\begin{array}{ccccccccccccccc}
 & & & & 0 & & 0 & & 0 & & 0 & & 0 & & \\
 & & & & \downarrow & & \downarrow & & \downarrow & & \downarrow & & \downarrow & & \\
 & 0 & \rightarrow & \hat{\Theta} & \xrightarrow{j_3} & 15 & \xrightarrow{d_1} & 60 & \xrightarrow{d_2} & 90 & \xrightarrow{d_3} & 60 & \xrightarrow{d_4} & 15 & \rightarrow 0 \\
 & & & & \downarrow & & \downarrow & & \downarrow & & \downarrow & & \downarrow & & \\
 & 0 & \rightarrow & 4 & \underset{3}{\xrightarrow{j_3}} & 140 & \xrightarrow{d_1} & 420 & \xrightarrow{d_2} & 504 & \xrightarrow{d_3} & 280 & \xrightarrow{d_4} & 60 & \rightarrow 0 \\
 & & & \| & & \downarrow \Phi_0 & & \downarrow \Phi_1 & & \downarrow \Phi_2 & & \downarrow \Phi_3 & & \downarrow \Phi_4 & \\
0 \rightarrow & \hat{\Theta} & \rightarrow & 4 & \underset{3}{\xrightarrow{\hat{D}}} & 125 & \underset{1}{\xrightarrow{\hat{D}_1}} & 360 & \underset{1}{\xrightarrow{\hat{D}_2}} & 414 & \underset{1}{\xrightarrow{\hat{D}_3}} & 220 & \underset{1}{\xrightarrow{\hat{D}_4}} & 45 & \rightarrow 0 \\
 & & & & & \downarrow & & \downarrow & & \downarrow & & \downarrow & & \downarrow & \\
 & & & & & 0 & & 0 & & 0 & & 0 & & 0 &
\end{array}
$$

The top Spencer sequence is the tensor product of the Poincaré sequence by the Lie algebra $\hat{\mathcal{G}}$ of dimension 15 and we may use the inclusions $R_2 \subset \bar{R}_2 \subset \hat{R}_2 \subset J_2(T)$ with $10 < 11 < 15 < 60$. Working by induction, the minimum formally exact resolution on the jet level is:

$$0 \longrightarrow \hat{\Theta} \longrightarrow 4 \longrightarrow 9 \longrightarrow 10 \longrightarrow 9 \longrightarrow 4 \longrightarrow 0$$

with "up and down" orders that must be compared to the above canonical Janet sequence. Of course, finding such numbers can be done by means of computer algebra (arXiv: 1603.05030) or through combinatorics (exercise !) but it will never prove that such a sequence is formally exact as it will involve enormous matrices (up to 840 x 1134 !!!) and cannot be achieved without the help of the Spencer δ -cohomology, still never introduced in GR or conformal geometry [20, 26].

When ω is the M metric, it follows that $\gamma=0$ and we obtain therefore:

$$X^r_{j,i} - X^r_{ri,j} = (\partial_i \xi^r_{rj} - \xi^r_{rij}) - (\partial_j \xi^r_{ri} - \xi^r_{rij}) = \partial_i \xi^r_{rj} - \partial_j \xi^r_{ri} = n\left(\partial_i \Lambda_j - \partial_j \Lambda_i\right))$$

Dividing by n , we may thus obtain $(F_{ij} = \partial_i \Lambda_j - \partial_j \Lambda_i) \in \wedge^2 T^*$ from $X^r_{rj,i} \in T^* \otimes \hat{g}_2 \subset C_1$ with $dF=0$ because $\hat{g}_3=0$ and thus $\xi^k_{rij}=0$ in $S_3T^* \otimes T$.

This result is solving the dream of H . Weyl for exhibiting the conformal origin of electromagnetism in [22]. It is however completely contradicting the standard approach of classical gauge theory based on the group $U(1)$ which is not acting on space-time. In addition, the EM field F is a section of the first Spencer bundle C_1 in the image of D_1 because $(\Lambda, \Lambda_i) \in C_0 = \hat{R}_3 \simeq \hat{R}_2$.

We apply the linearization procedure to the Riemann tensor:

$$\rho = (\rho^k_{l,ij} = \partial_i \gamma^k_{lj} - \partial_j \gamma^k_{li} + \gamma^r_{lj}\gamma^k_{ri} - \gamma^r_{li}\gamma^k_{rj}) \in \Lambda^2 T^* \otimes T^* \otimes T$$

Now, as the linearization $\Gamma \in S_2T^* \otimes T$ of γ is a tensor, the linearization R of ρ becomes:

$$R^k_{l,ij} = d_i \Gamma^k_{lj} - d_j \Gamma^k_{li} + \gamma^r_{lj}\Gamma^k_{ri} - \gamma^r_{li}\Gamma^k_{rj} + \gamma^k_{ri}\Gamma^r_{lj} - \gamma^k_{rj}\Gamma^r_{li}$$

If ∇ is the covariant derivative, we have $\nabla_r \omega_{ij} = \partial_r \omega_{ij} - \gamma^s_{ir}\omega_{sj} - \gamma^s_{jr}\omega_{is} = 0$ and we may move down the index k . Then, using r as a dumb index, we may consider the first order equations:

$$(L(\xi_1)\rho)_{kl,ij} \equiv R_{kl,ij} \equiv \rho_{rl,ij}\xi^r_k + \rho_{kr,ij}\xi^r_l + \rho_{kl,rj}\xi^r_i + \rho_{kl,ir}\xi^r_j + \xi^r \partial_r \rho_{kl,ij} = 0$$

that can be considered as an infinitesimal first order variation of ρ . As for the Ricci tensor $(\rho_{ij}) \in S_2T^*$, we notice that $\rho_{ij} = \rho^r_{i,rj} = 0 \Rightarrow R_{ij} \equiv \rho_{rj}\xi^r_i + \rho_{ir}\xi^r_j + \xi^r \partial_r \rho_{ij} = 0$. Using now a cyclic sums on (ijr) , the Bianchi identities are:

$$\beta_{kl,ijr} \equiv \nabla_r \rho_{kl,ij} + \nabla_i \rho_{kl,jr} + \nabla_j \rho_{kl,ri} = 0 \qquad \Leftrightarrow \qquad \beta \equiv \sum_{cycl} (\partial\rho - \gamma\rho) = 0$$

Their linearizations $B_{kl,ijr}=0$ are sections of the vector bundle F_2 in the short exact sequence:

$$0 \rightarrow F_2 \rightarrow \wedge^3 T^* \otimes g_1 \xrightarrow{\delta} \wedge^4 T^* \otimes T \rightarrow 0$$

$$\begin{aligned}
\dim(F_2) &= \left(\frac{n(n-1)(n-2)}{6}\right)\left(\frac{n(n-1)}{2}\right) - \left(\frac{n(n-1)(n-2)(n-3)}{24}\right)n \\
&= \frac{n^2(n^2-1)(n-2)}{24}
\end{aligned}$$

because $dim(g_1) = n(n-1)/2$ for any nondegenerate metric, that is $24-4=20$ when $n=4$. Such results cannot be even imagined by somebody not aware of the δ -cohomology [30-32].

We have the linearized cyclic sums of covariant derivatives both with their respective symbolic descriptions, not to be confused with the non-linear corresponding ones:

$$\begin{aligned} B_{kl,rij} &\equiv \nabla_r R_{kl,ij} + \nabla_i R_{kl,jr} + \nabla_j R_{kl,ri} \\ &= 0 \quad \mathrm{mod}\ (\Gamma) \\ &\Leftrightarrow \frac{\Sigma}{\mathrm{cycl}}(dR - \gamma R - \rho\Gamma) = 0 \end{aligned}$$

We have thus $\omega \longrightarrow \gamma \longrightarrow \rho \longrightarrow \beta$ and the respective linearizations $\Omega \longrightarrow \Gamma \longrightarrow R \longrightarrow B$.

3.4 Einstein Versus Weyl

It remains to prove that, in this new framework, the Ricci tensor only depends on the symbol $\hat{g}_2 \simeq T^* \subset S_2T^*\otimes T$ deroonation $\hat{R}_2 \subset J_2(T)\, \hat{R}_1 \subset J_1(T)$ $\hat{g}_1 \subset T^*\otimes T \quad \omega_{rj}\xi^r_i + \omega_{ir}\xi^r_j - \frac{2}{n}\omega_{ij}\xi^r_r = 0$ ing on any conformal factor. The next commutative diagram covers both situations, taking into account that the equations of both the classical and conformal Killing operator are homogeneous. The purely algebraic Spencer map $\delta : g_{q+1}T^* \otimes g_q$ with symbol $g_q = R_q \cap S_qT^* \otimes E \subset J_q(E)$ is induced by $-d$ and all the sequences are exact by definition but perhaps the left column:

$$\begin{array}{cccccccc}
 & 0 & & 0 & & 0 & & \\
 & \downarrow & & \downarrow & & \downarrow & & \\
0 \rightarrow & g_3 & \rightarrow & S_3T^* \otimes T & \rightarrow & S_2T^* \otimes F_0 & \rightarrow F_1 \rightarrow 0 \\
 & \downarrow \delta & & \downarrow \delta & & \downarrow \delta & & \\
0 \rightarrow & T^* \otimes g_2 & \rightarrow & T^* \otimes S_2T^* \otimes T & \rightarrow & T^* \otimes T^* \otimes F_0 & \rightarrow 0 \\
 & \downarrow \delta & & \downarrow \delta & & \downarrow \delta & & \\
0 \rightarrow & \boxed{\wedge^2T^* \otimes g_1} & \rightarrow & \wedge^2T^* \otimes T^* \otimes T & \rightarrow & \wedge^2T^* \otimes F_0 & \rightarrow 0 \\
 & \downarrow \delta & & \downarrow \delta & & \downarrow & & \\
0 \rightarrow & \wedge^3T^* \otimes T & = & \wedge^3T^* \otimes T & \rightarrow & 0 & & \\
 & \downarrow & & \downarrow & & & & \\
 & 0 & & 0 & & & &
\end{array}$$

Chasing in this diagram, we discover that F_1 is just the cohomology $H^2_1(g_1)$ of the first vertical column at $\wedge^2T^* \otimes g_1$ that is the quotient of the cocycle bundle $Z^2_1(g_1)$ kernel of the map $\delta : \wedge^{\cdot 2}T^* \otimes g_1 \wedge^3 T^* \otimes T$ by the coboundary bundle $B^2_1(g_1)$ image of the map $\delta : T^* \otimes g_2\wedge^2 \otimes g_1$. Needless to say that such mathematical methods have never been used in the stuy of classical or conformal Riemannian geometry and the reason for which the reader will never find other references in the mathematical or physical literature (!).

THEOREM 3.D.1: Introducing the δ -cohomology bundles $Riemann = H^2_1(g_1)$ at $\wedge^2T^* \otimes g_1$ and $Weyl = H^2_1(\hat{g}_1)$ at $\wedge^2T^* \otimes \hat{g}_1$ while taking into account that $g_1 \subset \hat{g}_1$, $g_2 = 0\, \hat{g}_2 \simeq T^*$ and $\hat{g}^3 = 0$, we have the commutative and exact " fundamental diagram II " found in 1983 [30]:

$$
\begin{array}{ccccccccccc}
 & & & & & & & & 0 & & \\
 & & & & & & & & \downarrow & & \\
 & & & & & & 0 & & Ricci & & \\
 & & & & & & \downarrow & & \downarrow & & \\
 & & & & 0 & \longrightarrow & Z_1^2(g_1) & \longrightarrow & Riemann & \longrightarrow & 0 \\
 & & & & \downarrow & & \downarrow & & \downarrow & & \\
 & & 0 & \longrightarrow & T^* \otimes \hat{g}_2 & \stackrel{\delta}{\longrightarrow} & Z_1^2(\hat{g}_1) & \longrightarrow & Weyl & \longrightarrow & 0 \\
 & & & & \downarrow & & \downarrow & & \downarrow & & \\
0 & \longrightarrow & S_2T^* & \stackrel{\delta}{\longrightarrow} & T^* \otimes T^* & \stackrel{\delta}{\longrightarrow} & \wedge^2 T^* & \longrightarrow & 0 & & \\
 & & & & \downarrow & & \downarrow & & & &
\end{array}
$$

The splitting sequence $0 \rightarrow Ricci \rightarrow Riemann \rightarrow Weyl \rightarrow 0$ provides an unusual interpretation of the successive Ricci, Riemann and Weyl tensor bundles. Similarly, the well known splitting sequence $0 \rightarrow S_2T^* \stackrel{\delta}{\rightarrow} T^* \otimes T^* \stackrel{\delta}{\rightarrow} \wedge^2 T^* \rightarrow 0$ provides an unusual conformal interpretation of the EM field $F = (F_{ij} = -F_{ji}) \in \wedge^2 T^*$ in a coherent way with the tentative of H. Weyl in 1918 [22].

$$
\begin{aligned}
\dim(\text{Riemann}) - \dim(\text{Weyl}) &= \frac{n^2(n^2-1)}{12} - \frac{n(n+1)(n+2)(n-3)}{12} \\
&= \frac{n(n+1)}{2} \\
&= \dim(\text{Ricci})
\end{aligned}
$$

and the Weyl operator is of order 3 when $n = 3$ but of order 2 when $n \geq 4$, a result still neither known but nor even acknowledged today (See arXiv: 1603.05030 for a computer algebra checking by my former PhD student A. Quadrat and [31]). We finally point out that the Bianchi-type operator is of order 2 when $n = 4$ but of order 1 when $n = 5$ (See [26] for more details).

3.5 Applications

Before comparing the Minkowski, Schwarzschild and Kerr metrics as in [13] while comparing to [14], we point out the purely mathematical fact explaining why gravitational waves and black holes cannot exist, not because of an experimental problem of detection but because of a structural problem of equation. Indeed, introducing the Ricci tensor $\rho_{ij} = \rho^r_{i,rj} = \rho_{ji}$ as a linear combination of the second order derivatives of the metric ω , we may linearize it over the locally constant Euclidean or Minkowskian metric in order to obtain a second order linear homogeneous Ricci operator $S_2T^* \rightarrow S_2T^* : (\Omega_{ij}) \rightarrow (R_{ij})$ with 4 terms along the formula:

$$2R_{ij} = \omega^{rs}(d_{rs}\Omega_{ij} + d_{ij}\Omega_{rs} - d_{ri}\Omega_{sj} - d_{sj}\Omega_{ri}) = 2R_{ji}$$

which is also valid when $n = 2$ with $2R_{11} = 2R_{22} = d_{11}\Omega_{22} + d_{22}\Omega_{11} - 2d_{12}\Omega_{12}$ and $R_{12} = 0$. Such a result is showing that the important object is not the Riemann tensor or the Einstein tensor but the Ricci tensor according to the previous fundamental diagram II. We obtain therefore:

THEOREM 4.1: The so-called defining equations of the gravitational waves that can be found in any textbook of general relativity like [19], are nothing else that the adjoint of the Ricci operator which is parametrizing the $Cauchy = ad(Killing)$ operator but is going " backwards", that is from right to left as we saw in the Introduction.

Proof. Introducing the test functions $\lambda^{ij} = \lambda^{ji}$, we get:

$$\lambda^{ij}R_{ij} = \omega^{rs}\lambda^{ij}(d_{rs}\Omega_{ij} + d_{ij}\Omega_{rs} - d_{ri}\Omega_{sj} - d_{sj}\Omega_{ri})$$

Integrating by parts while setting as usual $\Pi = \omega^{ij}d_{ij}$ for the Dalembert operator and exchanging the dumb indices, we get for the adjoint operator:

$$\boxed{\omega^{ij}d_{ij}\lambda^{rs} + \omega^{rs}d_{ij}\lambda^{ij} - \omega^{sj}d_{ij}\lambda^{ri} - \omega^{ri}d_{ij}\lambda^{sj} = \sigma^{rs}}$$

that is exactly the equations of the gravitational waves leading to the Cauchy identities:

$$d_r\sigma^{rs} \equiv \omega^{ij}d_{rij}\lambda^{rs} + \omega^{rs}d_{rij}\lambda^{ij} - \omega^{sj}d_{rij}\lambda^{ri} - \omega^{ri}d_{rij}\lambda^{sj} = 0$$

There is absolutely no need to set $d_i\lambda^{ij} = 0$ and we obtain the adjoint sequences when $n = 4$.

$$\begin{array}{ccccccc} & & 4 & \xrightarrow{Killing} & 10 & \xrightarrow{Ricci} & 10 \\ 0 & \leftarrow & 4 & \xleftarrow{Cauchy} & 10 & \xleftarrow{ad(Ricci)} & 10 \end{array}$$

without any reference to the Bianchi operator and the induced div operator or even to the Einstein operator. Hence, gravitational waves cannot exist, not for a problem of detection but for a problem of equation, as we have only obtained " a " parametrization of the Cauchy operator which is not even minimum but we can find a minimum one by keeping only λ_{ij} with $i < j$ as in [18]. Indeed, we have already obtained another parametrization with 20 test functions by using the $Beltrami = ad(Riemann)$ operator in the Introduction with $n = 4$, a result proving that the Cauchy operator can be parametrized. For the advanced reader, this intrinsic structural fact means that the differential module defined by the Cauchy operator is torsion-free [4]. We finally point out that the Airy, Beltrami or Einstein parametrizations are not responsible for earthquakes as there is no relation between the test functions λ and the deformation Ω of the metric ω , even if $n = 2$ as we saw with $\lambda^{ij}R_{ij} = \phi(d_{11}\Omega_{22} + d_{22}\Omega_{11} - 2d_{12}\Omega_{12})$ and Airy function ϕ . We also point out that the differential module defined by the Riemann or Ricci operator has a nonzero torsion submodule generated by the 10 components of the Weyl tensor which are separately killed by the Dalembert operator.

In the case of the Killing operator for the Minkowski metric, according to H. Poincaré, the geometrical and adjoint physical long exact differential sequences of operators acting on tensors, giving order of operators and number of components, are exactly the ones we have presented in the Introduction for various dimensions n . The main problem is that the corresponding Killing operators and systems for the M, S or (worst !) K metrics are not involutive and not even formally integrable, a key problem because the Janet sequences cannot be easily constructed. Hence, our main target will be to apply the PP procedure in each case, a difficult task indeed.

As we know that the corresponding Spencer sequence is isomorphic to the tensor product of the Poincaré differential sequence for the exterior derivative by a Lie algebra of dimension $n(n+1)/2$, its adjoint sequence is also exact, the reason for which the physical sequence is also exact, that is each operator is generating the CC of the previous one. In particular, the $Cauchy = ad(Killing)$ operator generates the CC of the $Beltrami = ad(Riemann)$ operator which generates the CC of the $Lanczos = ad(Bianchi)$ operator. We have proved in many recent publications that this result cannot be extended easily to the conformal situation because the acyclicity properties of the symbols highly depend on the dimension n and order q [31]. It thus remains to study the cases of the Schwarzschild and Kerr metrics, a much more delicate problem.

EXAMPLE 4.2: (Kerr metric) We now write the Kerr metric in Boyer-Lindquist coordinates (t, r, θ, ϕ) .

$$\omega = \frac{\rho^2 - mr}{\rho^2}\, dt^2 - \frac{\rho^2}{\Delta}\, dr^2 - \rho^2\, d\theta^2 - \frac{2amr\sin^2\theta}{\rho^2}\, dt\, d\phi - \left(r^2 + a^2 + \frac{mra^2\sin^2\theta}{\rho^2}\right)\sin^2\theta\, d\phi^2$$

where we have set $\Delta = r^2 - mr + a^2$ and $\rho^2 = r^2 + a^2cos^2(\theta)$ as usual and we recover the S-metric when $a = 0$ with $A(r) = 1 - \frac{m}{r}$:

$$\omega = A(r)dt^2 - (1/A(r))dr^2 - r^2d\theta^2 - r^2sin^2(\theta)d\phi$$

We notice that t or ϕ do not appear in the coefficients of the metric. We shall change the coordinate system in order to confirm these results by using computer algebra. The idea is to use the so-called " rational polynomial " coefficients as follows with $c = cos(\theta) \Rightarrow dc = -sin(\theta)d\theta \Rightarrow dc^2 = (1 - c^2)d\theta^2$ and set $x^0 = t$, $x^1 = r$, $x^2 = c = cos(\theta)$, $x^3 = \phi$). We obtain over the differential field $K = \mathbb{Q}(a, m)(t, r, c, \phi)$:

$$\omega = \frac{\rho^2 - mr}{\rho^2}\, dt^2 - \frac{\rho^2}{\Delta}\, dr^2 - \frac{\rho^2}{1-c^2}\, dc^2 - \frac{2amr(1-c^2)}{\rho^2}\, dt\, d\phi - (1-c^2)\left(r^2 + a^2 + \frac{ma^2r(1-c^2)}{\rho^2}\right) d\phi^2$$

with now $\Delta = r^2 - mr + a^2$ and $\rho^2 = r^2 + a^2c^2$ and we have $det(\omega) = -(r^2 + a^2c^2)^2$ in a coherent way with the fact that the S metric that can be written in the new system of coordinates:

$$\omega = A(r)dt^2 - \frac{1}{A(r)}dr^2 + \frac{r^2}{(1-c^2)}dc^2 - r^2(1-c^2)d\phi^2$$

Looking at the symbol $g_1 \subset T^* \otimes T$, elementary linear combinatorics allow to prove [18, 22]:

$$\omega_{33}\xi^3_3 + \omega_{03}\xi^0_3 = 0\ mod(\xi), \omega_{33}\xi^3_0 + \omega_{00}\xi^0_3 = 0\ mod(\xi), \omega_{33}\xi^0_0 - \omega_{03}\xi^0_3 = 0\ mod(\xi),$$

Then, multiplying Ω_{22} by ω_{11} , Ω_{11} by ω_{22} and adding, we finally obtain:

$$2(\omega_{11}\omega_{22})(\xi^1_1 + \xi^2_2) + \xi\partial(\omega_{11}\omega_{22}) = 0$$

However, we have also successively:

$$\left\{\begin{array}{lll} R_{03,03} & \equiv & 2\rho_{03,03}(\xi^0_0 + \xi^3_3) + \xi\partial\rho_{03,03} = 0 \\ R_{12,12} & \equiv & 2\rho_{12,12}(\xi^1_1 + \xi^2_2) + \xi\partial\rho_{12,12} = 0 \\ R_{01,23} & \equiv & \rho_{01,23}(\xi^0_0 + \xi^1_1 + \xi^2_2 + \xi^3_3) + \xi\partial\rho_{01,23} = 0 \end{array}\right.$$

Now, the coefficients of the metric are rational functions in K and the various geometric objects appearing in $\omega\gamma\rho$ can be obtained through the rules of differential algebra. It is thus possible to obtain the 13 non-zero components of the Riemann tensor for the Kerr metric according to K. R. Koehler in (http://kias.dyndns.org/crg/blackhole.html) by adding factorizations as follows: We shall distinguish the 6 non-vanishing components:

$$\left\{\begin{array}{lcl} \rho_{01,01} & = & -\frac{mr(2(r^2-mr+a^2)+a^2(1-c^2))(r^2-3a^2c^2)}{2(r^2+a^2c^2)^3(r^2-mr+a^2)} \\ \rho_{02,02} & = & \frac{mr(r^2-mr+a^2+2a^2(1-c^2))(r^2-3a^2c^2)}{2(1-c^2)(r^2+a^2c^2)^3} \\ \rho_{03,03} & = & \frac{mr(1-c^2)(r^2-mr+a^2)(r^2-3a^2c^2)}{2(r^2+a^2c^2)^3} \\ \rho_{12,12} & = & -\frac{mr(r^2-3a^2c^2)}{2(1-c^2)(r^2+a^2c^2)(r^2-mr+a^2)} \\ \rho_{13,13} & = & -\frac{(1-c^2)mr(r^4-2a^2c^2r^2+4a^2r^2-2a^4c^2+3a^4-2a^2mr(1-c^2))(r^2-3a^2c^2)}{2(r^2+a^2c^2)^3(r^2-mr+a^2)} \\ \rho_{23,23} & = & \frac{mr(2r^4-a^2c^2r^2+5a^2r^2-a^4c^2+3a^4-a^2mr(1-c^2))(r^2-3a^2c^2)}{2(r^2+a^2c^2)^3} \end{array}\right.$$

from the 7 components that are vanishing when $a=0$.

$$\left\{\begin{array}{lcl} \rho_{01,23} & = & \frac{amc(2r^2-a^2c^2+3a^2)(3r^2-a^2c^2)}{2(r^2+a^2c^2)^3} \\ \rho_{02,31} & = & -\frac{amc(r^2-2a^2c^2+3a^2)(3r^2-a^2c^2)}{2(r^2+a^2c^2)^3} \\ \rho_{03,12} & = & -\frac{amc(3r^2-a^2c^2)}{2(r^2+a^2c^2)^2} \\ \rho_{02,10} & = & \frac{3a^2mc(3r^2-a^2c^2)}{2(r^2+a^2c^2)^3} \\ \rho_{02,32} & = & \frac{amr(3r^2-mr+3a^2)(r^2-3a^2c^2)}{2(r^2+a^2c^2)^3} \\ \rho_{13,23} & = & -\frac{3a^2mc(1-c^2)(r^2+a^2)(3r^2-a^2c^2)}{2(r^2+a^2c^2)^3} \\ \rho_{01,13} & = & \frac{amr(1-c^2)(3r^2+3a^2-2mr)(r^2-3a^2c^2)}{2(r^2+a^2c^2)^3(r^2-mr+a^2)} \end{array}\right.$$

We have finally to add the 8 vanishing components:

$$\rho_{01,03}=0, \quad \rho_{01,12}=0, \quad \rho_{02,03}=0, \quad \rho_{02,12}=0,$$
$$\rho_{03,13}=0, \quad \rho_{03,23}=0, \quad \rho_{12,13}=0, \quad \rho_{12,23}=0.$$

In fact, as the Riemann tensor has $n^2(n^2-1)/12$ components, that is 20 when $n=4$, we have to take into account the only identity:

$$\rho_{01,23}+\rho_{02,31}+\rho_{03,12}=0 \Rightarrow R_{01,23}+R_{02,31}+R_{03,12}=0$$

We obtain therefore $\xi\partial(\rho_{12,12}/(\omega_{11}\omega_{22})) = 0$ but we have also $\xi\partial(\rho_{03,03}\rho_{12,12}/det(\omega)) = 0$.
The following invariants are obtained successively in a coherent way:

$$\omega_{11}\omega_{22} = \frac{(r^2+a^2c^2)^2}{(1-c^2)(r^2-mr+a^2)} \Rightarrow \mid \rho_{12,12} \mid /(\omega_{11}\omega_{22}) = \frac{mr(r^2-3a^2c^2)}{2(r^2+a^2c^2)^3}$$

Also, as $a \in K$, then $\rho_{01,23}$ and $\rho_{02,13}$ can be both divided by a and we get the new invariant:

$$\rho_{01,23}/\rho_{03,12} = \frac{2r^2-a^2c^2+3a^2}{r^2+a^2c^2}$$

These results are leading to $\xi^1 = 0, \xi^2 = 0$, thus to $\xi_1^1 = 0, \xi_2^2 = 0$ and $\xi_0^0 + \xi_3^3 = 0$ after substitution in the equations defining the first order symbol g_1 of R_1 .

In the case of the S-metric with $a = 0$, the previous division has no meaning and we have only $\xi_1 = 0$ as the only equation of zero order.

Let us now introduce the new equation:

$$R_{01,13} \equiv \rho_{01,13}(\xi_0^0 + 2\xi_1^1 + \xi_3^3) - \rho_{13,13}\xi_0^3 - \rho_{01,01}\xi_3^0 + (\rho_{01,23}+\rho_{02,13})\xi_1^2 = 0$$

As we have $\xi_0^0 + \xi_3^3 = 0$ and $\xi_1^1 = 0$, we obtain therefore a linear equation of the form:

$$\rho_{13,13}\xi_0^3 + \rho_{01,01}\xi_3^0 - (\rho_{01,23}+\rho_{02,13})\xi_1^2 = 0$$

Similarly, we have also:

$$R_{01,02} \equiv \rho_{01,02}(2\xi_0^0 + \xi_1^1 + \xi_2^2) - (\rho_{01,23}+\rho_{02,13})\xi_0^3 + \rho_{01,01}\xi_2^1 + \rho_{02,02}\xi_1^2 = 0$$

and we obtain therefore a linear equation of the form:

$$2\rho_{01,02}\xi_0^0 - (\rho_{01,23}+\rho_{02,13})\xi_0^3 + \rho_{01,01}\xi_2^1 + \rho_{02,02}\xi_1^2 = 0$$

In the case of the S-metric, that is when $a = 0$, we obtain respectively $\xi_3^0 = 0$ and $\xi_2^1 = 0$ as in [18] because $\xi_0^0 \simeq \xi_3^0$ The previous linear system has thus a rank equal to 2 and we obtain therefore because $\xi_0^3 \simeq \xi_3^0, \xi_1^2 \simeq \xi_2^1$.

$$\xi_3^0 = 0, \xi_2^1 = 0, \Leftrightarrow \xi_0^3 = 0, \xi_1^2 = 0, \xi_0^0 = 0, \xi_3^3 = 0$$

It remains to study the following 4 linear equations, namely [13]:

$$R_{01,03} = 0,\ R_{03,23} = 0,\ R_{03,13} = 0,\ R_{02,03} = 0$$

The rank of the previous system with respect to the 4 jet coordinates $(\xi_0^1, \xi_0^2, \xi_3^1, \xi_3^2)$ is equal to 2, for both the S and K-metrics thanks to the two striking identities:

$$R_{03,13} + a(1-c^2)R_{01,03} = 0, \quad R_{02,03} + \frac{a}{(r^2+a^2)}R_{03,23} = 0$$

Two prolongations only provide 6 additional equations of order one that we provide in the following list which is obtained $mod(j_2(\Omega))$, namely:

$$\xi^1 = 0, \xi^2 = 0, \xi_2^1 = 0, \xi_3^0 = 0, \xi_3^1 + lin(\xi_0^1, \xi_0^2) = 0, \xi_3^2 + lin(\xi_0^1, \xi_0^2)$$

We have therefore obtained the inclusion of Lie algebroids $R_1^{(2)} \subset R_1^{(1)} = R_1 \subset J_1(T)$ with respective dimensions $4 < 10 = 10 < 20$. Using the standard $ker - coker$ long exaxt sequence of prolongations:

$$\boxed{0 \rightarrow R_3 \rightarrow J_3(T) \rightarrow J_3(S_2T^*) \rightarrow Q_2 \rightarrow 0, \quad 0 \rightarrow 4 \rightarrow 140 \rightarrow 150 \rightarrow 14 \rightarrow 0}$$

we discover that the initial Killing system for the Kerr metric has 14 compatibility conditions of second order contrary to the 20 existing for the Minkowski metric. Such a result has been obtained totally independently of any specific GR technical object like the Teukolski scalars or the Killing-Yano tensors introduced in [14, 15]. However, this system is not involutive because its symbol is finite type but non-zero.

Using one more prolongation, all the sections (care again) vanish but ξ^0 and ξ^3 , a result leading to $dim(R_1^{(3)}) = 2$ in a coherent way with the only nonzero Killing vectors $\{\partial_t, \partial_\phi\}$. We have indeed:

$$\xi_0^1 = 0\ \xi_0^2 = 0 \Big| \Leftrightarrow \xi_3^1 = 0,\ \xi_3^2 = 0 \Rightarrow \xi_1^0 = 0,\ \xi_1^0 = 0,\ \xi_2^0 = 0,\ \xi_2^3 = 0$$

Taking therefore into account that the metric only depends on ($x^1 = r, x^2 = cos(\theta)$) we obtain after three prolongations the inclusions of first order systems:

$$R_1^{(3)} \subset R_1^{(2)} \subset R_1^{(1)} = R_1 \subset J_1(T) \Leftrightarrow 2 < 4 < 10 = 10 < 20$$

Surprisingly and contrary to the situation found for the S metric, we have now an involutive first order system with only solutions ($\xi^0 = cst, \xi^1 = 0, \xi^2 = 0, \xi^3 = cst$) and notice that $R_1^{(3)}$ does not depend any longer on the parameters $(m, a) \in K$. The difficulty is to know what second members must be used along the procedure met for all the motivating examples, in particular we have again identities to zero like $d_0\xi^1 - \xi_0^1 = 0, d_0\xi^2 - \xi_0^2 = 0$.

We finally obtain 14 second order generating CC and their prolongations as we already said but also 6 third order CC coming from the 6 following components of the Spencer operator, namely:

$$d_1\xi^1 - \xi^1_1 = 0, \quad d_2\xi^1 - \xi^1_2 = 0, \quad d_3\xi^1 - \xi^1_3 = 0,$$
$$d_1\xi^2 - \xi^2_1 = 0, \quad d_2\xi^2 - \xi^2_2 = 0, \quad d_3\xi^2 - \xi^2_3 = 0.$$

a result that cannot be even imagined from [14]. Of course, proceeding like in the motivating examples, we must substitute in the right members the values obtained from $j_2(\Omega)$ and set for example $\xi^1_1 = -\frac{1}{2\omega_{11}}\xi^r\partial_r\omega_{11}$ while replacing ξ^1 and ξ^2 by the corresponding linear combinations of the Riemann tensor already obtained for the right members of the two zero order equations. The corresponding Fundamental Diagram I is no longer depending on (m, a) as follows:

$$\begin{array}{ccccccccccccccc}
 & & & & 0 & & 0 & & 0 & & 0 & & 0 & & \\
 & & & & \downarrow & & \downarrow & & \downarrow & & \downarrow & & \downarrow & & \\
 & 0 & \rightarrow & \Theta & \stackrel{j_1}{\rightarrow} & 2 & \stackrel{D_1}{\rightarrow} & 8 & \stackrel{D_2}{\rightarrow} & 12 & \stackrel{D_3}{\rightarrow} & 8 & \stackrel{D_4}{\rightarrow} & 2 & \rightarrow 0 \\
 & & & & \downarrow & & \downarrow & & \downarrow & & \downarrow & & \downarrow & & \\
 & 0 & \rightarrow & 4 & \stackrel{j_1}{\rightarrow} & 20 & \stackrel{D_1}{\rightarrow} & 40 & \stackrel{D_2}{\rightarrow} & 40 & \stackrel{D_3}{\rightarrow} & 20 & \stackrel{D_4}{\rightarrow} & 4 & \rightarrow 0 \\
 & & & \| & & \downarrow & & \downarrow & & \downarrow & & \downarrow & & \downarrow & \\
0 \rightarrow & \Theta & \rightarrow & 4 & \stackrel{D}{\rightarrow} & 18 & \stackrel{D_1}{\rightarrow} & 32 & \stackrel{D_2}{\rightarrow} & 28 & \stackrel{D_3}{\rightarrow} & 12 & \stackrel{D_4}{\rightarrow} & 2 & \rightarrow 0 \\
 & & & & & \downarrow & & \downarrow & & \downarrow & & \downarrow & & \downarrow & \\
 & & & & & 0 & & 0 & & 0 & & 0 & & 0 &
\end{array}$$

with the Euler-Poincaré characteristic $4 - 18 + 32 - 28 + 12 - 2 = 0$. However, the only intrinsic concepts associated with a differential sequence are the " extension modules " that only depend on the Kerr differential module but not on the differential sequence and we repeat once more that: THE ONLY IMPORTANT CONCEPT IS THE GROUP INVOLVED, NOT THE METRIC. Needless to say that the group involved in this case has no physical usefulness.

EXAMPLE 4.3: (Schwarzschild metric) According to what we said, the situation of the Schwarzschild metric is much simpler when $a = 0$ with only six non-zero components of the Riemannn tensor:

$$\begin{array}{lcl}
\rho_{01,01} & = & -\frac{m}{r^2(r-m)} \\
\rho_{02,02} & = & \frac{m}{2r} \\
\rho_{03,03} & = & \frac{m(1-c^2)}{2r} \\
\rho_{12,12} & = & -\frac{m}{2(r-m)} \\
\rho_{13,13} & = & -\frac{m(1-c^2)}{2(r-m)} \\
\rho_{23,23} & = & mr(1-c^2)
\end{array}$$

We have now the inclusions of algebroids:

$$R_1^{(3)} \subset R_1^{(2)} \subset R_1^{(1)} = R_1 \subset J_1(T) 4 < 5 < 10 = 10 < 20$$

The subsystem $R_1^{(2)}$ is def by g the 5 nest rd eutios:

$$| \ \xi^1 = 0, \xi^1_2 = 0, \xi^1_3 = 0, \xi^0_2 = 0, \xi^0_3 = 0$$

while $R_1^{(3)}$ is obtained by adding aain $\xi^{\perp}_0 = 0$. We have 15 generating second order CC and 3 third order CC provided by the Spencer operator:

$$d_1\xi^1 - \xi^1_1 = 0, d_2\xi^1 - \xi^1_2 = 0, d_3\xi^1 - \xi^1_3 = 0$$

in which we have to substitute $\xi^1 \in j_2(\Omega)$, $\xi^1_1 \in j_2(\Omega), \xi^1_2 \in j_2(\Omega), \xi^1_3 \in j_2(\Omega)$.

It thus follows from the previous results of this section, which have been obtained without the need of any purely relativistic tool, that black holes cannot exist as they are contradicting [14,15] while showing that the underlying mathematical problem is a purely formal one with no link with GR along the given motivating example. ï»¿

CONCLUSION

When a linear partial differential operator $\mathcal{D}\xi = \eta$ is given, a direct problem is to look for the generating compatibility conditions $\mathcal{D}_1\eta = 0$ that must be satisfied by η . Similarly, if $\mathcal{D}_1\eta = \zeta$ is given, one may look for CC of the form $\mathcal{D}_2\zeta = 0$ and so on. The mathematical community (and we do not speak about the physical community !) is of course aware of such a " step by step" way but is not at all aware of the existence of another "as a whole" procedure allowing to define the various differential operators of the differential sequence thus obtained apart from the very specific situation of the Poincaré (in France !) sequence for the exterior derivative that admits a unique defining formula for each operator separately. The best known case is that of Riemannian geometry and its application to general relativity with the successive Killing, Riemann and Bianchi operators of first, second and first order respectively. In particular, we may ask " Who knows about the Spencer operator and the corresponding Spencer sequence $\ell^{\,n}$ at the heart of this paper.

In the Introduction, we have explained and illustrated through many motivating examples that, when a second order differential operator $\mathcal{D}$ is depending on constant or variable coefficients, its generating compatibility conditions (CC) may be of first, second, third and even sixth or higher order, a result largely depending on the parameters. In the meantime, we have shown that the solution of this problem for a system of order q cannot be obtained without bringing such a system to an involutive form or at least to a formally integrable form of order $q+r$ after differentiating $r+s$ times the equations while keeping only the equations left up to order $q+r$ in such a way that the order of the CC is at most $r+s+1$.

From a very different point of view, the Spencer differential sequence is obtained by bringing any involutive system $R_q \subset J_q(E)$ to a first order involutive system $R_{q+1} \subset J_1(R_q)$ having an isomorphic space of solutions or, with a more precise language, allowing to define a differential module isomorphic to the differential module M defined by the initial system. The quotient of the Spencer sequence for the first order trivially involutive first order system $J_{q+1}(E) \subset J_1(J_q(E))$ by the previous Spence sequence which is induced by the inclusion $R_q \subset J_q(E)$ is the well defined finite length differential Janet sequence introduced by M. Janet as a footnote in 1920 which is thus providing another resolution of the same space of solutions or of the differential module M already defined. According to a very difficult theorem of (differential) homological algebra, the only objects that do not depend of the resolution used are the (differential) extension modules that are measuring the fact that the corresponding dual sequence made by the respective formal adjoint of the operators involved and going thus " backwards" (that is from right to left) may not be exact, that is each operator may not generate the CC of the preceding one. it thus follows that the Spencer and Janet sequences will bring the same formal informations as a whole, even though, in actual practice, we proved that they can be completely different.

It may happen, for example with the Schwarzschild and Kerr metrics, with $q = 1, r = 0, s = 3$, that the final corresponding FI systems will not depend any longer on the parameters involved initially. Accordingly, the only important object to consider is not the metric but its group G of invariance which is used through the fact that the Spencer sequence is the tensor product of the Poincaré sequence by its Lie algebra $\vec{\mathcal{G}}$, the main formal reason for which black holes cannot exist.

We have thus finally proved that the main idea, along the tentative of H. Weyl in 1918, is not to shrink the dimension of this group from 10 down to to 4 or 2 parameters by using the S or K metrics instead of the M metric but, on the contrary, to enlarge the group from 10 up to 11 or 15 parameters by using the Weyl or conformal group instead of the Poincar'e group of space-time while using the adjoint of the respective Spencer sequences [17]. It will follow that the first set of Maxwell equations is obtained by a projection of the second Spencer operator D_2 that can be parametrized by a projection of the first Spencer operator D_1 , a result contradicting the basic assumption of classical gauge theory in which they are induced by D_3 . The main problem today is that, in the minimum resolution of the conformal Killing operator, the generating CC of the second order Weyl operator are also made by a second order operator, a result confirmed by my PhD student A. Quadrat (INRIA) in 2016 (See [24, 26] or arXiv: 1603.05030) but still not acknowledged and showing that conformal geometry but me revisited by using the Spencer δ -cohomology [31].

Finally, in a more general framework, when a Lie group G is acting on a manifold X of dimension n , the Spencer sequence is always locally and formally exact, being isomorphic to the tensor product of the Poincaré sequence by the Lie algebra of G . On the contrary, the corresponding formally exact Janet sequence may have Janet bundles of high dimensions. The last operator $\mathcal{D}_n$ is always surjective while its adjoint is always injective. However, $ad(\mathcal{D}_{n-1})$ may not define all the CC of $ad(\mathcal{D}_n)$ because $ad(D_n)$ may fail to be injective. Applying these methods to the conformal group of transformations when $n = 4$, we discovered in the very recent [17] the common conformal origin of the Cauchy, Cosserat, Clausius/Poisson and Maxwell equations. For example the EM field F comes from the composition of epimorphisms ($60 \rightarrow 16 \rightarrow 6 \rightarrow 0$):

$$\boxed{\hat{C}_1 \rightarrow \hat{C}_1/\tilde{C}_1 = (T^* \otimes \hat{R}_2)/(T^* \otimes \tilde{R}_2) \simeq T^* \otimes (\hat{R}_2/\tilde{R}_2) \simeq T^* \otimes \hat{g}_2 \simeq T^* \otimes T^* \overset{\delta}{\rightarrow} \wedge^2 T^*}$$

while the EM potential comes from the composition of epimorphisms (1540):

$$\hat{C}_0\hat{C}_0/\tilde{C}_0 \simeq \hat{R}_2/\tilde{R}_2 \simeq \hat{g}_2 \simeq T^*$$

and the parametrization $dA = F$ is induced by D_1 while the Maxwell equation $dF = 0$ is induced by D_2 . Using the short exact splitting sequence $0 \rightarrow S_2T^* \overset{\delta}{\longrightarrow} T^* \otimes T^* \overset{\delta}{\longrightarrow} \wedge^2 T^* \rightarrow 0$ leading to the isomorphism $T^* \otimes T^* \simeq S_2T^* \oplus \wedge^2 T^* \simeq (R_{ij}) \oplus (F_{ij})$ with $16 = 10 + 6$, that only depends on the elations of the conformal group, along the Fundamental Diagram II showing the common conformal origin of electromagnetism and gravitation, already published in 1983 [30]. More generally, taking the quotient of the Spencer sequence for $\hat{C}_r$ by the Spencer sequence for $\tilde{\Theta}$, we obtain a formally exact sequence with bundles $\hat{C}_r/\tilde{C}_r$ which is isomorphic to the tensor product of the Poincar
'e sequence by a vector space of dimension $dim(\hat{g}_2) = dim(T^*) = 4$ that we can project onto the formally exact Poincaré sequence, with a shift by one step contradicting the use of $U(1)$ in GT. We obtain therefore the following commutative and exact diagram in which we notice that the first vertical short exact sequence on the left is nothing else than the bottom short exact sequence of the previous fundamental diagram II:

$$
\begin{array}{ccccccccccccccc}
 & & & & 0 & & 0 & & 0 & & 0 & & & & \\
 & & & & \downarrow & & \downarrow & & \downarrow & & \downarrow & & & & \\
 & & 1 & \rightarrow & 10 & \rightarrow & 20 & \rightarrow & 15 & \rightarrow & 4 & \rightarrow & 0 & & gravitation \\
 & & & & \downarrow & & \downarrow & & \downarrow & & \| & & & & \\
 & & 4 & \xrightarrow{d} & 16 & \xrightarrow{d} & 24 & \xrightarrow{d} & 16 & \xrightarrow{d} & 4 & \rightarrow & 0 & & \\
 & & \| & & \downarrow & & \downarrow & & \downarrow & & \downarrow & & & & \\
1 & \xrightarrow{d} & 4 & \xrightarrow{d} & 6 & \xrightarrow{d} & 4 & \xrightarrow{d} & 1 & \rightarrow & 0 & & & & electromagnetism \\
 & & & & \downarrow & & \downarrow & & \downarrow & & & & & & \\
 & & & & 0 & & 0 & & 0 & & & & & &
\end{array}
$$

A snake chase in this diagram proves that gravitation has to do with the conformal factor ϕ when $F = 0$ as the first operator on the upper left is just the composition $D_1 \circ d : \phi \rightarrow \partial_i \phi \rightarrow \partial_{ij} \phi$ according to the fundamental diagram II. Also, using the dual summation $\rho(x)(\partial_4 \xi^4 - \xi^4_4) + g^i(x)(\partial_i A - A_i) + g^{ij}(x)(\partial_i A_j - 0)$ with $\xi^k_{ijr} = 0$ and integrating by parts, we get the induction equations:

$$\xi^4 \partial_4 \rho = 0, \xi^4_4 = A \partial_i g^i + \rho = 0, \xi^4_{4i} = A_i \rightarrow \partial_r g^{ri} + g^i = 0$$

leading to the Poisson equation for ϕ when $g^{ij} = \phi \omega^{ij}$ and thus to a new conformal scheme for electromagnetism and gravitation. It is also a reason for which elations are also sometimes called and confused with “accelerations” because and accelerometer on an inertial platform in a rocket can only measure the difference $\partial_4 \xi^k_4 - \xi^k_{44}$ with $k = 1, 2, 3$ between the acceleration (time derivative of the speed as a rotation of space-time) and the gravitational field, while one has $\xi^k_{44} = \omega^{kr} A_r$ and the ditive ruleof secn rderts

$$\boxed{\bar{f} = g \circ f \Rightarrow \bar{f}^k_{44} = f^k_{44} + g^k_{44}}$$

holds whenever $f_1 = g_1 = id_1 = j_1(id)$ for the one jet of the identity transformation $y = x$ (Compare [25] to [33]). However, no one of these results could have been even imagined by Weyl because the Riemann operator must be replaced by the Weyl operator while the Bianchi operator must be replaced by a second order CC operator, a result still not known today in the conformal framework [33, 34].

In the spirit of the Cosserat brothers on elasticity in 1909 and H. Weyl on electromagnetism in 1918, we have tried to explain and illustrate why the structure of physical theories must depend on a Lie group of transformations considered as a Lie pseudogroup. The main idea is then to introduce the corresponding Janet (1920) or Spencer (1970) differential sequences both with their respective adjoint differential sequences needed for variational calculus [28, 35]. In a coherent way with the dream of Weyl, the most striking result is the “shift” that must be used in the physical interpretation of the sequences obtained, in the sense that the EM field as a 2-form is coming from the first Spencer bundle and not from the second (See [16] for other examples). These two sequences may be sometimes quite different though always homologically equivalent and we have tried to illustrate them through the study of gravitational waves and black holes. As both of them are largely unknown, no other reference can be found and only the future will decide about the best one that must be used !.

APPENDIX

After 1950 the introduction of homological algebra in pure mathematics has been more than an evolution but rather quite a revolution in algebraic geometry. Following the wish of one of the reviewers that we thank, our aim in this appendix is to explain that differential homological algebra, namely the way to add the word ” differential ” in front of ALL the concepts already introduced (module, resolution, duality, extension modules, ..) will bring quite a revolution in physics. The main problem is that a full account should need a whole paper [35] or even a whole book [21] and that we have seen in the core of this paper that the differential geometric framework is already difficult while the geometric part is somehow even more difficult. By chance, in a more general framework, we have proved that the controllability of a control system is a structural property of the control system, not depending on the choice of inputs and outputs among the control variables and can be described in terms of vanishing of extension modules [4]. Roughly, it means that a control system is controllable if and only if the system can be parametrized or, equivalently, if there does not exist any observable quantity which is solution of an autonomous system for itself, a more physical way to say that the differential module defined by the system is torsion-free [35]. Accordingly we shall explain through two examples how to pass ” beyond the mirror”.

First of all, we sketch the idea hidden beyond ” differential extension modules” by using only the language of operators along the content of this paper. For this, we notice that, if a given linear differential operator $\mathcal{D}_1 \eta = \zeta$ is give, a ” direct problem ” is to look for compatibility conditions (CC) in the form of a linear operator $\mathcal{D}_2 \zeta = 0$ and so on. We hope that the reader is now convinced that it may already be a difficult problem to provide ” a prior” any idea of the order of the CC operator as we have provided examples in which the order is ranging from 1 up to 6. However, conversely, if a system described by $\mathcal{D}_1 \eta = 0$, a much more difficult ” inverse problem ” is to find a parametrization, that is an operator $\mathcal{D} \xi = \eta$ having exactly such CC. Now, using the well known properties of the adjoint procedure $\mathcal{D} ad(\mathcal{D})$ with $ad(ad(\mathcal{D})) = \mathcal{D}$, if $\mathcal{D} \xi = \eta$ has generating CC $\mathcal{D}_1 \eta = 0$, then $\mathcal{D}_1 \circ \mathcal{D} = 0 \Rightarrow ad(\mathcal{D}) \circ ad(\mathcal{D}_1) = 0$ but $ad(\mathcal{D})$ may not generate all the CC of $ad(\mathcal{D}_1)$ while $ad(D_1)$ may not generate all the CC of $ad(D_2)$ and $ad(\mathcal{D}_2)$ may not generate all the CC of $ad(\mathcal{D}_3)$ and so on, as can be seen in the motivating examples. The introduction of extension modules is a way to measure such a gap.

Starting with the system, we sketch on an example the five steps of the differential double duality test must be used in order to know whether this system can be parametrized or not:

STEP 1: Write down the system $\mathcal{D}_1\eta = \zeta : d_{12}\eta^1 + d_{22}\eta^2 = \zeta$.

STEP 2: Write down the adjoint operator $\cdots$ backwards: multiplying on the left by a test function λ and integrating by parts, we get

$$\boxed{\eta^1 \rightarrow d_{12}\lambda = \mu^1, \eta^2 \rightarrow d_{22}\lambda = \mu^2}$$

STEP 3: As any operator is the adjoint of its adjoint, find its CC as an operator $ad(\mathcal{D})\mu = \nu\ d_2\mu^1 - d_1\mu^2 = \nu$.

STEP 4: Write down its adjoint as an operator $\mathcal{D}\xi = \eta$. $\mu^1 \rightarrow -d_2\xi = \eta^1, \mu^2 \rightarrow d_1\xi = \eta^2$

Step 5: Find its CC as an operator $\mathcal{D}'_1\eta = 0$ and compare to $\mathcal{D}_1$.

CONCLUDE: If $\mathcal{D}_1$ and $\mathcal{D}'_1$ are identical or have the same space of solutions, that is produce the same involutive system, then $\mathcal{D}_1$ is parametrized by $\mathcal{D}$. Otherwise, if the space of solutions of $\mathcal{D}'_1$ is smaller than that of $\mathcal{D}_1$, then $\mathcal{D}_1$ cannot be parametrized. It means that there is at least one new CC which is an autonomous element which is satisfying at least one OD or PD equation for itself, a fact showing that the initial system, considered as a control system, cannot be controllable (See [21, 35] or Zbl 179.93001 for more details and examples, in particular the study of RCL electrical circuits). We notice that we don't need to separate (η^1, η^2) into input and output.

END: In the present example, $\mathcal{D}'_1$ is defined by $d_1\eta^1 + d_2\eta^2 = \zeta'$ and we have $d_2\zeta' = \zeta$, that is $d_2\zeta' = 0$ whenever $\zeta = 0$. It follows that $\mathcal{D}$ CANNOT be parametrized. Ofc course, such a result could have been found directly in this elementary example but such a test is unavoidable in general.

In order to recapitulate, our purpose in this appendix is to explain how differential homological algebra is able to combine these two procedures.

For this we ask the reader to spend a few dollars in order to realize the next experiment and try to understand why such a fact is clearly showing that gravitational waves cannot exist as we have explained in the Introduction and in theorem 4.1 or in [36].

Example 5.1: (Double pendulum) Let us consider a thin rigid bar of length L able to slide horizontally with a position x function of time t and time derivative d . We may attach a pendulum of length l_1 , mass m_1 , (small) angle θ_1 from the vertical at one end and a pendulum of length l_2 , mass m_2 , (small) angle θ_2 from the vertical at the other end. At equilibrium, the two pendulums are fixed. If one of the pendulums is slightly moved and $l_1 \neq l_2$, moving the bar with enough skill, one can bring the full system to equilibrium, that is $x = cst, \theta_1 = \theta_2 = 0$ and we say that the full system is controllable by using the movement of the bar.

Now, if $l_1 = l_2 = l$ and one pendulum is moved while the other is untouched, then any way to stop the first wll bring the other to have the same movement and the system is not controllable that is, in particular, there is no way to stop both pendulums as before.

In order to write down the two OD equations of the system, one has to consider the Newton law applied to the inertial forces $d^2(x + l\theta)$, the gravity force mg and the tension of the thread. Projecting on the perpendicular to each pendulum to eliminate the last one, we may divide by the respective mass in order to get the two OD equations in the form of a surjective operator $\mathcal{D}_1\eta = \zeta$ with $\eta = (\eta^1 = \theta^1, \eta^2 = \theta^2, \eta^3 = x$):

$$d^2x + l_1 d^2\theta^1 + g\theta^1 = \zeta^1, \qquad d^2x + l_2 d^2\theta^2 + g\theta^2 = \zeta^2$$

Multiplying the firstOD equation by the test function λ^1 , the seond by the test fncin λ^2 , adding and integrating by parts, we obtain the adjoint operator in the form $ad(\mathcal{D}_1)\lambda = \mu$, namely:

$$\theta^2 l_2 d^2\lambda^2 + g\lambda^2 = \mu^2, x d^2\lambda^1 + d^2\lambda^2 = \mu^3$$

First of all, if $\mu^1 = \mu^2 = \mu^3 = 0$, we obtain two zero order OD equations where the second one is obtain by differentiating twice the first and substituting:

$$l_2\lambda^1 + l_1\lambda^2 = 0, \qquad (l_2/l_1)\lambda^1 + (l_1/l_2)\lambda^2 = 0$$

As the determinant of this linear system is equal to $l_1 - l_2$, it follows that $ad(\mathcal{D}_1)$ is injective if and only if $l_1 \neq l_2$.

Let us now prove that $\mathcal{D}_1$ can be parametrized if and only if such a condition is satified. First of all we notice that $\lambda^1, \lambda^2 \in j_2(\mu)$ and, using a tricky PP procedure or computer algebra, we discover that $ad(\mathcal{D}_1)$ has only one CC $ad(\mathcal{D})\mu = \nu$ of order 4. Taking the adjoint, we obtain a well defined fourth order injective parametrization in the form $\mathcal{D}\xi = \eta$ as follows:

$$\boxed{-l_1 l_2 d^4\xi - g(l_1 + l_2)d^2\xi - g^2\xi = x,\ l_2 d^4\xi + g d^2\xi = \theta^1,\ l_1 d^4\xi + g d^2\xi = \theta^2}$$

This parametrization is injective and we have the short exact adjoint sequences:

$$\begin{array}{ccccccccc} 0 & \longrightarrow & 1 & \overset{D}{\longrightarrow} & 3 & \overset{D_1}{\longrightarrow} & 2 & \longrightarrow & 0 \\ \\ 0 & \longleftarrow & 1 & \overset{ad(D)}{\longleftarrow} & 3 & \overset{ad(D_1)}{\longleftarrow} & 2 & \longleftarrow & 0 \end{array}$$

At no moment we have ever been speaking about inputs, outputs and Kalman test !.

It remains to study the case $l_1 = l_2 = l$. Subtracting the second equation from the first while setting $\theta = \theta^1 - \theta^2$, we get $ld^2\theta = g\theta = 0$, that is the standard Od equation of a single pendulum. Of course, we notice at once that the observable θ is an autonomous element and its behaviour cannot be controlled. Equivalently, θ is generating the torsion submodule $t(M)$ of the differential module M defined by $\mathcal{D}_1$. The main fact is that now $\mathcal{D}_1$ cannot any longer be parametrized?. For this, we may multiply each OD equation by two test functions as before and integrate by parts in order to obtain:

$$ld^2\lambda^1 + g\lambda^1 = \mu^1, ld^2\lambda^2 + g\lambda^2 = \mu^2, d^2(\lambda^1 + \lambda^2) = \mu^3$$

Summing the two first OD equations while setting $\lambda = \lambda^1 + \lambda^2$, we get:

$$d^2\lambda = \mu^3,\ ld^2\lambda + g\lambda = \mu^1 + \mu^2$$

It follows that $ad(\mathcal{D}_1)$ is no longer injective with kernel $\lambda = 0 \Leftrightarrow \lambda^1 + \lambda^2 = 0$. We also obtain $g\lambda = \mu^1 + \mu^2 - l\mu^3$ and, substituting, we obtain one single CC of order 2 for $ad(\mathcal{D}_1)$, namely $ad(\mathcal{D})$ as follows:

$$d^2(\mu^1 + \mu^2 - l\mu^3) - g\mu^3 = \nu$$

Multiplying by the test function ξ and integrating by parts, we get $\mathcal{D}$:

$$\mu^1 d^2\xi = \theta^1, \mu^2 d^2\xi = \theta^2, \mu^3 - ld^2\xi - g\xi = x$$

The 3 CC are described by $\mathcal{D}'_1 \neq \mathcal{D}_1$ as follows:

$$d^2x + ld^2\theta^1 + g\theta^1 = 0, d^2x + ld^2\theta^2 + g\theta^2 = 0, \theta^1 - \theta^2 = 0$$

We recover the fact that the new CC is introducing $\theta = \theta^1 - \theta^2$ which is indeed a torsion element with autonomous OD equation $d^2\theta + g\theta = 0$.

This operator $\mathcal{D}$ of order 2 is injective and we have the short exact adjoint sequences:

$$\begin{array}{ccccccccc}
 & & & & & & 3 & & \\
 & & & & & D'_1 \nearrow & & & \\
0 & \longrightarrow & 1 & \xrightarrow{D} & 3 & \xrightarrow{D_1} & 2 & \longrightarrow & 0 \\
 & & & & & & & & \\
0 & \longleftarrow & 1 & \xleftarrow{ad(D)} & 3 & \xleftarrow{ad(D_1)} & 2 & &
\end{array}$$

It is absolutely impossible to recover all these results and understand their meaning without differential double duality and differential homological algebra.

Example 5.2: (General relativity) We now prove that the above situation is .. exactly similar to the one we have described in GR in order to explain why GW cannot exist.

When $n = 4$, let us prove that the 10 Einstein equations cannot admit a potential or, equivalently, that the Ricci operator cannot be parametrized and that the Einstein operator is therefore useless as it cannot have a mathematical origin contrary to the Ricci operator, according to the fundamental diagram II.

We shall discover that the existence of autonomous elements (torsion elements in the module framework) ... are nothing else than the $20 - 10 = 10$ components of the Weyl bundle already introduced in the fundamental diagram II, a result highly not evident at first sight !.

First of all, according to the parametrization test, to the result of the Introduction and to Theorem 4.1, we have at once the negative test procedure:

$$\begin{array}{ccccccc}
 & & & & & Riemann & 20 \\
 & & & & & \nearrow & \\
 & & 4 & \xrightarrow{Killing} & 10 & \xrightarrow{Ricci} & 10 \\
 & & & & & & \\
0 & \longleftarrow & 4 & \xleftarrow{Cauchy} & 10 & \xleftarrow{ad(Ricci)} & 10
\end{array}$$

The 5 steps are indicated as follows while taking into account that $Cauchy = ad(Killing)$, a result that can be found in any textbook of continuum mechanics or elasticity:

$Ricci \longrightarrow ad(Ricci) \longrightarrow Cauchy \longrightarrow Killing \longrightarrow Riemann$

Accordingly and in a coherent way with the previous example, the Ricci operator and thus the Einstein operator cannot be parametrized and we have $20 - 10 = 10$ generating torsion elements, that is to say elements satisfying at least one PD equation for each one. Of course, such an approach has never been followed because the fundamental diagram II is not known though it provides the splitting $Riemann = Ricci \oplus Weyl$ coming from the splitting $T^* \otimes T^* = S_2T^* \oplus \wedge^2 T^*$. My chance has been to know very well the results of A. Lichnerowicz who has been my advisor during 25 years from 1973 to his death in 1998. Indeed, I got in mind the so-called (in France !) " Lichnerowicz waves " and I am now able to give a short proof of the linearized case [18]:

Theorem 5.3: The Dalembertian of each component of the Weyl tensor is a linear differential consequence of the 10 Einstein equations $R_{ij} = 0$.

Proof. Linearizing over the Euclide or Minkowski metric ω while using the Bianchi identities and taking into account that $R_{kl,ij} = R_{ij,kl}$, we get with $d^r = \omega^{ri} d_i$:

$$d_r R_{kl,ij} + d_i R_{kl,jr} + d_j R_{kl,ri} = 0 \Rightarrow d^r R_{rl,ij} = d^r R_{ij,rl} = d_i R_{lj} - d_j R_{li}$$

$$d_{rs} R_{kl,ij} + d_{is} R_{kl,jr} + d_{js} R_{kl,ri} = 0 \Rightarrow \Box R_{kl,ij} + \omega^{rs} d_{is} R_{kl,jr} + \omega^{rs} d_{js} R_{kl,ri} = 0$$

$$\Box R_{kl,ij} = d_i(d_k R_{lj} - d_l R_{kj}) - d_j(d_k R_{li} - d_l R_{ki})$$

Finally, using the splitting formula for defining the components $\sigma^k_{l,ij} = \rho^k_{l,ij} - (\sum \rho_{rs})$ of the Weyl tensor from the components of the Riemann tensor with now $\sigma^r_{l,rj} = 0$, we obtain by linearization $\Sigma^k_{l,ij} = R^k_{l,ij} - (\sum R_{rs})$

It is absolutely impossible to extend the above result to the conformal Riemannian geometry because the analogue of the Bianchi operator is now of order 2, a result still neither known and nor even acknowledged today in the long exact sequence that we have already provided at the end of Section 3C, where $\mathcal{D}$ is the conformal Killing operator and $\mathcal{D}_1$ is the Weyl operator [15, 26, 31]. This is the main reason for which the Spencer sequences and their adjoint sequences must be used !.

REFERENCES

[1] Janet, M. Sur les Systèmes aux Dérivées Partielles, Journal de Math. 1920; 8: 65-151.

[2] Cosserat, E., Cosserat, F. Théorie des Corps Déformables, 1909, Herman, Paris.

[3] Zerz, E. Topics in Multidimensional Systems Theory, Springer LNCIS 256, 2000.

[4] Pommaret, J-F. Algebraic Analysis of Control Systems Defined by Partial Differential Equations, in “Advanced Topics in Control Systems Theory”, Springer, Lecture Notes in Control and Information Sciences LNCIS 311, 2005, Chapter 5, pp. 155-223.

[5] Vessiot, E. Sur la Théorie des Groupes Infinis. 1903; 20:411-451.

[6] Pommaret, J.-F. How Many Structure Constants do Exist in Riemannian Geometry ?, Mathematics in Computer Science. 2022; 16: 23, DOI: 10.1007/s11786-022-00546-3.

[7] Klainerman S. Linear Stability of Black Holes, Astérisque. Séminaire Bourbaki, exp:1015. 2011; 339: 91-139, (Accessible through http://www.numdam.org).

[8] Klainerman, S. Are Black Holes real ? A Mathematical Perspective, You Tube, IHES, 22/04/2011

[9] Damour, T. Gravitational Waves and Binary Black Holes, http://www.bourbaphy.fr/december20 (https://seminaire-poincare.pages.math.cnrs.fr/damourgrav.pdf)

[10] Pommaret, J.-F. The Mathematical Foundations of General Relativity Revisited, Journal of Modern Physics. 2013; 4: 223-239. DOI: 10.4236/jmp.2013.48A022.

[11] Pommaret, J.-F. Minimum Parametrization of the Cauchy Stress Operator, Journal of modern Physics. 2021; 12: 453-482. DOI: 10.4236/jmp.2021.124032.

[12] Pommaret, J.-F. Why Gravitational Waves Cannot Exist, Journal of Modern Physics. 2017; 8: 2122-2158. DOI: 10.4236/jmp.2017.813130.

[13] Pommaret, J-F. Killing Operator for the Kerr Metric, (https://arxiv.org/abs/2211.00064) DOI: 10.4236/jmp.2023.141003

[14] Aksteiner, S., Andersson L., Backdahl, T., Khavkine, I., Whiting, B. Compatibility Complex for Black Hole Spacetimes, Commun. Math. Phys. 2021; 384: 1585-1614. https://doi.org/10.1007/s00220-021-04078-y (arXiv:1910.08756)

[15] Pommaret, J.-F. The Conformal Group Revisited. Journal of Modern Physics Revisited, 2021; 12:1822-1842. DOI: 10.4236/jmp.2021.1213106.

[16] Pommaret, J.-F. Cauchy, Cosserat, Clausius, Einstein, Maxwell, Weyl equations revisited, Journal of Modern Physics. 2024; 15: 2365-2397, DOI: 10.4236/jmp.2024.1513097

[17] Poincaré, H. Sur une Forme Nouvelle des Equations de la Mécanique, C. R. Acad. Sc. Paris. 1901; 132: 369-371.

[18] Pommaret, J.-F. Gravitational Waves and Parametrizations of Linear Differential Operators, 2024; DOI: 10.5772/intechopen.1000851 (In Frajuca, Gravitational Waves - Theory and Observations, DOI: 10.5772/intechopen.1000226) p 3-39.

[19] Foster, J., Nightingale, J.D. A Short Course in General Relativity, New York, Longman, 1979.

[20] Pommaret, J.-F. Partial Differential Equations and Group Theory, Kluwer, 1994. DOI: 10.1007/978-94-017-2539-2

[21] Pommaret, J.-F. Partial Differential Control Theory, Kluwer, Dordrecht. 2001 (Zbl 1079.93001). ISBN: 978-94-010-3845-4

[22] Weyl, H. (1918, 1952) Space, Time, Matter, 1918, 1952, Dover, New York.

[23] Pommaret, J.-F. Parametrization of Cosserat Equations, Acta Mechanica. 2010; 215: 43-55. DOI: 10.1007/s00707-010-0292-y.

[24] Quadrat, A., Robertz, D. A Constructive Study of the Module Structure of Rings of Partial Differential Operators, Acta Applicandae Mathematicae, 2014; 133: 187-234.

[25] Pommaret, J.-F. The Mathematical Foundations of Elasticity and Electromagnetism Revisited, Journal of Modern Physics. 2019; 10: 1566-1595. DOI: 10.4236/jmp.2019.1013104.

[26] Pommaret, J.-F. Deformation Theory of Algebraic and Geometric Structures, Lambert Academic Publisher (LAP), 2016, Saarbrucken, Germany.

[27] Spencer, D.C., Kumpera, A. Lie Equations, 1972, Princeton University Press.

[28] Pommaret, J.-F. Spencer Operator and Applications: From Continuum Mechanics to Mathematical Physics, in "Continuum Mechanics-Progress in Fundamentals and Engineering Applications", Dr. Yong Gan (Ed.), ISBN: 978-953-51-04476, InTech (2012) Available from: DOI: 10.5772/35607 .

[29] Pommaret, J.-F. Partial Differential Equations and Lie Pseudogroups, 1978, Gordon and Breach, New York.

[30] Pommaret, J.-F. (1983) The Structure of Electromagnetism and Gravitation, C. R. Acad. Sc. Paris, Serie I, 1983, 297 (7 Novembre) 493-496.

[31] Pommaret, J.-F. Gravitational Waves and the Foundations of Riemann Geometry , Advances in Math. Research, Volume 35, p. 95 - 61, NOVA Science Publisher, Advances in Mathematical Research. 2024; 35: 95-105, Chapter 6, ISBN: 979-8-89113-607-6

[32] Pommaret, J.-F. From Differential Sequences to Black Holes, Journal of Modern Physics, 16 (2025) 410-440, https://doi.org/10.4236/jmp.2025.163023

[33] Mashhoon, B. Conformal Symmetry, Accelerated Observers and Nonlocality, (2019) arXiv: 1906.06667 .

[34] Osborn, H. Lectures on Conformal Field Theories in More than two Dimensions, 2025 Lecture Notes at DAMTP, Cambridge, England.

[35] Pommaret, J.-F. From Kalman to Einstein and Maxwell: The Structural Controllability Revisited, Advances in Pure Mathematics, 15 (2025) 570-628. https://doi.org/10.4236/apm.2025.159031

[36] Pommaret, J.-F. Why Gravitational waves cannot exist, https://doi.org/10.56367/OAG-045-11836

Great Britain Journals Press

RESEARCH FINGERPRINT

IDENTIFIER
LJRS-226172

PEER REVIEW
Double Blind

SIMILARITY CHECK
Perplexity AI and iThenticate

ACCESS
Open Access

LANGUAGE
English

PRINT ISSN
2631-8490

ONLINE ISSN
2631-8504

EDITION

ABBREVIATION
LJRS

VOLUME
26

ISSUE
4

YEAR
2026

KEY DATES

RECEIVED
2026-03-03

ACCEPTED
2026-03-09

ONLINE PUBLISHED
2026-06-01

PUBLISHED
2026-06-16

CATALOGING

CROSSMARK DOI
10.34257/LJRS226172UK

JEL CLASS
Q23, Q56, R40

AGRIS CLASS
K10

ACCESS ONLINE

London Journal of Research In Science: Natural and Formal

General Section

Article Record

Cost of Sustainable Timber Forest Management in the State of Acre, Brazilian Amazon

CORRESPONDENCE

AUTHORS & AFFILIATIONS

Dr. Catherine Cristina Claros Leite ¶*

Forest Engineer

Zenobio Abel Perelli Gouvêa da Gama e Silva ‖

ζ Professor

Gilson Fernandes da Silva §

ζ Professor

¶ Freelancer

‖ Universidade Federal do Acre, Rio Branco, Brazil (OA)

§ Universidade Federal do Espírito Santo, Vitória, Brazil (OA)

ABSTRACT

This study aimed to generate economics information on sustainable forest management in the state of Acre.

Data collection addressed the following points: 1) prices of forest land and timber logs; 2) development and implementation of the Sustainable Forest Management Plan (SFMP) and the Annual Operational Plan (AOP); 3) forest harvesting and 4) timber transport to the sawmill. Basic data were obtained through interviews with forest consultants, timber industry entrepreneurs, and owners of firms involved in forest extraction.

Different scenarios were considered: forests located 50 mathrmkm, 100 mathrmkm, and 150 mathrmkm from the city of Rio Branco; managed areas with and without permanent plots; and with the application of silvicultural treatments. The production cost was obtained using different interest rates, and a 25-year cutting cycle was adopted. In economic terms, forest management activities were evaluated by calculating the net present value (NPV) and the production of log delivered to the sawmill yard was evaluated by calculating the marketing margin. The results generated in this study on forest management practices in the state of Acre allowed us to infer the following main conclusions: 1) the average cost of producing standing timber in an area located 50 mathrmkm from the Rio Branco timber

Index Terms: Forest economics • Permanent plots • Sustainable Forest Management

FUNDING
No external funding was declared for this work.

CONFLICTS
The authors declare no conflict of interest.

AI USAGE
No generative AI was used for analysis or results.

HOW TO CITE
Leite et al. (2026). Cost of Sustainable Timber Forest Management in the State of Acre, Brazilian Amazon. London Journal of Research In Science: Natural and Formal, 26(4), 45-60. DOI: 10.34257/LJRS226172UK

METADATA CONTINUATION

AUTHOR CONTACT QR LEDGER

Dr. Catherine Cristina Claros Leite¶∐*

ARCHIVAL RECORD

LJRS · Vol 26 · Issue 4 · 2026

Article ID LJRS-226172 · DOI 10.34257/LJRS226172UK

Print ISSN 2631-8490 · Online ISSN 2631-8504

 CROSSREF DOI 10.34257/LJRS226172UK

RESEARCH ARTICLE

Cost of Sustainable Timber Forest Management in the State of Acre, Brazilian Amazon

Dr. Catherine Cristina Claros Leite[¶∐*], Zenobio Abel Perelli Gouvêa da Gama e Silva[‖ζ], and Gilson Fernandes da Silva[§ζ]

QUALIFICATIONS / ROLES

∐ Forest Engineer
ζ Professor

AFFILIATIONS

¶ Freelancer
‖ Universidade Federal do Acre, Rio Branco, Brazil (**OA**)
§ Universidade Federal do Espírito Santo, Vitória, Brazil (**OA**)

Abstract

This study aimed to generate economics information on sustainable forest management in the state of Acre.
Data collection addressed the following points: 1) prices of forest land and timber logs; 2) development and implementation of the Sustainable Forest Management Plan (SFMP) and the Annual Operational Plan (AOP); 3) forest harvesting and 4) timber transport to the sawmill. Basic data were obtained through interviews with forest consultants, timber industry entrepreneurs, and owners of firms involved in forest extraction.
Different scenarios were considered: forests located $50 mathrmkm$, $100 mathrmkm$, and $150 mathrmkm$ from the city of Rio Branco; managed areas with and without permanent plots; and with the application of silvicultural treatments. The production cost was obtained using different interest rates, and a 25-year cutting cycle was adopted. In economic terms, forest management activities were evaluated by calculating the net present value (NPV) and the production of log delivered to the sawmill yard was evaluated by calculating the marketing margin. The results generated in this study on forest management practices in the state of Acre allowed us to infer the following main conclusions: 1) the average cost of producing standing timber in an area located $50 mathrmkm$ from the Rio Branco timber hub increases by approximately 0.82% with the installation and measurement of permanent plots throughout the cutting cycle and 2) the marketing margin for logs indicates that for more distant areas ($150 mathrmkm$)) this activity is unfeasible.

Keywords: *Forest economics, Permanent plots, Sustainable Forest Management*

Correspondence: Dr. Catherine Cristina Claros Leite

1 Introduction

Morales-Hidalgo et al. (2015) state that forests provide ecosystem goods and services, as food, water, shelter, and nutrient cycling, and play a key role in biodiversity conservation. Macdicken et al. (2015), in turn, argues that these resources can contribute significantly to the economy and ensure livelihoods and environmental protection.

Keenan et al. (2015) reveal that forests cover about 30% of the global land area, and 44% of these are distributed in tropical countries. Food and Agriculture Organization of the United Nations (FAO) (2016) states that the second largest forest area in the world is in Brazil. Strand et al. (2017) add that the Amazon Basin occupies about 60% of Brazilian territory, which, according to Assunção et al. (2017), is the largest continuous expanse of tropical forests in the world. Given this reality, Fearnside (1997) and Hamaoui JR. et al. (2016) consider that the proper use of this biome is key to global balance, as it plays an important role in global carbon and water cycles and temperature patterns.

However, Azevedo-Ramos (2010) warns that the timber sector in the Amazon, for decades, using techniques with high environmental impact and high wood waste, has been associated with the destruction of the forest. In view of this fact, Higuchi (1994) and Sabogal et al. (2006) suggest Sustainable Forest Management (SFM) as the forest exploitation practice that has the potential to ensure the sustainable use of this natural resource. Brandt et al. (2016) point out that a growing portion of tropical forests is managed to achieve biodiversity conservation, forest protection, and increased income.

It is worth to highlight that in sustainable forest management is knowledge of its economic aspects. In timber production in the Amazon, this study would have the potential to support decision-making by local forest firms, and the identification of costs will underpin other economic research in the region. These ideas are based on Barreto et al. (1998), who argue for the need for detailed cost-benefit analyses of management to support the debate on forest use. Furthermore, Applegate et al. (2004) argue that most timber entrepreneurs are not fully aware of the costs of timber harvesting.

It is worth noting that Barreto et al. (1998), Boltz et al. (2001), De Graaf et al. (2003), Holmes et al. (2001) and Holmes et al. (2002) identified the costs of forest management in the Amazon. However, each region of the Amazon has peculiarities, such as forest stock and variation in the stumpage price which affect costs. Thus, it is recommended to carry out studies using data collected in different areas of this biome.

According to Amaral et al. (2012), the state of Acre has 87% of its territory covered by natural forest. Given this scenario, studies such as Machado (2013), Silva (2003), Silva and Santos (2011) and Silva (2015) have calculated the management costs in Acre. However, research identifying the cost of forest management implemented at different forest-to-sawmill distances is needed, considering or not the installation and measurement of permanent plots (PP) and the adoption of silvicultural treatments (ST).

Given the above, this study aimed to generate economics information on sustainable forest management in the state of Acre. Specifically, it aimed to: 1) quantify the cost of producing logs delivered to sawmills, at different forest-to-sawmill distances, considering management with or without the installation and measurement of permanent plots (PP) and the application or not of silvicultural treatments (ST) and 2) identify the profit margin for logs delivered to sawmills in Acre.

2 MATERIALS AND METHODS

2.1 Materials

2.1.1 Study Area. The study area is the state of Acre, in the Amazon, between latitudes 07°07' S and 11°08' S and longitudes 66°30' W and 74° W. This state has an area of 164,221.36 km² (4% of the Brazilian Amazon), and borders Peru, Bolivia, and the states of Amazonas and Rondônia (Acre, 2010). Figure 1 summarizes this information.

Figure 1. Location map of the state of Acre, Brazil.

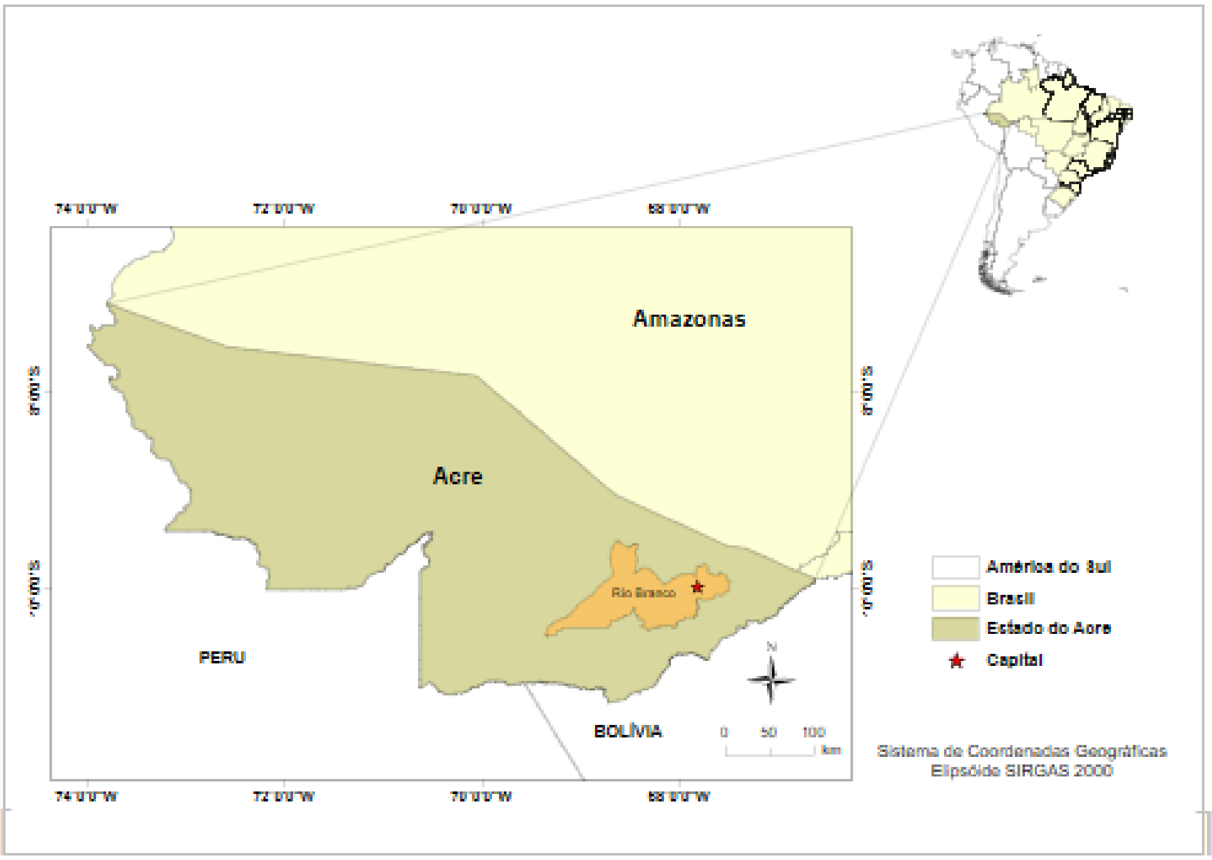

According to the Brazilian Institute of Geography and Statistics (IBGE) (2016), the population of Acre is 816,687 inhabitants, of which 46.17% reside in Rio Branco.

In the state of Acre, the climate is of the hot and humid equatorial type, characterized by high temperatures, high rainfall levels, and high relative humidity, with an average annual temperature of around 24.5°C (ACRE, 2010). According to the Köppen-Geiger climate classification, Acre presents two climate subtypes: Tropical humid or Equatorial (Af) and Tropical monsoon (Am) (Kottek et al., 2006).

The main hydrographic basins of Acre are the Purus River and the Juruá River basins, located in the central and eastern region and in the west of state, respectively. All rivers and streams belong to the Amazon River hydrographic network (Guilherme, 2016).

Argisol soil classes cover approximately 40% of the state's area, followed by Cambisols, which occupy about 30% of the territory (ACRE, 2006).

According to Acre (2010), two large phytoecological regions predominate: Dense Ombrophilous Forest and Open Ombrophilous Forest, with the individual or simultaneous occurrence of different plant formations (vines, bamboos, palm trees). There is a third region, the *Campinarana*, restricted to the northwestern part of the State.

2.1.2 Local Forestry-Timber Production Process. The stages of log production, originating from management plans in Acre, adopt the procedures required by federal legislation, such as Decree 5.975/2006 (Brazil, 2006a); Normative Instruction (IN) of the Ministry of the Environment (MMA) No. 05/2006 (Brazil, 2006b); IBAMA Execution Standard No. 01/2007 (Brazil, 2007); Conama Resolution No. 406/2009 (Brazil, 2009); MMA IN 01/2015 (Brazil, 2015); and state legislation: Joint Resolution CEMACT/CFE No. 003/2008 (Neves, 2009).

The stage of preparing the Sustainable Forest Management Plan (SFMP) and the Annual Operational Plan (AOP) includes pre-exploration activities, carried out one year before exploitation, and necessary for the licensing of these documents (Thaines, 2013). The first phase of the process is the preparation of the SFMP, with the execution of a sample forest inventory in the Forest Management Unit (FMU) (Espada et al., 2013), in order to collect qualitative and quantitative data on the forest (BRASIL, 2009).

The area to be exploited in a given year is called the Annual Production Unit (APU), where a 100% forest inventory is carried out (Balieiro et al., 2010). Microzoning identifies permanent preservation areas, areas of liana thickets and bamboo (BRASIL, 2007). Then, the Annual Operational Plan (AOP) is prepared, which is the planning document for exploitation in the APU (Balieiro et al., 2010), containing data on the species and volume to be exploited, trees to be maintained, planned activities such as road and yard construction, exploitation and post-exploration procedures (BRASIL, 2007).

Once the AOP is prepared, in accordance with Joint State Resolution CEMACT/CFE No. 003/2008, legislation that guides the licensing, monitoring, and inspection of forest management in Acre, the Sustainable Forest Management Plan (SFMP) and the AOP are submitted to the Acre Institute of the Environment (IMAC).

To assess the damage caused by logging, permanent plots (PPs) are installed and measured before intervention in the forest, and remeasured after exploitation (Oliveira et al., 2004). The cutting of vines occurs before harvesting, when planned (BRASIL, 2007).

According to Joint Resolution CEMACT/CFE No. 003/2008, after the licensing of the SFMP/AOP, the responsible environmental agency, within its attributions, issues the Operating License (OL) and the Authorization for Exploitation (AUTEX).

Logging activities are carried out after the issuance of the OL and AUTEX, which, according to Thaines (2013), include the construction of roads and storage yards; tree cutting; skidding planning, marking of skidding trails; skidding of logs to the yards; yard operation, such as log measurement, organization, loading, and transshipment (intermediate transport of logs from storage yards in the forest to a central yard usually located near consolidated transport infrastructure, such as paved roads. Espada et al. (2013) comment that the transport of logs occurs from the forest to the industry yard.

After the exploitation of the APU, an Activity Report must be submitted to the environmental agency (Brazil, 2009), detailing the activities carried out and the volume effectively exploited in this APU (Brazil, 2006b). Among the post-exploration activities, there are also: infrastructure maintenance; monitoring of forest growth (when foreseen in the SFMP), through measurement of the installed PP and carrying out silvicultural treatments and forest protection, when foreseen in the management plan (Thaines, 2013).

2.2 Data Collection

Considering procedures adopted by Silva (2015) and Silva and Santos (2011), data collection for this study focused on the following factors: 1) Price of unmanaged forest land; 2) Price of forest raw materials; 3) Development and execution of the SFMP/AOP; 4) Forest harvesting; and 5) Transportation of logs to the sawmill.

The basic data used to quantify the cost of log production were obtained through interviews using a specific questionnaire. Interviews were chosen because, according to Gil (2008), this procedure allows for greater contact with the reality experienced by social actors and, according to May (2004), this form of data collection generates rich understandings of experiences and opinions on a given subject.

The interviews focused on the city of Rio Branco, since according to Acre (2010), this city concentrates 63% of the Acrean timber industries, in addition to 69% of the direct jobs in the timber industry sector throughout the state of Acre. According to Lentini et al. (2005), Rio Branco represents the main timber hub of this state.

The interviews took place in December 2016 and addressed the agents involved in activities related to SFM carried out in Acre: 1) Forestry engineers who prepare and execute SFMP and AOP in the region; 2) Sawmill owners who carry out SFM to supply wood to their companies; 3) Logging executor and 4) Forestry engineers, responsible, at IMAC, for licensing forest management activities.

Data collection was carried out according to an accessibility sampling method, as described by Gil (2008). Thus, interviewees were selected according to the interviewer's accessibility to them, assuming that the interviewees could, in some way, be representative of the researched universe.

The engineers from IMAC provided specific data on the SFMP licensing process and its respective fees, such as the amounts charged for inspection and the license. These interviewees also contributed data on the management practices in Acre, such as the length of roads (km) and the number of storage yards in the AOPs.

The questionnaire was applied to consultants, sawmill owners, and the forestry extraction company. Data regarding land prices at different forest-to-Rio Branco distances were obtained from a real estate agency located in Rio Branco.

The timber entrepreneurs and forest consultants interviewed provided data on the price of logs, delivered to sawmills, for different species, as practiced in the local market.

Following the procedure adopted by Silva and Santos (2011), the data were broken down into physical and economic values, as indicated below.

The physical values obtained, as suggested by Machado (2013) and Silva and Santos (2011), were those inherent to the SFMP/AOP: 1) average total area of the Annual Production Units, in hectares; 2) average annual volume of timber in logs (m^3 $year^{-1}$) and 3) average volume harvested in the AOPs, per unit area of effective harvesting (m^3 ha^{-1}).

Table 1 presents the average data used in quantifying the production cost.

Table 1. Characterization of Annual Production Units (APUs), state of Acre, 2016.

Items	Unit	Value
Average total area of the APUs	(ha)	1,030.56
Average annual volume of timber logs	(m^3 $year^{-1}$)	12,400.00
Average volume extracted at the APUs	(m^3 ha^{-1})	14.71

Economic data refers to land prices, log prices, service provision and operational costs, according to Silva (2015) and Silva and Santos (2011).

It should be noted that, due to the difficulty in obtaining detailed cost data for certain activities, the price charged for carrying out these operations was considered as a *proxy* value to represent these costs, according to the procedure adopted by Silva (2015). Thus, for the items of preparation of the SFMP/AOP, forest census, installation and measurement of permanent plots and post-exploration report, the prices charged by forestry consultants to perform such services were taken into account. In the operations of cutting, skidding, loading, transshipment, reloading, support camp, and forest transport, the price paid by sawmills to the firms providing these services was adopted.

In the planning of a APU, according to IN 05/2006 (BRAZIL, 2006b), the volume exploited is that per area of effective forest exploitation: the area effectively exploited in the APU, not counting the Areas of Permanent Preservation (APP) and infrastructure.

The costs of SFM were quantified per area of effective exploitation. From the data collected on AOPs, it was considered that the unexploited areas (APPs) correspond on average to 18% of the total area of the APU. Thus, an average area of 845.06 ha of effective exploitation was obtained (82% of a UPA with 1,030.56 ha).

Thus, the prices charged for the total area of the APU were converted to effective area, multiplying the conversion factor (1.21951 - obtained by dividing the average total area of the APU by the effective harvest area).

It was found that sawmill owners in Acre, when they do not own their own forest area, enter into a contract with the owners of forest lands. The landowner charges a price per unit area (hectares) for this timber firm to exploit the forest under a Sustainable Forest Management Plan (SFMP) regime. This allows these companies to be responsible for the execution and holders of the SFMP/POA.

The average price obtained in the interviews was R$ 557.14 ha^{-1}. According to those interviewed, the payment method, which depends on the negotiation, may have the following options: 1) the total amount is paid in three installments; 1st installment 30% after issuance of the AUTEX; 2nd installment 30 days after the start of exploitation and the 3rd installment 90 days after the start of exploitation; 2) the total amount is paid in twelve installments, with the first installment paid after issuance of the AUTEX and the remaining installments monthly; and 3) the total amount is paid in three installments, 1st installment 30% after issuance of the AUTEX, the 2nd installment 40% in the month the exploitation begins and the 3rd installment 30% at the end of the exploitation.

To calculate the stumpage price, the average contract price (R$ 557.14 ha^{-1}) was divided by the average volume harvested from the APUs (14.71 m^3 ha^{-1}), resulting in R$ 37.86, which corresponds to the value paid per cubic meter of log harvested.

The average price to prepare and execute the SFMP/AOP is R$ 87.50 ha^{-1} (for the total area of the APU). The price for the area of effective harvesting was R$ 106.71 ha^{-1}.

The taxes levied on the preparation of the SFMP/AOP are related to the provision of services: 1) Withholding Income Tax (IRRF); 2) Social Integration Program (PIS); 3) Contribution to Social Security Financing (COFINS); 4) Social Contribution on Net Profit (CSLL) and 5) Tax on Services of Any Nature (ISS).

It should be noted that these taxes correspond to 16.15% of the price charged for preparing the SFMP/AOP. Thus, considering that the average price for preparing the SFMP/AOP is R$ 106.71 ha^{-1}, a value of R$ 17.23 ha^{-1} was obtained.

The average cost of notary documentation was R$ 0.28 ha^{-1}, obtained by dividing the cost by the average area of effective exploitation (845.06 ha). The notary fees involve the following items: 1) signature authentication; 2) registration of the legal reserve area on the margins of the rural property registration; 3) property certificate; registration of the Term of Responsibility for the Maintenance of Managed Forest (TRMFM) and 4) Term of Forest and Technical Responsibility (TRFT), if the preparation of the SFMP is carried out by a technician different from the preparation and execution of the AOP.

The fees with the Regional Council of Engineering and Agronomy (CREAA)/Technical Responsibility Annotation (ART) refer to the payment of the ART of the technician responsible for the preparation and/or execution of the SFMP/AOP. The average cost with ART was R$ 0.10 ha^{-1}, obtained by dividing the cost by the average area of effective exploitation (845.06 ha).

In addition to federal legislation, SFM licensing follows guidelines and procedures from Joint Resolution No. 003, of August 12, 2008, of the State Council for the Environment, Science and Technology and the State Forestry Council.

The licensing costs are the costs for licensing the SFMP and the AOP with IMAC. The items involved in this process are licensing fee, calculated based on the total area of the APU; technical inspection fee; travel fee, calculated based on the distance to the managed area and administrative fee. The total value is multiplied by two years, the validity of the OL and AUTEX. A simulation was carried out, together with a person responsible for the Forest Management sector in the environmental agency. The average total area of the APUs (Table 1) was considered, located at different distances from Rio Branco (50 km, 100 km and 150 km). The cost for the total area was R$ 3.82 ha-1 (50 km), R$ 4.55 ha^{-1} (100 km), and R$ 5.27 ha^{-1} (150 km). The cost converted to effective area was R$ 4.66 ha^{-1} (50 km), R$ 5.55 ha^{-1} (100 km), and R$ 6.43 ha^{-1} (150 km).

The interviewees revealed that the average price charged by consulting firms for conducting a 100% forest inventory was R$ 42.80 ha^{-1}. It should be noted that this value is included in the price charged for preparing the SFMP/AOP.

Permanent plots (PPs), as reported by Silva et al. (2005), serve to monitor the growth dynamics of managed forests through continuous forest inventory (CFI), and should be established in forest production areas. However, conducting the CFI is optional, being mandatory only to justify the adoption of parameters different from those presented in Normative Instruction No. 5, of the MMA, of December 11, 2006, such as, for example, the alteration of the cutting cycle.

To identify the costs of implementing and measuring PPs, two data sources were used: the responses of the interviewees and the work of Santos (2007). Thus, the data obtained generated an average cost of R$ 3.00 ha^{-1}. In Santos (2007), studying the installation and measurement of a permanent plot in the Antimary State Forest, in the state of Acre, in 2005, the cost found was US$ 432.26 per plot. Following procedures presented by Oliveira et al. (2004), it was assumed that a PP should be installed for every 250 ha of managed area. Thus, a cost of US$ 1.73 ha^{-1} was obtained. Given these values, the average cost to install and measure permanent plots was found to be US$ 1.15 ha^{-1}.

Oliveira et al. (2004) state that plots should be measured again the year after harvest, and from then on the intervals between measurements should be two to five years. To identify the costs of this activity, in addition to data obtained through interviews, with an average value of R$ 2.50 ha^{-1}, the cost of US$ 314.11 for remeasurement of plots, found by Santos (2007), was used. Considering that a permanent plot should be installed for every 250 ha of managed area, the cost for remeasurement of plots is US$ 1.26 ha^{-1}. The average cost of remeasurement of permanent plots obtained was US$ 0.89 ha^{-1}.

As verified in the interviews, the holder of the management plan must present to IMAC copies of the publication in the State Official Gazette and a local daily newspaper of the licensing request and receipt. Furthermore, according to Joint Resolution CEMACT/CFE No. 003/2008, upon receiving the LO and the AUTEX, the holder must affix signs indicating the forest management area on the property before exploitation. The average cost of these activities, obtained by dividing the cost by the average area of effective exploitation (845.06 ha), was R$ 0.52 ha^{-1}.

According to CEMACT/CFE Resolution No. 003/2008, the post-exploration (or activity) report must be submitted to IMAC before requesting a new AOP or up to one hundred and eighty days after the completion of the actions described in the AOP of the exploited APU (Neves, 2009). Consultants charge an average price of R$ 4.46 ha^{-1} (total area) to prepare the document, or, R$ 5.40 ha^{-1} to the area of effective exploitation.

Logging is generally carried out by third-party firms, which are responsible for all operations, from felling to unloading the logs at the storage yard. To quantify the costs of this process, the price paid by the timber industries to the contracted firms was considered, as well as the price charged by the service provider itself. It should be noted that payment for these activities is based on the cubic meter of logs exploited, in commercial measure. The commercial measure adopted in Acre's sawmills is an adaptation of the Francon method or the reduced 4th method. This method yields the volume of a squared log (BRASIL, 2003). According to information obtained in interviews, the measurement adopted by Acre's timber merchants involves a modification, in which the sapwood is deducted from one of the measurements of the smaller diameter face of the log.

The average price paid/charged for the construction of roads and yards, obtained from data collection, was R$ 9.75 m^{-3}. However, it was decided to calculate the cost separately for roads and yards, based on AOPs data obtained from the interviews.

The average price for renting machinery to open the infrastructure, obtained from the interviews, of R$ 2,150.00/km of road (4 m wide) was adopted. In addition, since the management projects have an average of 0.032 km of roads/ha (effective area), a cost of R$ 68.80 ha^{-1} was obtained. This value was divided by the average volume exploited in the APUs (14.71 m^3 ha^{-1}), and a cost of R$ 4.68 m^{-3} was obtained for opening roads.

For the activity of opening yards, according to AOPs data, it was considered that on average, an yards infrastructure of 500 m^2 (20 x 25m) corresponds to 0.44% of the effective area of a APUP. The average effective exploitation area obtained in this study (845.06 ha) was used, resulting in a total yard area of 37,182.64 m^2. Thus, considering that 1 km of road 4 m wide corresponds to 4,000 m^2 (0.4 ha), and that the cost for opening 4,000m^2 is R$ 2,150.00, the total cost for yards is R$ 19,985.67. Considering the average effective area and the average exploited volume obtained in this study, the cost for opening yards is R$ 23.65 ha^{-1} or R$ 1.61 m^{-3}.

Another point to highlight is that, in calculating the cost of forest extraction, it was assumed that this activity can occur in two ways: one operation including the transport of logs between storage yards in the forest and a yard located near a paved highway; and another without this kind of transport. It should be noted that kind of transport allows the company to supply itself with logs year-round, because during the rainy season, trucks are prevented from traveling on unpaved roads within forest areas, and companies are supplied by logs deposited in the yard near paved roads, known as the "esplanada" (storage area). From the above, this study presents a scenario where a company in Rio Branco operates year-round. Thus, during the dry season (four months), it supplies itself without using that kind of transport, while during the remaining eight months, it uses this kind of transport to supply its logs. Therefore, the average final cost of forest exploitation for this firm resulted from a weighted average of the costs with and without this kind of transport, where the weight used was the percentage share that each of these exploitation systems has in the total volume of logs processed by the firm, 67% and 33%, respectively.

The average prices for cutting, skidding, loading, transshipment, reloading, and support camp operations were R$ 9.38 m^{-3}, R$ 25.36 m^{-3}, R$ 8.58 m^{-3}, R$ 15.00 m^{-3}, R$ 7.75 m^{-3}, and R$ 11.75 m^{-3}, respectively. Support infrastructure costs include camp, helper, food, and cook. The average costs of exploitation, with transshipment, were R$ 84.11 m^{-3} and without transshipment, were R$ 61.36 m^{-3}.

The transportation of timber is carried out by service providers, with the log placed in the sawmill yard. The freight costs for forest-sawmill distances of 50, 100, and 150 km were R$ 40.83 m^{-3}, R$ 72.00 m^{-3}, and R$ 93.33 m^{-3}, respectively.

Silva et al. (2005) comment that administrative costs account, on average, for 17.5% of the annual subtotal costs. These costs, according to Silva and Santos (2011), involve costs for accounting, office, and field supervision services.

During the interviews, data on the costs of issuing invoices for rural producers were obtained. Subsequently, a document issued by the State Finance Secretariat was found to indicate that, for the transport of logs within the state of Acre, the issuance of an Electronic Invoice is not required. However, the document states that if an invoice is issued for the raw product (logs), the field relating to the Tax on the Circulation of Goods and Services (ICMS) does not need to be filled in.

Therefore, it was decided to consider the issuance of the invoice when quantifying the production cost. In addition, it was taken into account that, according to interview data, an invoice must be issued for each truckload, with a volume between 40 and 60 cubic meters, and the cost to issue an invoice is R$ 3.00. Thus, a cost of R$ 0.06 m^{-3} was obtained for issuing the invoice, for an average volume per truckload of 50 m^3.

Some respondents reported that there are tax costs associated with the sale of logs, with 2.25% of the gross value of the logs being collected for the Rural Worker Support Fund (Funrural). Thus, since the average price practiced in the local market for logs delivered to sawmills was R$ 256.7 m^{-3}, the cost of Funrural collection is R$ 5.78 m^{-3}.

Forestry consultants and sawmill owners reported that income tax costs account for 27.5% of the net profit from the sale of logs.

The secondary data used in this study were data from AOPs executed in the state of Acre, referring to the length of roads (km) and total area of storage yards (m^2).

Operational cost data for PP in a management area in Acre were used, from Santos (2007). Costs concerning post-exploration silvicultural treatments in a management area in the Amazon were obtained from the study by Ferreira (2012). Cost data for the pre-exploration activity of vine cutting were obtained from the work of Thaines (2013).

Cutting vines intertwined with the trees to be harvested and neighboring trees is recommended to avoid the undue fall of trees and the risk of accidents for the field team (Balieiro et al., 2010). It is recommended that this activity be carried out at least one year before harvesting, preferably along with or immediately after a 100% forest inventory (Fundação Floresta Tropical (FFT), 2002).

Due to the difficulty in obtaining data for cutting vines activity during data with the interviewees, the cost presented by Thaines (2013) was considered. This author takes into account that the vine cutting team in an exploration area of 1,000 hectares, in the Tapajós National Forest, in Pará, was composed of four workers, and the remuneration for the 1,000 ha undertaking was R$ 6,000.00, which corresponds to R$ 6.00 ha^{-1}.

Post-logging silvicultural treatments include the release of remaining commercial trees through thinning, girdling of competing trees, or cutting of vines; the management of natural regeneration; enrichment plantings in clearings, among others (Espada et al., 2013). The cutting of vines should be repeated after logging on the remaining trees to facilitate their development (FFT, 2002).

The adoption of silvicultural treatments (TT) in managed areas in Acre is incipient or non-existent, which made it impossible to obtain data for this activity. However, since this study considered scenarios that include such activity, data from Ferreira (2012) were used, who determined the installation, monitoring, and maintenance costs of different post-harvest silviculture systems in a managed area in the municipality of Paragominas, Pará. The treatment selected contained the activities: 1) thinning for release, by girdling; 2) cutting of vines in the treated trees and 3) planting in clearings. The installation cost was R$ 96.80 ha^{-1} while the monitoring and maintenance costs was R$ 37.70 ha^{-1}.

To correct for inflationary effects on the economic values used in this study, the prices and costs considered were converted from Brazilian Real (R$) to US Dollar (US$). To do this, the official exchange rate for the sale of the US dollar was consulted on the website of the Central Bank of Brazil (BCB). Therefore, using the 15th (or the next business day) of each month of 2016 as a reference, the average exchange rate obtained was US$ 1.00 = R$ 3.5009.

3 Methods

Quantification of the cost of producing logs, harvested in a managed area and delivered to the timber company's yard, in the state of Acre

This calculation is justified by the words of Sasaki et al. (2016), who state that cost is the main concern for adopting Reduced Impact Logging (RIL). Thus, since RIL is the concept used in forest exploitation adopted in the state of Acre, its economics evaluation will contribute to the evaluation of sustainable forest management as a whole.

The quantification of the cost of log production followed a procedure adapted from the method indicated by Silva (2015), summarized in the following expression.

$$C_{pf} = C_{mp} + C_{ef} + C_{tf} + C_{nf} + C_{Funrural} + C_{IR} \quad (1)$$

Where: C_{pf} is the production cost (minimum price) of logs harvested in a managed area and delivered to the sawmill's yard (US$ m^{-3}); C_{mp} refers to the production cost (minimum price) of stumpage in a managed area; C_{ef} refers to the cost of logging activities in an area under the SFM regime (US$ m^{-3}); C_{tf} is the cost of transporting logs from the managed area to the sawmill (US$ m^{-3});

C_{nf} is the cost of issuing the invoice for the logs (US$ m^{-3}); $C_{Funrural}$ is the cost related to the collection of Funrural (US$ m^{-3}); and C_{IR} is the cost of income tax on net profit (US$ m^{-3}).

Cost of production of stumpage in a forest management area in the state of Acre

The cost of production of stumpage was calculated as indicated by Silva (2003), being obtained through expression (2):

$$C_{mp} = P_{mp} + C_{mf} \quad (2)$$

Where: P_{mp} refers to the average stumpage price (US$ m^{-3}); C_{mf} is the cost of producing the SFM to be carried out (US$ m^{-3}).

The P_{mp}, as indicated by Silva (2003), is the price paid for stumpage to the forest owner, described previously. The C_{mf} involves the costs of forest management operations (in R$ ha^{-1}), described in the previous section, obtained through expression (3):

$$C_{mf} = \frac{\sum_{t=0}^{n} \frac{C_t}{(1+i)^t}}{\frac{V_m}{(1+i)^{t_e}}} \quad (3)$$

Where: C_t represents the total cost of AFM activities in the year t (US$ ha^{-1}); V_m refers to the average volume harvested per area of effective exploitation (m³ ha^{-1}); i is the opportunity cost of capital (interest rate), expressed as a decimal (p.a.); t represents the year in which a given cost occurs; and t_e is the year in which logging takes place.

Net present value (NPV) of SFM activities

The economic viability of MFS activities was verified by calculating the NPV, according to the following expression (4), presented by Rezende and Oliveira (2011):

$$VPL = \sum_{t=0}^{n} R_t(1+i)^{-t} - \sum_{t=0}^{n} C_t(1+i)^{-t} \tag{4}$$

Where: VPL is the net present value of SFM activities (US$ ha^{-1}); C_t is the cost of SFM operations at the end of the year t (US$ ha^{-1}); R_t is the revenue at the end of the year t (US$ ha^{-1}); n is the project duration, in years and t is the year in which the revenue or cost occurs.

Revenue was obtained by multiplying the minimum price of stumpage by the average volume harvested in the APUs (14.71 m^3 ha^{-1}). According to Silva and Fontes (2005), when a project that has an NPV greater than zero, it is economically viable.

The cost of production C_{ef} comprises activities related to logging, which includes the costs of road and yard infrastructure, cutting, skidding, loading, timber forwarding, reloading, and support infrastructure.

It should be noted that the final cost of the operation was obtained by the weighted average of the costs of the logging systems with and without timber forwarding. To meet the demand for wood, a sawmill may or may not carry out timber forwarding during forest exploitation. It was considered that a sawmill operates year-round, when the system without timber forwarding occurs in four months (weight of 0.33), during a year of operation of the timber company, while the system with timber forwarding has a participation of eight months (weight of 0.67) in production. Thus, during logging in the dry season, for every three trucks, two carry out timber forwarding of the production and one goes directly to the sawmill in Rio Branco.

C_{tf} involves the cost of transporting the log from the forest to the sawmill yard in Rio Branco. C_{nf} in turn includes the cost of issuing the invoice for transporting the log within the state of Acre. While $C_{Funrural}$ is the cost generated by the collection of Funrural, at the time of sale of the log. Finally C_{IR} indicates the cost of Income Tax on the net profit from the sale of the log.

The net profit was obtained using expression (5):

$$L = R - C \tag{5}$$

Where: L is the net profit from the sale of logs (US$ m^{-3}); R is the gross revenue from the sale of logs, in other words, the average local price of logs (US$ m^{-3}); and C is the sum of the costs of log production (US$ m^{-3}), obtained using the expression (6):

$$C = C_{mp} + C_{ef} + C_{tf} + C_{nf} + C_{Funrural} \tag{6}$$

Next, the income tax (C_{IR}) was calculated using the following expression (7):

$$C_{IR} = L \times 0.275 \tag{7}$$

Where C_{IR} is the income tax on the net profit from the sale of the log (US$ m^{-3}).

The cost of production was quantified and analyzed considering three types of situations: 1) based on the distance from the forest to the sawmill in Rio Branco; 2) whether or not the forest has permanent plot (PP) measurements and 3) based on the application or not of post-harvest silvicultural treatments (ST).

It is worth mentioning that the scenarios with plots include the installation, measurement, and remeasurement of PP. The situations with treatments, in turn, in addition to the installation, measurement, and remeasurement of PP, include the activities of installation, monitoring, and maintenance of silvicultural treatments (ST). Furthermore, a 25-year cutting cycle was adopted as the planning horizon for the SFM, which complies with CONAMA Resolution No. 406/2009.

As already mentioned, for quantifying the cost of log production from SFM, addressed three scenarios, namely, forest located 50 km, 100 km and 150 km from the sawmill in Rio Branco. In addition, for each of these scenarios, the possibility of the SFM analyzed having or not having the installation and measurements of permanent plots (PP) was given. Finally, for each of the situations mentioned, the possibility of carrying out or not silvicultural treatments (STs) in the management addressed was considered.

In addition, different interest rates were used to analyze the behavior of forest production costs, as recommended by Pearse (1990) and Wagner (2012). As suggested by Lima Júnior et al. (1997), the rates used in forest projects vary from 6 to 12% per year. Therefore, discount rates of 6% a.a., 8% a.a., 10% a.a. and 12% a.a. were adopted, following the procedure of Silva and Santos (2011).

It should be noted that the price of land was included in the cash flow as a cost in year zero and an income at the end of year 24, as adopted by Silva and Santos (2011). Thus, it is assumed that the land is acquired at the beginning of the cutting cycle and sold at the end of it.

Regarding silvicultural treatments (TTs), for the cash flow, the following guidelines from Ferreira (2012) were followed: the installation costs of the TTs occur one year after exploitation, while maintenance and monitoring costs occur annually for the first five years, and thereafter, every five years, until the end of the cutting cycle.

Marketing Margin for Logs Delivered to Sawmills

The absolute (or gross) marketing margin for logs was calculated using expression (8), indicated by Mendes and Padilha Júnior (2007):

$$M = P_{mt} - C_{pf} \tag{8}$$

Where: M is the absolute marketing margin for logs from managed areas in Acre (US$ m^{-3}); P_{mt} is the average price of logs, harvested in managed areas and delivered to the sawmill yard, played in the local market (US$ m^{-3}) and C_{pf} is the production cost of logs, harvested in a managed area and delivered to the sawmill yard (US$ m^{-3}).

The marketing margin was used as an indicator of profit or loss in log production, in the different scenarios adopted. For this, the average price of logs practiced in the local market, obtained in the data collection, used as income, was R$ 256.7 m^{-3}.

4 RESULTS AND DISCUSSION

Cost of stumpage production in the state of Acre, 2016

The average selling price of stumpage in the Acrean timber market in 2016 was US$ 10.82 m^{-3}. It should be noted that it was verified that there is no differentiation in prices for the different groups of species, of higher or lower commercial value, since the negotiation occurs according to the size of the UPA. However, by way of comparison, the stumpage price in Acre in 2008, presented by Silva (2015), was differentiated for three groups of commercial species: noble species (US$ 27.12 m^{-3}); hardwood species (US$ 21.81 m^{-3}) and softwood species (US$ 22.76 m^{-3}). In turn, the average market price of stumpage, presented by Silva and Santos (2011), in a study carried out in the state of Acre in 2011, was US$ 25.16 m^{-3}. From the above, it can be seen that the price found in this study is considered lower compared to the values presented in previous studies.

It was noted that the average volume harvested in the managed forests of Acre, according to the data obtained in this study (14.71 m^3 ha-1), did not reach the maximum cutting intensity of 30 m^3 ha-1 (when using machines for log skidding), foreseen in Conama Resolution No. 406/2009 (BRAZIL, 2009). The volume harvested is considered low, compared to the average harvest value of 25.36 m^3 ha^{-1}, observed in the study by Holmes et al. (2002), carried out in Paragominas, state of Pará. It is emphasized that the volume exploited directly affects the costs of log production.

The interviewees stated that the commercial volume harvested in managed areas in the state of Acre rarely reaches the maximum allowed by law. One of the main factors that interfere with the volume harvested in a managed area refers to the species demanded by the market. For example, in the preparation phase of an Annual Operational Plan (AOP), it is planned to exploit a certain species, selecting it for cutting. However, in the year of harvesting, this species has a low commercial value, causing the decision-maker to choose not to exploit all the individuals of this species selected for cutting, or even to decide not to exploit it, thus reducing the volume of cutting. In addition to this factor, the characteristics of the forest considerably interfere with the volume harvested. According to Hosokawa et al. (1998), the productivity of native forests is influenced by the productive capacity of the soil and the heterogeneous distribution of species in the area.

Ferreira (2014) states, the Acrean forests are characterized by the dominant presence of bamboo species of the genus *Guadua*. According to Silveira (2001), bamboo dominance can limit the competitive ability of tree species with low adaptive capacity to the environment, leading to alterations in floristic composition and a reduction of almost 40% of species in a one-hectare sample. Furthermore, that bamboo alters the forest structure, decreasing density and basal area. Ferreira (2014) cites that, during logging, clearings are created in the forest canopy, providing abundant physical space and light, which are extremely favorable to bamboo development. So, it is emphasized the need to understand the conditions that favor the appearance of bamboo, its growth rate, and the time it takes to dominate a given forest area. This author also argues that this information is urgent for the case of the forests of Acre, since it is in the central and eastern regions of the state, where the bamboo forests are concentrated, that logging is most intense.

Thus, it is understood that timber production in these forests can vary from region to region and according to the predominant type of vegetation, where certain areas may present a higher occurrence of individuals of species with greater commercial value.

The costs of SFM, in native forest areas in the state of Acre, for the year 2016, are presented in Table 2.

Table 2. Composition of MFS cost for a 25-year cutting cycle, converted to effective management area, state of Acre, 2016.

YEAR	ITEM	50 km			100 km			150 km		
		With PP	**Without PP**	**With PP and TS**	**With PP**	**Without PP**	**With PP and TS**	**With PP**	**Without PP**	**With PP and TS**
0	Land price	243.84	243.84	243.84	200.30	200.30	200.30	148.05	148.05	148.05
	Preparation of SFMP/AOP	30.48	30.48	30.48	30.48	30.48	30.48	30.48	30.48	30.48
	Taxes	4.92	4.92	4.92	4.92	4.92	4.92	4.92	4.92	4.92
	Fees for CREA/ART	0.03	0.03	0.03	0.03	0.03	0.03	0.03	0.03	0.03
	Registry Office	0.08	0.08	0.08	0.08	0.08	0.08	0.08	0.08	0.08
	Licensing/IMAC	1.33	1.33	1.33	1.58	1.58	1.58	1.84	1.84	1.84
	Installation/Measurement PPs	1.15	-	1.15	1.15	-	1.15	1.15	-	1.15
	Cutting of Vine Trees*	1.71	1.71	1.71	1.71	1.71	1.71	1.71	1.71	1.71
	Publication and SFMP Sign	0.15	0.15	0.15	0.15	0.15	0.15	0.15	0.15	0.15
	Subtotal	**283.69**	**282.54**	**283.69**	**240.40**	**239.26**	**240.40**	**188.41**	**187.26**	**188.41**
	Administration	49.65	49.45	49.65	42.07	41.87	42.07	32.97	32.77	32.97
	Total	**333.34**	**331.99**	**333.34**	**282.47**	**281.13**	**282.47**	**221.38**	**220.03**	**221.38**
1	Post-exploratory report	1.54	1.54	1.54	1.54	1.54	1.54	1.54	1.54	1.54
	Administration	0.27	0.27	0.27	0.27	0.27	0.27	0.27	0.27	0.27
	Total	**1.81**	**1.81**	**1.81**	**1.81**	**1.81**	**1.81**	**1.81**	**1.81**	**1.81**
2	Remediation of permanent plots	0.89	-	0.89	0.89	-	0.89	0.89	-	0.89
	Silvicultural treatments	-	-	27.65	-	-	27.65	-	-	27.65
	Subtotal	**0.89**	**-**	**28.54**	**0.89**	**-**	**28.54**	**0.89**	**-**	**28.54**
	Administration	0.16	-	5.00	0.16	-	5.00	0.16	-	5.00
	Total	**1.05**	**-**	**33.54**	**1.05**	**-**	**33.54**	**1.05**	**-**	**33.54**
3–6	Silvicultural treatments**	-	-	10.77	-	-	10.77	-	-	10.77
	Administration	-	-	1.88	-	-	1.88	-	-	1.88
	Total	**-**	**-**	**12.65**	**-**	**-**	**12.65**	**-**	**-**	**12.65**

Continued

YEAR	ITEM	50 km			100 km			150 km		
		With PP	Without PP	With PP and TS	With PP	Without PP	With PP and TS	With PP	Without PP	With PP and TS
7, 12, 17, 22	Remediation of permanent plots	0.89	-	0.89	0.89	-	0.89	0.89	-	0.89
	Silvicultural treatments**	-	-	10.77	-	-	10.77	-	-	10.77
	Subtotal	**0.89**	**-**	**11.66**	**0.89**	**-**	**11.66**	**0.89**	**-**	**11.66**
	Administration	0.16	-	2.04	0.16	-	2.04	0.16	-	2.04
	Total	**1.05**	**-**	**13.70**	**1.05**	**-**	**13.70**	**1.05**	**-**	**13.70**

Source: *Thaines (2013). ** Fonte: Ferreira (2012).

The price of forest land located 100 km from Rio Branco is 17.86% lower compared to the price of land 50 km from that city. Conversely, the price of an area 150 km from Rio Branco is approximately 40% lower than the price of land located 50 km from that city. The costs related to forest management licensing increase as the management area becomes more distant. In the simulation carried out in this study, the increase in licensing costs, changing the distance from 50 km to 150 km between the forest and the sawmill in Rio Branco, was about 39%, due to the costs of displacement.

The price of land corresponds, on average, to 70.31% of the total cost of year zero for scenarios with PP and 70.66% for scenarios without PP. The lowest costs correspond to the costs of Technical Responsibility Report (ART), notary documentation, and costs of publication and management signage. It is important to mention that, according to the interviewees, the costs of notary documentation are generally the responsibility of the landowner. It is also noted that the cost for remeasurement of permanent plots decreases by about 23% compared to the cost of implementing and measuring PP in year zero.

The SFM costs at different interest rates are shown in Table 3.

Observing the values indicated in Table 3, it can be seen that the cost of SFM activities tends to decrease with increasing distance from the forest to the sawmill yard. This decrease is related to the price of forest land, which becomes lower as the distance from the timber hub in Rio Branco increases. The average cost of SFM for scenarios with plots was US$ 253.94 ha^{-1}, US$ 250.05 ha^{-1} for scenarios without PP and US$ 322.81 ha^{-1} for scenarios with PP and TS.

Table 4 presents a summary of the production cost (or minimum price) of this timber product in managed areas in the state of Acre.

The cost of producing stumpage also decreases with increasing distance, due to the costs of SFM activities. The average cost of stumpage producing, for the different rates analyzed, in an area located 50 km from the timber hub in Rio Branco, increases by approximately 0.82% with the installation, measurement, and remeasurement of PP throughout the cutting cycle. For areas 100 km and 150 km away, the average cost of producing stumpage increases by 0.91% and 1.05%, respectively, with the addition of continuous forest inventory activities.

For areas 100 km and 150 km away, the average cost of stumpage producing increases by 0.91% and 1.05%, respectively, with the addition of Continuous Forest Inventory (CFI)/Permanent Plot (PP) measurement activities.

Table 3. Cost of MFS in forest areas, the state of Acre, 2016.

Scenario	Description	Interest rate (% p.a.)	SFM Cost (US$ ha^{-1})
1	Management area located 50 km from the sawmill in Rio Branco, with PP	6	277.67
		8	298.97
		10	312.31
		12	320.72
2	Management area located 50 km from the sawmill in Rio Branco, without PP	6	273.48
		8	295.21
		10	308.88
		12	317.54
3	Management area located 50 km from the sawmill in Rio Branco, with PP and TS	6	368.52
		8	380.91
		10	386.89
		12	389.11
4	Management area located 100 km from the sawmill in Rio Branco, with PP	6	237.55
		8	254.98
		10	265.87
		12	272.72
5	Management area located 100 km from the sawmill in Rio Branco, without PP	6	233.37
		8	251.22
		10	262.44
		12	269.55
6	Management area located 100 km from the sawmill in Rio Branco, with PP and TS	6	328.40
		8	336.91
		10	340.45
		12	341.12
7	Management area located 150 km from the sawmill in Rio Branco, with PP	6	189.36
		8	202.12
		10	210.07
		12	215.06
8	Management area located 150 km from the sawmill in Rio Branco, without PP	6	185.17
		8	198.36
		10	206.64
		12	211.89

Continued

Scenario	Description	Interest rate (% p.a.)	SFM Cost (US$ ha^{-1})
9	Management area located 150 km from the sawmill in Rio Branco, with PP and TS	6	280.21
		8	284.06
		10	284.65
		12	283.46

It is noted that, if the holder of the Sustainable Forest Management Plan (SFMP) chooses to carry out the CFI in the managed forest, considering the results obtained in this study, there is little change in the final cost. This result was also observed by Machado (2013), when evaluating the cost of timber management in the state of Acre in 2012. The difference in cost in the scenario without PPM allocation compared to the one with plot allocation was 0.80%.

The difference between the average cost of producing stumpage, at different interest rates, with measurement and remeasurement of PP and application of TS after extraction, at 50 km, 100 km and 150 km from Rio Branco, represented an increase of 18.5%, 20.6% and 23.7% in the final cost, respectively, compared to scenarios without these operations.

Table 4. Composition of the cost of producing stumpage, for a 25-year cutting cycle, in a managed area, state of Acre, 2016.

Scenario	Description	Interest Rate (% a.a.)	Cost of SFM (US$ m^{-3})	Cost of stumpage production (US$ m^{-3})	Revenue (US$ ha^{-1})
1	Management area located 50 km from the sawmill in Rio Branco, with PP	6	20.00	30.82	453.36
		8	21.94	32.76	481.90
		10	23.35	34.17	502.64
		12	24.41	35.23	518.23
2	Management area located 50 km from the sawmill in Rio Branco, without PP	6	19.70	30.52	448.95
		8	21.67	32.49	477.93
		10	23.09	33.91	498.82
		12	24.17	34.99	514.70
3	Management area located 50 km from the sawmill in Rio Branco, with PP and TS	6	26.55	37.37	549.71
		8	27.96	38.78	570.45
		10	28.92	39.74	584.58
		12	29.62	40.44	594.87
4	Management area located 100 km from the sawmill in Rio Branco, with PP	6	17.11	27.93	410.85
		8	18.71	29.53	434.39
		10	19.88	30.70	451.60
		12	20.76	31.58	464.54
5	Management area located 100 km from the sawmill in Rio Branco, without PP	6	16.81	27.63	406.44
		8	18.44	29.26	430.41
		10	19.62	30.44	447.77
		12	20.52	31.34	461.01
6	Management area located 100 km from the sawmill in Rio Branco, with PP and TS	6	23.66	34.48	507.20
		8	24.73	35.55	522.94
		10	25.45	36.27	533.53
		12	25.96	36.78	541.03
7	Management area located 150 km from the sawmill in Rio Branco, with PP	6	13.64	24.46	359.81
		8	14.83	25.65	377.31
		10	15.70	26.52	390.11
		12	16.37	27.19	399.96
8	Management area located 150 km from the sawmill in Rio Branco, without PP	6	13.34	24.16	355.39
		8	14.56	25.38	373.34
		10	15.45	26.27	386.43
		12	16.13	26.95	396.43
9	Management area located 150 km from the sawmill in Rio Branco, with PP and TS	6	20.19	31.01	456.16
		8	20.85	31.67	465.87
		10	21.28	32.10	472.19
		12	21.58	32.40	476.60

Note: The average market price of standing timber considered was US$ 10.82 m^{-3}.

It is observed that the cost of production of stumpage increases with the increase in the discount rate. As an example, this value in scenario 1, calculated at a rate of 12% p.a., is 14.3% higher than that obtained at a rate of 6%. The average revenue for the evaluated rates, for management areas located 50 km, 100 km and 150 km from Rio Branco, is US$ 516.35 ha^{-1}, US$ 467.64 ha^{-1} and US$ 409.13 ha^{-1}, respectively.

It is also observed that the average production cost in scenarios with PP is US$ 29.71 m-3, US$ 29.45 m-3 for situations without PP, and US$ 35.55 m-3 for scenarios with PP and TS, providing an increase of 174.6%, 172.2%, and 228.6%, respectively, in the minimum price of stumpage.

The increased cost in scenarios with PP and TS is due to the inclusion of different treatments (girdling, vine cutting, and planting in clearings) in the cash flow of MFS activities. According to data obtained from interviews, it was found that the holders of management plans do not include post-harvest treatments in the planning of the UPAs. It should be noted that current legislation does not require the application of these activities, nor the installation of permanent plots; that is, both activities are optional. Only for forest certification purposes, to meet Principle No. 8 (Monitoring and Evaluation) of the Forest Stewardship Council (FSC), should continuous forest inventory be carried out in the management area. It is emphasized that managers do not apply silvicultural treatments after harvesting because they do not believe that this activity provides benefits to the managed forests, and mainly due to the additional costs.

In the state of Pará, research focusing on silvicultural treatments in managed forests is more advanced. Studies such as those by Gomes et al. (2010); Sandel and Carvalhos (2000); Souza et al. (2015) and Taffarel et al. (2014) have been carried out. However, there are few studies involving economic analyses of the application of post-harvest treatments in native forests in the Amazon, among these are: Ferreira (2012), Pinho et al. (2009) and Pires (2014). Despite the studies carried out, Gomes et al. (2010) comment that silvicultural techniques after timber harvesting are rarely adopted due to the scarcity of information on the subject in the Brazilian Amazon.

4.1 Net Present Value of MFS

The NPV of MFS activities is presented in Table 5. Positive NPV values indicate that management projects are economically viable. The NPV decreases with increasing interest rates. The average NPV in scenarios with PP is US$ 145.99 ha^{-1} while US$ 146.02 ha^{-1} in scenarios without PP and US$ 146.0 ha^{-1} in scenarios with PP and TS, showing little difference in values.

Despite the profitability of management, there are barriers to applying it on a large scale in the Amazon, such as the higher profitability of agriculture in the short term compared to management and the need for a forest policy including control of forest exploitation, economic incentives for management and logging (Barreto et al., 1998).

Table 5. Net present value of MFS, the state of Acre, 2016.

Scenario	Description	Interest rate (% p.a.)	NPV (US$ ha^{-1})
1	Management area located 50 km from sawmill, with PP	6	150.04
		8	147.23
		10	144.64
		12	141.99
2	Management area located 50 km from sawmill, without PP	6	150.06
		8	147.31
		10	144.59
		12	142.01
3	Management area located 50 km from sawmill, with PP and TS	6	150.08
		8	147.29
		10	144.54
		12	142.02
4	Management area located 100 km from sawmill, with PP	6	150.04
		8	147.23
		10	144.68
		12	142.05
5	Management area located 100 km from sawmill, without PP	6	150.07
		8	147.32
		10	144.63
		12	142.07
6	Management area located 100 km from sawmill, with PP and TS	6	150.09
		8	147.29
		10	144.58
		12	141.95
7	Management area located 150 km from sawmill, with PP	6	150.08
		8	147.24
		10	144.57
		12	142.05
8	Management area located 150 km from sawmill, without PP	6	150.10
		8	147.33
		10	144.66
		12	142.07
9	Management area located 150 km from sawmill, with PP and TS	6	150.13
		8	147.30
		10	144.61
		12	142.08

The average costs of logging activities in Acre are presented in Table 6.

Table 6. Average cost of logging, state of Acre, 2016.

Logging Activities	Cost (US$ m^{-3})
Road opening	1.34
Yard opening	0.46
Cutting	2.68
Skidding	7.24
Loading	2.45
Forwarding of timber	4.28
New Loading	2.21
Support camp	3.36
Total with forwarding of timber	24.02
Total without forwarding of timber	17.53
Final Cost	**21.87**

The results, shown in Table 6, demonstrate that skidding accounts for the largest share of logging costs, followed by hauling, support camp and tree felling operations, which represent approximately 73% of the total logging cost with hauling. The lowest costs are incurred by yard and road construction operations (7.5%) and loading logs onto trucks (10.2%).

Barreto et al. (1998), conducted in the municipality of Paragominas, state of Pará, with a timber volume of 38.6 m^3 ha^{-1}, the costs of road and yard opening, felling, skidding, and loading activities were US\$ 0.22 m^{-3}, US\$ 0.07 m^{-3}, US\$ 0.25 m^{-3}, US\$ 1.31 m^{-3}, US\$ 2.59 m^{-3}, respectively. Holmes et al. (2002), analyzing the financial aspects of RIL at Fazenda Cauaxi, also in Pará, the costs of road and yard opening were US\$ 0.16 m^{-3} for each activity. In cutting, skidding and yard operations, the costs were US\$ 0.62 m^{-3}, US\$ 1.24 m^{-3} and US\$ 1.28 m^{-3}, respectively. It is noted that the costs found in the present study for such activities are higher. However, it is worth mentioning that characteristics of SFMP, which vary over the years from region to region, influence costs. According to Amaral et al. (1998), the cost of management varies according to the type of forest.

Variations in the stock of commercial species and differences in harvesting projects affect estimates of productivity, costs, waste, and damage (Holmes et al., 2002). Financial comparisons of reduced-impact logging depend on forest and terrain conditions, logging operation planning, the market, and other factors (Putz et al., 2008). Applegate et al. (2004), in turn, argue that the heterogeneity of areas, the time scale of harvesting operations, the impact of topography, and operational conditions during harvesting significantly influence costs.

4.2 Production cost and marketing margin of log, in state of Acre

Values of the composition of the production cost, calculated using different interest rates, of log originating from managed areas in the state Acre, and delivered at sawmill yards in the city of Rio Branco, and the absolute marketing margin, at different distances from the timber hub in this city, are indicated in Table 7.

Table 7. Composition of production cost and gross marketing margin of timber logs in the state of Acre, 2016.

Scenario	Description	Rate	Stumpage Cost	Net Profit	Income Tax	Log Cost	Gross Margin
1	Management area located 50 km from the sawmill in Rio Branco, with PP	6	30.82	7.30	2.01	68.03	5.30
		8	32.76	5.36	1.48	69.44	3.89
		10	34.17	3.95	1.09	70.46	2.87
		12	35.23	2.89	0.80	71.23	2.10
2	Management area located 50 km from the sawmill in Rio Branco, without PP	6	30.52	7.60	2.09	67.81	5.51
		8	32.49	5.63	1.55	69.24	4.08
		10	33.91	4.21	1.16	70.27	3.06
		12	34.99	3.13	0.86	71.05	2.27
3	Management area located 50 km from the sawmill in Rio Branco, with PP and TS	6	37.37	0.75	0.21	72.78	0.55
		8	38.78	0.00	0.00	73.98	-0.66
		10	39.74	0.00	0.00	74.94	-1.62
		12	40.44	0.00	0.00	75.64	-2.32
4	Management area located 100 km from the sawmill in Rio Branco, with PP	6	27.93	1.29	0.36	72.39	0.94
		8	29.53	0.00	0.00	73.63	-0.31
		10	30.70	0.00	0.00	74.80	-1.48
		12	31.58	0.00	0.00	75.68	-2.36
5	Management area located 100 km from the sawmill in Rio Branco, without PP	6	27.63	1.59	0.44	72.17	1.15
		8	29.26	0.00	0.00	73.36	-0.04
		10	30.44	0.00	0.00	74.54	-1.22
		12	31.34	0.00	0.00	75.44	-2.12
6	Management area located 100 km from the sawmill in Rio Branco, with PP and TS	6	34.48	0.00	0.00	78.58	-5.26
		8	35.55	0.00	0.00	79.65	-6.33
		10	36.27	0.00	0.00	80.37	-7.05
		12	36.78	0.00	0.00	80.88	-7.56
7	Management area located 150 km from the sawmill in Rio Branco, with PP	6	24.46	0.00	0.00	74.66	-1.33
		8	25.65	0.00	0.00	75.85	-2.52
		10	26.52	0.00	0.00	76.72	-3.39
		12	27.19	0.00	0.00	77.39	-4.06
8	Management area located 150 km from the sawmill in Rio Branco, without PP	6	24.16	0.00	0.00	74.36	-1.03
		8	25.38	0.00	0.00	75.58	-2.25
		10	26.27	0.00	0.00	76.47	-3.14
		12	26.95	0.00	0.00	77.15	-3.82
9	Management area located 150 km from the sawmill in Rio Branco, with PP and TS	6	31.01	0.00	0.00	81.21	-7.88
		8	31.67	0.00	0.00	81.87	-8.54
		10	32.10	0.00	0.00	82.30	-8.97
		12	32.40	0.00	0.00	82.60	-9.27

Note: Values in US\$ m^{-3}. Cost of forest exploitation: US\$ 21.87 m^{-3}; Cost of forest transport: US\$ 11.66 m^{-3} (50 km), US\$ 20.57 m^{-3} (100 km) and US\$ 26.66 m^{-3} (150 km); Cost of invoice: US\$ 0.02 m^{-3} and FUNRURAL: US\$ 1.65 m^{-3}.

The cost of production tends to increase as managed areas become more distant from Rio Branco. This is due to the variation in transportation costs, which increase by almost 129% when the distance changes from 50 to 150 km from Rio Branco. The cost of producing stumpage, for scenarios with PP, without PP, and with PP and TS, increases on average by about 10%, changing the distance from 50 to 150 km. Thus, even though the cost of producing stumpage decreases with increasing distance, a higher transportation cost ends up increasing the cost of producing stumpage.

The average cost of producing stumpage, for scenarios with permanent plots, was US\$ 73.36 m^{-3}. The average cost of producing stumpage, of logging activities, and the average cost of transporting log to the sawmill yard represent approximately 40.5%, 29.8% and 26.8% of the final average cost, respectively. Costs related to invoices and Funrural and Income Tax have the smallest share in the cost of producing log (2.9%).

The average production cost for scenarios without PP, at different interest rates, was US\$ 73.12 m^{-3}. Activities related to the average cost of producing standing timber represent almost 40.3% of the average cost of producing log timber. Transporting the log to the sawmill and the costs related to invoices and taxes represent, respectively, 29.9%, 26.8% and 3.0% of the average production cost for scenarios without permanent parcels.

In scenarios with permanent plots and TS, the average production cost was US\$ 78.73 m^{-3}, where the average cost of stumpage production accounts for 45.2% of the final cost, while forest harvesting represents 27.8%. The average freight cost and the costs of invoices and taxes, in turn, correspond to 24.9% and 2.1% of the average log production cost, respectively.

The average price of logs delivered to the sawmill is US$ 73.32 m^{-3}, while the average production cost, considering different scenarios and rates, is US$ 75.07 m^{-3}, indicating a negative average profit margin.

5 Conclusions

The results generated in this study on forest management practices in the state of Acre allowed us to infer the following main conclusions: 1) the average cost of producing standing timber in an area located 50 km from the Rio Branco timber hub increases by approximately 0.82% with the installation and measurement of permanent plots throughout the cutting cycle; and 2) the profit margin for logs indicates that for more distant areas (150 km) this activity is unfeasible.

REFERENCES

[1] ACRE. Governo do Estado do Acre. **Zoneamento Ecológico-Econômico do Acre Fase II**: documento síntese. 2. ed. Rio Branco: SEMA, 2010.

[2] ACRE. Governo do Estado do Acre. **Zoneamento Ecológico-Econômico do Acre Fase II**: documento síntese. Rio Branco: SEMA, 2006. 354 p.

[3] AMARAL, E. F. et al. Circunstâncias Estaduais. In: COSTA, F. S. et al. (Ed.) **Inventário de emissões antrópicas e sumidouros de gases de efeito estufa do estado do Acre**: ano-base 2010. Rio Branco: Embrapa Acre, 2012.

[4] AMARAL, P. et al. Floresta para sempre: um manual para a produção de madeira na Amazônia. Belém: Imazon, 1998. 130 p.

[5] APPLEGATE, G.; PUTZ, F. E.; SNOOK, L. K. **Who pays for and who benefits from improved timber harvesting practices in the tropics?** Lessons learned and information gaps. Bogor: Center for International Forestry Research, 2004.

[6] ASSUNÇÃO, J. et al. Property-level assessment of change in forest clearing patterns: the need for tailoring policy in the Amazon. **Land Use Policy**, Amsterdan, v. 66, p. 18-27, 2017.

[7] AZEVEDO-RAMOS, C. Desenvolvimento sustentável sob a ótica da floresta. In: AZEVEDO-RAMOS, C. **Amazônia e desenvolvimento sustentável**. Rio de Janeiro: Fundação Konrad Adenauder Stiftung, 2010. 98 p. (Cadernos Adenauer X, n. 4).

[8] BALIEIRO, M. R. et al. **As concessões de florestas públicas na Amazônia Brasileira**: um manual para pequenos e médios produtores. 2. ed. Piracicaba; Belém: Imaflora/ IFT. 2010. 204p.

[9] BARRETO, P. et al. Costs and benefits of forest management for timber production in eastern Amazonia. **Forest Ecology and Management**, Amsterdan, v. 108, p. 9-26, 1998.

[10] BOLTZ, F. et al. Financial returns under uncertainty for conventional and reduced-impact logging in permanent production forests of the Brazilian Amazon. **Ecological Economics**, Amsterdan, v. 39, n. 3, p. 387-398, 2001.

[11] BRANDT, J. S.; NOLTE, C.; AGRAWAL, A. Deforestation and timber production in Congo after implementation of sustainable forest management policy. **Land Use Policy**, Amsterdan, v. 52, p. 15-22, 2016.

[12] BRASIL. Decreto nº 5.975, de 30 de novembro de 2006. **Diário Oficial da República Federativa do Brasil**, Brasília, DF, 01 dez. 2006a. Seção 1, p. 01-03. Disponível em:<http://pesquisa.in.gov.br/imprensa/jsp/visualiza/index.jsp?data=01/12/2006&jornal=1&pagina=1&totalArquivos=132>. Acesso em: 23 fev. 2017.

[13] BRASIL. Instrução normativa nº 1, de 12 de fevereiro de 2015. **Diário Oficial da República Federativa do Brasil**, Brasília, DF, 13 fev. 2015. Seção 1, p. 67. Disponível em: <http://pesquisa.in.gov.br/imprensa/jsp/visualiza/index.jsp?data=13/02/2015&jornal=1&pagina=67>. Acesso em: 24 fev. 2017.

[14] BRASIL. Instrução normativa nº 30, de 31 de dezembro de 2002. **Diário Oficial da República Federativa do Brasil**, Brasília, DF, 01 jan. 2003.

[15] BRASIL. Instrução normativa nº 5, de 11 de dezembro de 2006. Diário Oficial da República Federativa do Brasil, Brasília, DF, 13 dez. 2006b. Seção 1, p. 155-159. Disponível em: <http://pesquisa.in.gov.br/imprensa/jsp/visualiza/index.jsp?data=13/12/2006&jornal=1&pagina=155&totalArquivos=232>. Acesso em: 23 fev. 2017.

[16] BRASIL. Norma de execução nº 1, de 24 abril de 2007. Diário Oficial da República Federativa do Brasil, Brasília, DF, 30 abr. 2007. Seção 1, p. 405. Disponível em: <http://pesquisa.in.gov.br/imprensa/jsp/visualiza/index.jsp?data=30/04/2007&jornal=1&pagina=405&totalArquivos=428>. Acesso em: 23 fev. 2017.

[17] BRASIL. Resolução Conama nº 406, de 02 de fevereiro de 2009. **Diário Oficial da República Federativa do Brasil**, Brasília, DF, 06 fev. 2009. Seção 1, p. 100. Disponível em: <http://pesquisa.in.gov.br/imprensa/jsp/visualiza/index.jsp?data=06/02/2009&jornal=1&pagina=100&totalArquivos=160>. Acesso em: 17 ago. 2016.

[18] DE GRAAF, N. R.; FILIUS, A. M.; SANTOS, A. R. H. Financial analysis of sustained forest management for timber: perspectives for application of the CELOS management system in Brazilian Amazonia. **Forest Ecology and Management**, Amsterdan, v. 177, p. 287-299, 2003.

[19] ESPADA, A. L. V. et al. **Manejo florestal e exploração de impacto reduzido em florestas naturais de produção da Amazônia**. Belém: IFT, 2013. 31 p. (Instituto Floresta Tropical. Informativo Técnico, 1).

[20] FEARNSIDE, P. M. Environmental services as a strategy for sustainable development in rural Amazonia. **Ecological Economics**, Amsterdan, v. 20, n. 1, p. 53-70, 1997.

[21] FERREIRA, E. J. L. O bambu é um desafio para a conservação e o manejo de florestas no sudoeste da Amazônia. **Ciência e Cultura**, São Paulo, v. 66, n. 3, p. 46-51, 2014.

[22] FERREIRA, M. V. S. **Avaliação econômica do manejo florestal em floresta de terra firme na Amazônia brasileira com aplicação de silvicultura pós-colheita**. 2012. 81 f. Dissertação (Mestrado em Ciências Florestais) – Universidade Federal Rural da Amazônia, Belém, 2012.

[23] FOOD AND AGRICULTURE ORGANIZATION OF THE UNITED NATIONS – FAO. **Global forest resources assessment 2015**: How are the world's forests changing? 2. ed. Roma: FAO, 2016.

[24] FUNDAÇÃO FLORESTA TROPICAL (FFT). **Manual de procedimentos técnicos para condução de manejo florestal e exploração de impacto reduzido (versão 4.0)**. Belém: FFT, 2002.

[25] GIL, A. C. **Métodos e técnicas de pesquisa social**. 6. ed. São Paulo: Atlas, 2008.

[26] GOMES, J. M. et al. Sobrevivência de espécies arbóreas plantadas em clareiras causadas pela colheita de madeira em uma floresta de terra firme no município de Paragominas na Amazônia brasileira. **Acta Amazonica**, Manaus, v. 40, n. 1, p. 171-178, 2010.

[27] GUILHERME, E. **Aves do Acre**. Rio Branco: Edufac, 2016. 897 p. Disponível em: <https://issuu.com/edufac/docs/livro_aves_do_acre_miolo_05_08_2016>. Acesso em: 03 fev. 2017.

[28] HAMAOUI JR., G. S. et al. Land-use change drives abundance and community structure alterations of thaumarchaeal ammonia oxidizers in tropical rainforest soils in Rondônia, Brazil. **Applied Soil Ecology**, Amsterdan, v. 107, p. 48-56, 2016.

[29] HIGUCHI, N. Utilização e manejo dos recursos madeireiros das florestas tropicais úmidas. **Acta Amazonica**, Manaus, v. 24, n.3-4, p. 275-288, 1994.

[30] HOLMES, T. P. et al. Financial and ecological indicators of reduced impact logging performance in the eastern Amazon. **Forest Ecology and Management**, Amsterdan, v. 163, n. 1-3, 28 p. 93-110, 2002.

[31] HOLMES, T. P. et al. Financial indicators of reduced impact logging performance in Brazil: case study comparisons. p. 152-162. In: ENTERS, T. et al. (Eds.). **Applying reduced impact logging to advance sustainable forest management**. Bangkok: Food and Agriculture Organization of the United Nations, 2001. (FAO. RAP Publication, 14).

[32] HOSOKAWA, R. T.; MOURA, J. B.; CUNHA, U. S. **Introdução ao manejo e economia de florestas**. Curitiba: UFPR, 1998. 162 p.

[33] INSTITUTO BRASILEIRO DE GEOGRAFIA E ESTATÍSTICA (IBGE). **Estimativas da população residente no brasil e unidades da federação com data de referência em 1º de julho de 2016**. IBGE, 13 set. 2016. Disponível em: <ftp://ftp.ibge.gov.br/Estimativas_de_Populacao/Estimativas_2016/estimativa_dou_2016_20160913.pdf>. Acesso em: 02 fev. 2017.

[34] KEENAN, R. J.; REAMS, G.A.; ACHARD, F. et al. Dynamics of global forest area: Results from the FAO Global Forest Resources Assessment 2015. **Forest Ecology and Management**, Amsterdan, v. 352, p. 9-20, 2015.

[35] KOTTEK, M. et al. World map of the Köppen-Geiger climate classification updated. **Meteorologische Zeitschrift**, Stuttgart, v. 15, n. 3, p. 259-263, 2006.

[36] LENTINI, M.; VERÍSSIMO, A.; PEREIRA, D. **A expansão madeireira na Amazônia**. Belém: Imazon. 2005. (Imazon. Série O Estado da Amazônia, 02).

[37] LIMA JÚNIOR, V. B.; REZENDE, J. L. P.; OLIVEIRA, A. D. Determinação da taxa de desconto a ser usada na análise econômica de projetos florestais. **Cerne**, Lavras, v. 3, n. 1, p. 45-66, 1997.

[38] MACDICKEN, K. G.; SOLA, P.; HALL, J. E.; SABOGAL, C.; TADOUM, M.; Wasseige, C. de. Global progress toward sustainable forest management. **Forest Ecology and Management**, Amsterdam, v. 352, p. 47-56, 2015.

[39] MACHADO, M. P. O. **Custo do manejo florestal madeireiro na Amazônia**: um estudo de caso no Estado do Acre, 2012. 2013. 76 f. Monografia (Bacharelado em Engenharia Florestal) – Universidade Federal do Acre, Rio Branco, 2013.

[40] MAY, T. Pesquisa social: questões, métodos e processos. Porto Alegre: Artmed, 2004.

[41] MENDES, J. T. G.; PADILHA JÚNIOR, J. B. **Agronegócio**: uma abordagem econômica. Nova Jersey: Pearson Prentice Hall, São Paulo, 2007.

[42] MORALES-HIDALGO, D.; OSWALT, S. N.; SOMANATHAN, E. Status and trends in global primary forest, protected areas, and areas designated for conservation of biodiversity from the Global Forest Resources Assessment 2015. **Forest Ecology and Management**, Amsterdan, v. 352, n. 7, p. 68-77, 2015.

[43] NEVES, R. F. (Org.). **Coletânea de normas ambientais do Estado do Acre**. 2. ed. Rio Branco: Procuradoria Geral do Estado/ Procuradoria Especializada do Meio Ambiente, 2009.

[44] OLIVEIRA, L. C. et al. **Diretrizes simplificadas para instalação e medição de parcelas permanentes em florestas naturais da Amazônia brasileira**. Manaus: GT Monitoramento de Florestas, 2004.

[45] PEARSE, P. H. **Introduction to forestry economics**. Vancouver: University of British Columbia Press, 1990.

[46] PINHO, G. S. C. et al. Análise de custos e rendimentos de diferentes métodos de corte de cipós para produção de madeira na Floresta Nacional de Tapajós. **Acta Amazônica**, Manaus, v. 39, n. 3, p. 555-560, 2009.

[47] PIRES, I. P. **Crescimento, mortalidade e viabilidade técnica e financeira do desbaste de liberação de copas em uma floresta ombrófila úmida, no leste do Pará**. 2014. 117 f. Dissertação (Mestrado em Ciências Florestais) – Universidade Federal Rural da Amazônia, Belém, 2014.

[48] PUTZ, F. E. et al. Reduced-impact logging: challenges and opportunities. **Forest Ecology and Management**, Amsterdan, v. 256, n. 7, p. 1427-1433, 2008.

[49] REZENDE, J. L. P.; OLIVEIRA, A. D. **Análise econômica e social de projetos florestais**. 2. ed. Viçosa, MG: UFV, 2011.

[50] SABOGAL, C. et al. **Manejo florestal empresarial na Amazônia brasileira**: restrições e oportunidades: relatório síntese. Belém: CIFOR, 2006. 72 p.

[51] SANDEL, M. P.; CARVALHOS, J. O. P. Anelagem de árvores como tratamento silvicultural em florestas naturais da Amazônia brasileira. **Revista de Ciências Agrárias**, Belém, n. 33, p. 9-32, 2000.

[52] SANTOS, R. A. **Custo do manejo florestal madeireiro, estudo de caso**: Floresta Estadual do Antimary. 2007. 109 f. Monografia (Bacharelado em Economia) – Universidade Federal do Acre, Rio Branco, 2007.

[53] SASAKI, N. et al. Sustainable management of tropical forests can reduce carbon emissions and stabilize timber production. **Frontiers in Environmental Science**, Lausanne, v. 4, n. 50, p. 1-13, 2016.

[54] SILVA, J. M. N. et al. **Diretrizes para instalação e medição de parcelas permanentes em florestas naturais da Amazônia Brasileira**. Belém: Embrapa Amazônia Oriental, 2005. 68 p.

[55] SILVA, M. L.; FONTES, A. A. Discussão sobre os critérios de avaliação econômica: valor presente líquido (VPL), valor anual equivalente (VAE) e valor esperado da terra. **Árvore**, Viçosa, MG, v. 29, n. 6, p. 931-936, 2005.

[56] SILVA, M. L.; JACOVINE, L. A. G.; VALVERDE, S. R. **Economia florestal**. 2. ed. Viçosa, MG: UFV, 2005. 178 p.

[57] SILVA, Z. A. G. P. G. Concessão florestal: governo e iniciativa privada interagindo para implementar o manejo florestal sustentável na Amazônia. In: SEMINÁRIO ECONOMIA DO MEIO AMBIENTE: REGULAÇÃO ESTATAL E AUTO-REGULAÇÃO EMPRESARIAL PARA O DESENVOLVIMENTO SUSTENTÁVEL, 3., 2003, Campinas. **Anais**... Campinas: UNICAMP, 2003.

[58] SILVA, Z. A. G. P. G. Raio econômico como um indicativo para a definição de concessões florestais: um estudo de caso no estado do Acre. In: MATOS et al. (Ed.). **II Prêmio Serviço Florestal Brasileiro em Estudos de Economia e Mercado Florestal**: coletânea de monografias premiadas. Brasília: ESAF, 2015. p. 205-244.

[59] SILVA, Z. A. G. P. G.; SANTOS, R. A. Custo do manejo florestal madeireiro em floresta pública: estudo de caso no Acre, 2011. **Amazônia**: Ciência & Desenvolvimento, Belém, v. 7, n. 3, p. 79-96, 2011.

[60] SILVEIRA, M. **A floresta aberta com bambu no sudoeste da Amazônia**: padrões e processos em múltiplas escalas. 2001. 109 f. Tese (Doutorado em Ecologia) – Universidade de Brasília, Brasília, 2001.

[61] SOUZA, D. V. et al. Crescimento de espécies arbóreas em uma floresta natural de terra firme após a colheita de madeira e tratamentos silviculturais, no município de Paragominas, Pará, Brasil. **Ciência Florestal**, Santa Maria, v. 25, n. 4, p. 873-883, 2015.

[62] STRAND, J.; CARSON, R.T.; NAVRUD, S. et al. Using the Delphi method to value protection of the Amazon rainforest. **Ecological Economics**, Amsterdam, v. 131, p. 475-484, 2017.

[63] TAFFAREL, M. et al. Efeito da silvicultura pós-colheita na população de *Lecythis lurida* (Miers) Mori em uma floresta de terra firme na Amazônia brasileira. **Ciência Florestal**, Santa Maria, v. 24, n. 4, p. 889-898, 2014.

[64] THAINES, F. **Coeficientes técnicos para o manejo florestal comunitário com fins madeireiros no bioma Amazônia**. Brasília: Serviço Florestal Brasileiro, 2013. 135 p.

[65] TIMOFEICZYK JUNIOR, R. et al. Estrutura de custos do manejo de baixo impacto em florestas tropicais – um estudo de caso. **Floresta**, Curitiba, v. 35, n. 1, p. 89-103, 2005.

[66] WAGNER, J. E. **Forestry economics**: a managerial approach. New York: Routledge – Taylor & Francis Group, 2012.

Great Britain Journals Press

RESEARCH FINGERPRINT

IDENTIFIER
LJRS-226274

PEER REVIEW
Double Blind

SIMILARITY CHECK
Perplexity AI and iThenticate

ACCESS
Open Access

LANGUAGE
English

PRINT ISSN
2631-8490

ONLINE ISSN
2631-8504

EDITION

ABBREVIATION
LJRS

VOLUME
26

ISSUE
4

YEAR
2026

KEY DATES

RECEIVED
2026-03-11

ACCEPTED
2026-03-16

ONLINE PUBLISHED
2026-06-10

PUBLISHED
2026-06-16

CATALOGING

CROSSMARK DOI
10.34257/LJRS226274UK

LCC CLASS
TD196.C45, RA1247.C45

ACCESS ONLINE

London Journal of Research In Science: Natural and Formal
General Section

Article Record

Chemical-Environmental Aspects of Measures to Eliminate the Chemical Weapon Destruction Consequences

CORRESPONDENCE →

AUTHORS & AFFILIATIONS

Dr. Alexey V. Trubachev ¶*
Expert of the Federal Register of Experts

Dr. Larisa V. Trubacheva ‖
ζ Head

¶ Expert of the Federal Register of Experts of the Scientific Research Institute – Federal Research Center for Projects Evaluation and Consulting Services,Russia

‖ Department of the Institute of Natural Sciences, Udmurt State University, Izhevsk, Russia (OA)

ABSTRACT

The paper presents the basic requirements for carrying out measures to eliminate the consequences of activities at chemical weapons destruction facilities, describes technological approaches for implementing measures to eliminate the consequences of the destruction of skin abscesses and phosphorus-organic toxic substances, and evaluates their effectiveness. The chemical-toxicological characteristic of the waste generated during the implementation of liquidation measures is given, the environmental risks of these measures are analyzed, including the risks of long-term storage of toxic waste in appropriate storage areas. The ways to reduce the negative environmental impact of the consequences of carrying out liquidation measures at the facilities for the destruction of lewisite, sarin and soman are proposed

Index Terms: chemical weapons destruction facilities • environmental risks • liquidation measures

FUNDING
No external funding was declared for this work.

CONFLICTS
The authors declare no conflict of interest.

AI USAGE
No generative AI was used for analysis or results.

HOW TO CITE
Trubachev, A. V. & Trubacheva, L. V. (2026). Chemical-Environmental Aspects of Measures to Eliminate the Chemical Weapon Destruction Consequences. London Journal of Research In Science: Natural and Formal, 26(4), 74-77. DOI: 10.34257/LJRS226274UK

METADATA CONTINUATION

AUTHOR CONTACT QR LEDGER

Dr. Alexey V. Trubachev¶∐*

ARCHIVAL RECORD

LJRS · Vol 26 · Issue 4 · 2026

Article ID LJRS-226274 · DOI 10.34257/LJRS226274UK

Print ISSN 2631-8490 · Online ISSN 2631-8504

RESEARCH ARTICLE

Chemical-Environmental Aspects of Measures to Eliminate the Chemical Weapon Destruction Consequences

Dr. Alexey V. Trubachev[¶ ∐ *] and Dr. Larisa V. Trubacheva[‖ ζ]

QUALIFICATIONS / ROLES

∐ Expert of the Federal Register of Experts
ζ Head

AFFILIATIONS

¶ Expert of the Federal Register of Experts of the Scientific Research Institute – Federal Research Center for Projects Evaluation and Consulting Services,Russia
‖ Department of the Institute of Natural Sciences, Udmurt State University, Izhevsk, Russia (**OA**)

Abstract

The paper presents the basic requirements for carrying out measures to eliminate the consequences of activities at chemical weapons destruction facilities, describes technological approaches for implementing measures to eliminate the consequences of the destruction of skin abscesses and phosphorus-organic toxic substances, and evaluates their effectiveness. The chemical-toxicological characteristic of the waste generated during the implementation of liquidation measures is given, the environmental risks of these measures are analyzed, including the risks of long-term storage of toxic waste in appropriate storage areas. The ways to reduce the negative environmental impact of the consequences of carrying out liquidation measures at the facilities for the destruction of lewisite, sarin and soman are proposed

Keywords: *chemical weapons destruction facilities, environmental risks, liquidation measures*

Correspondence: Dr. Alexey V. Trubachev

1 Introduction

During 2005-2017, in accordance with the Federal Target Program "Destruction of Chemical Weapons Stocks in the Russian Federation", chemical weapons were completely destroyed in all 7 storage arsenals in Russia. In order to involve the property complexes of former chemical weapons destruction facilities in economic turnover, a number of measures was carried out to eliminate the consequences of their activities - liquidation measures (hereinafter referred to as LM). The main task of LM was to perform the following works: reducing the content of the toxic substances residual amounts in the buildings, structures on the territories of industrial sites to hygienic standards, neutralizing and disposing the waste generated during the implementation of chemical safety measures at the storage landfills. The achievement of the necessary parameters for the fulfillment of these tasks was largely determined by the nature of the technologies used to destroy toxic substances, ensuring the environmental safety of these technologies implementation, and creating new approaches to organizing and conducting environmental-analytical monitoring in the areas where the chemical weapons destruction facilities were located[1-3].

The main technological approaches to eliminating the consequences of the destruction of skin-abscess (hereinafter referred to as SATS) and phosphorus-organic (hereinafter referred to as POTS) toxic substances (hereinafter referred to as TS) are largely identical. These approaches include operations of decontamination, dismantling, fragmentation and thermal neutralization of the construction materials and metal structures, technological and engineering equipment, communications, and appliances in the rooms where the chemical weapons are stored and destruction operations are carried out[4,5]. Of great importance in carrying out such work is the effectiveness of decontamination of the technological and other surfaces that have come into contact with the detoxification products of TS, the reliability of the isolation of compacted waste, and precision chemical and analytical control of the TS residual amounts[6].

In the process of conducting the liquidation measures not only the residual amounts of toxic substances themselves can have a negative impact on the ecosystem and human health, but also the products of their neutralization, such as inorganic arsenic compounds (in the case of lewisite detoxification[7]), as well as the derivatives of methylphosphonic acid and inorganic fluorides (in the case of sarin and soman detoxification[8,9]), trapped into the aquatic environment, the air environment (during the incineration of relevant waste), as well as the soil horizons. In this regard, the task arises of operational control of these substances content in various matrices at the level of maximum permissible concentrations.

The purpose of this work was to analyze the effectiveness of technological approaches in the implementation of LM at the facilities for the destruction of chemical weapons "Kizner" (POTS), "Kambarka" (SATS) in the Udmurt Republic and "Maradykovsky" (POTS, SATS) in the Kirov region, to present the characteristics of the products of toxic substances neutralization formed during the implementation of technological operations, as well as to make an assessment of the associated environmental risks and possible ways to minimize them.

2 The main stages of the liquidation measures

The activities to eliminate the consequences of chemical weapons destruction are a set of measures aimed at making the chemical weapons destruction facilities and the territories they occupy safe for the environment and humans[10].

Before the start of LM in the working spaces of the facility, sampling and analysis of samples for the content of TS on the surfaces of the building structures and technological equipment was carried out. After the residual amounts of TS had been detected, the surfaces were decontaminated. According to the research results, the working spaces were divided into three groups: I hazard group – the «dirty rooms» in which toxic substances were found on the surface, in the samples "bulk" and scrapings in the concentrations above the hygienic standards; II hazard group – the «conditionally dirty rooms» in which the concentrations of toxic substances did not exceed the hygienic standards; group III - the «clean rooms» where no toxic substances were detected on the samples surface and in which no work with toxic substances had previously been carried out. When confirming the absence of the TS in the "deep" samples, after removing the contaminated layers of the building structure material, the rooms were "opened" for the actual LM.

The main stages of LM in the elimination of the consequences of the destruction of POTS were:

- dismantling and fragmentation of the technological equipment and construction structures of the buildings of hazard groups I and II;
- thermal neutralization of the metal waste and construction dust from after the removal of the top contaminated layer from the rooms of groups I and II;
- isolation of the neutralized waste obtained as a result of LM by encapsulation and their removal to a solid waste storage landfill;
- performing laboratory tests to determine the contamination of the soil of the industrial site and the sanitary protection zone with residual amounts of toxic substances, their degradation products and general industrial pollutants. In case of exceeding the established hygienic standards certain measures were taken to dispose of soil and remediate the site of the facility.

The main stages of LM in the elimination of the consequences of the destruction of SATS were:

- dismantling the technological equipment, cutting the tanks in the storage facilities and at the storage sites of the reaction masses into fragments;
- decontamination and detoxification of the metal fragments, building structures and soil;
- thermal neutralization of the solid waste and wastewater (by the fire method);
- isolation of the neutralized waste obtained as a result of LM by encapsulation or concreting and their removal to the solid waste storage landfill;
- analysis of the soil contamination on the territory of the industrial site and the sanitary protection zone for the content of the residual amounts of organic pollutants, their degradation products and general industrial pollutants. In case of exceeding the established hygienic standards, certain measures were taken to dispose of soil and remediate the territory of the facility.

3 Technological solutions implemented during liquidation measures

To ensure the safe implementation of LM, the use of thermal neutralization of the metal structures fragments, production equipment and other fireproof waste contaminated with POTS was proposed as a priority[7].

Thermal neutralization was carried out in two stages: at the first stage the internal and external surfaces were decontaminated by complete immersion in baths with an aqueous peroxide-alkaline solution for 2 hours. After decontamination, the fragments were washed with water and blown round with compressed air, while the quality control of the decontamination was carried out according to the content of TS in the rinsing water in accordance with the hygienic standards. At the second stage the obtained fragments were neutralized in thermal neutralization units in the temperature range from 500 to 650°C. The mode of thermal neutralization in the specified temperature range was determined depending on the type of TS, fragments and substances to be neutralized according to the technological regulations. Chemical-analytical control of the decontamination level of the thermally neutralized fragments has shown that the content (C) in the rinses from decontaminated surfaces does not exceed the maximum permissible levels-MPL (e.g. for sarin $C < 0.4 \cdot 10^{-5}$ mg/dm^2, MPL $= 1.0 \cdot 10^{-4}$ mg/dm^2; for soman $C < 0.1 \cdot 10^{-6}$ mg/dm^2, MPL $= 1.0 \cdot 10^{-5}$ mg/dm^2). These neutralized fragments can be used as scrap metal at metal processing plants. The neutralized construction waste and spent sorbents are sent for isolation to the industrial waste storage landfills as production waste after the liquidation work.

In the process of implementation of the liquidation measures at the POTS destruction facilities, decontamination with mixtures based on monoethanolamine and waste encapsulation technology were used, resulting in bitumen-salt masses containing calcium salts of methylphosphonic acid and its acid ester, diisopropyl ether of methylphosphonic acid, aminoethylisopropyl-methylphosphonate, calcium fluoride, sarin in the amount of less than $1 \cdot 10^{-8}$% and bitumen (up to 97.5%)[9]. These bitumen-salt masses as waste of hazard class III were sent for burial at the special waste storage landfills.

The main operation when performing LM at the SATS destruction facilities was surface decontamination. Decontamination of fragmented parts of the technological equipment and construction fractions was carried out with a 3.0% aqueous solution of sodium hydroxide by soaking them in degassing baths for 24 hours (a 10.0% aqueous solution of NaOH was used for additional preventive decontamination). 1.0% aqueous solution of sodium hydroxide was used to treat the exterior surfaces of the equipment and building structures of the buildings in which arsenic-containing lewisite detoxification products were handled in order to decontaminate the rags, activated carbon, plastic and metal gaskets and plugs contaminated with arsenic, and personal protective equipment.

The water-polymer composition based on hydrogen peroxide containing a quaternary ammonium compound, acetic or oxalic acid, starch and water was used to decontaminate the external surfaces of equipment, pipelines and building structures. Decontamination of surfaces using this composition was carried out three times with a consumption of 0.3 l/m^2 per treatment, with 30% of the formulation being retained on the metal surfaces and 70% draining away. After decontamination the treated materials were dried at a temperature not lower than 20°C and the humidity not more than 60%. This composition was also used to decontaminate the fragmented equipment parts by soaking them in decontaminating baths for 1 hour. An aqueous solution of sodium hypochlorite with an active chlorine concentration of 5–10 g/l was used for soil decontamination, with 50–100 kg of solution being consumed per 1 ton of soil, depending on the achieved soil moisture. Spent decontaminating solutions were incinerated in a liquid waste incinerator.

To isolate arsenic-containing wastewater formed during the detoxification of lewisite, the technology of their encapsulation in the form of a concrete-salt mass was used, and concreting was used to isolate metal waste products. The concrete-salt mass was a solid product of the composition: 0.30% arsenic, 4.15% sodium sulfate, 1.85% calcium sulfate, 93.70% silicon dioxide (concrete), and the concreted metal waste consisted of 0.10% arsenic, 1.23% calcium sulfate, 19.13% metallic iron, 79.54% silicon dioxide (concrete). These concrete masses, as the waste of hazard class II, obtained as a result of LM operations at SATS destruction facilities, were sent for burial at the special landfills.

4 Environmental risks of the elimination of the chemical weapons destruction consequences and ways to minimize them

The chemical weapons destruction facilities where liquidation measures are carried out are classified as category II facilities (moderate negative impact), and waste disposal facilities resulting from LM (burial landfills) are classified as category I facilities (significant negative impact).

The impact on the environment during LM is caused by emissions into the atmosphere during the dismantling, fragmentation and decontamination of the technological equipment, metal and building structures, the combustion of decontaminating solutions and wastewater[11]. Thus, during the implementation of liquidation measures at SATS destruction facilities, the emissions of pollutants containing inorganic arsenic compounds may occur during operations for cutting and dismantling decontaminating baths, as well as during the incineration of spent decontaminating solutions at the thermal neutralization plant. Inorganic arsenic compounds have an acute toxic effect on human internal organs, cause skin diseases, and have a carcinogenic effect (their maximum permissible concentration in the air must be $3 \cdot 10^{-6}$ g/m^3).

As noted above, the mixtures for decontaminating the external surfaces of the equipment, fragmented parts and soil include organic substances (acetic acid, oxalic acid, starch), as well as the products containing active chlorine (sodium hypochlorite). For thermal neutralization of the waste mixtures, incineration by fire is used. It is known[12] that the simultaneous presence of chlorine, oxygen-, hydrogen-, and carbon-containing compounds in the reaction medium in the temperature range from 230 to 530°C significantly leads to the formation of polychlorinated dibenzo-p-dioxins and dibenzofurans. Such conditions are realized at the plant for combustion of these mixtures, which leads to the formation of dioxins in the combustion products and their release into the atmosphere. Dioxins are one of the most highly toxic compounds, they are able to accumulate in the human and animal bodies without decomposition, exerting an embryotoxic and carcinogenic effect (the maximum permissible concentration of dioxins in air must be $5 \cdot 10^{-13}$ g/m^3).

Thus, one of the possible negative environmental consequences of LM implementation at facilities where SATS are destroyed is atmospheric air pollution with arsenic compounds and dioxins.

Concrete-salt and bitumen-salt masses, concreted metal waste containing arsenic compounds, methylphosphonic acid derivatives and other substances can pose a danger to the environment. For one reason or another, prolonged storage at burial landfills may result in depressurization of containers filled with these wastes, followed by leaching of arsenic-containing and other toxic components releasing into the environment (soil, water horizons). For example, the main migration products from bitumen-salt masses obtained during the neutralization of sarin are monoethanolamine and isopropyl esters of methylphosphonic acid. These substances, having sensitizing, gonadotropic, teratogenic and mutagenic effects on the body of warm-blooded animals, can integrally turn out to be toxic when released into the environment. This is also one of the possible negative environmental consequences of the liquidation measures implementation.

LM environmental safety should be ensured by a number of organizational, technical and technological measures aimed at the safe management of the working processes and the prevention of toxic emissions of chemicals. Among them, it should be noted there are such as: using the sealed equipment and materials; multi-stage flue gas purification of the thermal neutralization plants; equipping the places of mechanical processing and flame cutting of fragments with mobile filtration units to remove and filter the welding fumes and dust from the temporary and non-stationary work posts; protecting the underground part of the toxic waste storage bunkers from atmospheric precipitation infiltration and groundwater inflow, etc.

Industrial chemical-analytical control of the LM implementation, monitoring the pollution of the atmospheric air, soil, water horizons, snow cover at the industrial zone facilities and adjacent territories is important for minimizing environmental risks during the elimination of the consequences of the chemical weapons destruction. At waste disposal facilities, it is necessary to regularly monitor the atmospheric air pollution to check the content of the lewisite and inorganic arsenic compounds, the groundwater and soils pollution to check the content of the total arsenic, lewisite, phosphate and fluoride ions, as well as the content of the methylphosphonic acid derivatives and POTS themselves.

Performing precision chemical analytical measurements of the concentrations of the above-mentioned toxicants in multicomponent natural matrices requires the development and creation of new instruments and methods of analysis, including on-line sensors for monitoring their content in environmental objects that meet the requirements of high accuracy, expressiveness and selectivity.

Carrying out the work to eliminate the consequences of the chemical weapons destruction is an environmentally significant challenge that requires the use of specific technological approaches and methods of chemical and analytical control to minimize the associated environmental risks.

5 Conclusions

It has been shown that the measures to eliminate the consequences of the chemical weapons destruction are a number of organizational, technical and technological measures aimed at making the facilities for the destruction of toxic substances safe for the environment and humans. The possible negative environmental consequences of the liquidation measures have been analyzed. These effects may be associated with the release of inorganic arsenic and dioxin compounds into the environment during detoxification of residual amounts of lewisite, as well as the derivatives of methylphosphonic acid and fluorides during detoxification of residual amounts of sarin and soman. Burial landfills of concrete-salt and bitumen-salt masses as waste of hazard classes II and III obtained during the liquidation measures implementation can also have a negative impact on the environment. The ways to minimize possible environmental risks associated with the liquidation measures implementation at the chemical weapons destruction facilities have been described. These ways include the prevention of chemicals emissions and the creation of modern chemical-analytical methods and test systems to control environmental pollution with appropriate toxicants.

REFERENCES

[1] V.G. Petrov, A.V. Trubachev and A.M. Lipanov, "Analysis of technologies for lewisite destruction", Ecological Risks Associated with the Destruction of Chemical Weapons, Springer, 289-296 (2006).

[2] V.G. Petrov and A.V. Trubachev, "Some technical questions on destruction of chemical artillery arms for object in Kizner (Udmurtia)", *Proc. 7th Symposium on CBRNE threats*, Jyvaskyla, Finland, 171-179 (2009).

[3] V.G. Petrov, M.A. Shumilova, A.V. Trubachev, et.al., "New approaches to the organization of the control of pollution on objects on destruction of the chemical weapons and other dangerous industrial enterprises", *Abstr. 9th International Chemical and Biological Medical Treatment Symposium*, Spiez, Smitzerland, 242 (2012).

[4] V.P. Kapashin, V.G. Mandych, A.Y. Karmishin, I.N. Isaev, A.S. Lyakin, I.V. Kovalenko and V.D. Nazarov, "Optimization of technology for performing liquidation measures at chemical weapons destruction facilities", Journal of NBC Protection Corps. 4, 404-420 (2020). (In Russian) / [Капашин В.П., Мандыч В.Г., Кармишин А.Ю., Исаев И.Н., Лякин А.С., Коваленко И.В., Назаров В.Д. Оптимизация технологии выполнения ликвидационных мероприятий на объектах по уничтожению химического оружия. *Вестник войск РХЗ защиты,* 2020; 4(4):404-420].

[5] Yu.V. Novoydarsky, T.Ya. Ashikhmina, I.G. Shirokikh, L.N. Domracheva and S.Yu. Ogorodnikova, "Methodological aspects of work on the preparation of chemical weapons storage and destruction facilities for decommissioning activities", Theoretical and Applied Ecology. 4, 100-104 (2014). (In Russian) / [Новойдарский Ю.В., Ашихмина Т.Я., Широких И.Г., Домрачева Л.Н., Огородникова С.Ю. Методические аспекты проведения работ по подготовке объектов хранения и уничтожения химического оружия к мероприятиям по выводу их из эксплуатации. *Теоретическая и прикладная экология*, 2014; 4:100-104].

[6] B.N. Filatov, V.V. Klaucek and N.G. Britanov, "Toxic and hygienic safety during the destruction of chemical weapons, the elimination or conversion of chemically hazardous facilities", Medicine of extreme situations. 4(50), 35-47 (2014). (In Russian) / [Филатов Б.Н., Клаучек В.В., Британов Н.Г. Токсиколого-гигиеническое обеспечение безопасности при уничтожении химического оружия, ликвидации или перепрофилировании химически опасных объектов. *Медицина экстремальных ситуаций,* 2014;4(50):35-47].

[7] A.A. Maslennikova, N.G. Britanov, B.N. Filatov and S.A. Demidova, "Ecological and toxicological assessment of the danger of arsenic contamination of waste from building structures of facilities for the destruction of chemical weapons of skin-abscess action", Theoretical and Applied Ecology. 4, 49-53 (2010). (In Russian) / [Масленникова А.А., Британов Н.Г., Филатов Б.Н., Демидова С.А. Эколого-токсикологическая оценка опасности загрязнения мышьяком отходов строительных конструкций объектов по уничтожению химического оружия кожно-нарывного действия. *Теоретическая и прикладная экология*, 2010;4:49-53].

[8] E.I. Malochkina, Z.I.Gorbunova, O.A. Khodakovskaya, L.D. Glukhova and V.A. Petrunin, "Inhalation toxicity of bitumen-salt masses obtained during the destruction of sarin, soman and russian VX", Toxicological Bulletin. 4, 2-6 (2006). (In Russian) / [Малочкина Е.И., Горбунова З.И., Ходаковская О.А., Глухова Л.Д., Петрунин В.А. Ингаляционная токсичность битумно-солевых масс, полученных при уничтожении зарина, зомана и российского VX. *Токсикологический вестник*, 2006; 4: 2-6].

[9] O.M. Plotnikova, B.I. Kudrin and S.Y. Maksimovskikh, "Assessment of the toxicity of bitumen-salt masses obtained during the destruction of sarin at the "Shchuchye" facility in the Kurgan region", Theoretical and Applied Ecology. 3, 110-112 (2015). (In Russian) / [Плотникова О.М., Кудрин Б.И., Максимовских С.Ю. Оценка токсичности битумно-солевых масс, полученных при уничтожении зарина на объекте «Щучье» Курганской области. *Теоретическая и прикладная экология*, 2015;3: 110-112].

[10] Sanitary rules of SR 2.2.1.2513-09 / SR 2.2.1.2513-09. 2.2.1. Resolution of the Chief state sanitary doctor of the Russian Federation, dated 05.18.2009, № 34. (In Russian) / [Санитарные правила СП 2.2.1.2513-09 / СП 2.2.1.2513-09. 2.2.1. Постановление Главного государственного санитарного врача Российской Федерации от 18.05.2009, № 34].

[11] A.V. Trubachev and L.V. Trubacheva, "Environmental consequences of liquidation events at chemical weapons destruction facilities", *Proc. VIII International Scientific and Practical Conference on Environmental Safety in the Technosphere.* Yekaterinburg, 276-279 (2025) (In

Russian) / [Трубачев А.В., Трубачева Л.В. Экологические последствия ликвидационных мероприятий на объектах по уничтожению химического оружия. Материалы VIII Международной научно-практической конференции «Экологическая безопасность в техносферном пространстве»: Екатеринбург, 2025;276-279].

[12] V.G. Petrov, "Calculation of the amount of formed dioxins in the flue gases of waste incinerators and assessment of the toxicity of the gas mixture", Chemical physics and mesoscopy. 3, 460-467 (2016). (In Russian) / [Петров В.Г. «Расчет количества образовавшихся диоксинов в дымовых газах установок по сжиганию отходов и оценка токсичности газовой смеси». *Химическая физика и мезоскопия*, 2016;18,(3):460-467].

0 Research Index

Author Guidelines

London Journal of Research in Science

Journals Press | Open Access | Peer Reviewed | COPE Compliant

I. OUR EDITORIAL PHILOSOPHY

At Journals Press, we recognize that true scientific advancement relies on rigorous validation and unobstructed distribution. London Journal of Research in Science serves as a premium, open-access platform committed to upholding the highest echelons of academic integrity. Our objective is to streamline the publication journey, empowering researchers to focus resolutely on their discoveries rather than administrative burdens.

II. UNRESTRICTED MANUSCRIPT SUBMISSION

We believe rigid formatting requirements stifle innovation and delay dissemination. Therefore, we invite you to submit your manuscript in its current, natural format.

- **Accepted Formats:** Microsoft Word (.docx), LaTeX (.tex), PDF (.pdf), or standard Rich Text.
- **Requirements:** Only the manuscript file, corresponding author's name, and contact email.
- **Heading Style:** Final typeset articles normally use sentence case for author-created headings, while preserving acronyms, proper nouns, gene/species names, chemical notation, brand names, Roman numerals, and approved manual capitalization.
- **Submission Portal:** https://journalspress.com/submit-manuscript/

Upon submission, our elite pre-production team manages all typesetting and template conversion, establishing a sleek, review-ready manuscript.

III. NEXT-GENERATION PEER REVIEW

Credibility is forged through meticulous evaluation. London Journal of Research in Science deploys an innovative, multi-tiered double-blind peer review framework ensuring objective, uncompromised scrutiny.

1. **Algorithmic & Editorial Triage:** Submissions undergo AI-assisted screening for ethical compliance, originality, and scope alignment before human editorial assessment.
2. **Expert Panel Evaluation:** Manuscripts are routed to domain-specific scholars. Reviewers focus on methodological soundness, data integrity, and analytical rigor.
3. **Collaborative Refinement:** Authors receive comprehensive, line-numbered Review Reports, enabling precise, constructive dialogues. Modifications are requested natively via our intuitive Author Dashboard.

IV. THE PUBLICATION PIPELINE

We emphasize speed without compromising precision. Our publication lifecycle is entirely transparent:

1. **JournalPreview:** Following acceptance, a fully typeset galley proof is released to the authors. This version contains line numbers allowing for targeted, final typographical refinements.
2. **Online First:** Once the JournalPreview is ratified, the corrected article is officially launched online. It receives an active Digital Object Identifier (DOI), rendering it immediately citable while awaiting final issue compilation.
3. **Issue Compilation & Print Archive:** The paper is aggregated into its respective Volume and Issue. Premium, hardbound volumes are cataloged and distributed to premier academic institutions globally.

V. COMMITMENT TO OPEN SCIENCE

London Journal of Research in Science champions the unhindered flow of information.

- **Absolute Open Access:** All publications are universally accessible from the moment of launch under the CC BY-NC-ND 4.0 license, dismantling paywalls and democratizing knowledge.
- **Immutable Archiving:** Research is redundantly decentralized across state-of-the-art global data repositories, safeguarding the scholarly record for posterity.

Connect with Journals Press

Submit Manuscript: https://journalspress.com/submit-manuscript/
Official Gateway: https://journalspress.com
Editorial Assistance: support@journalspress.com

Redefining scholarly excellence. Shaping the narrative of tomorrow.

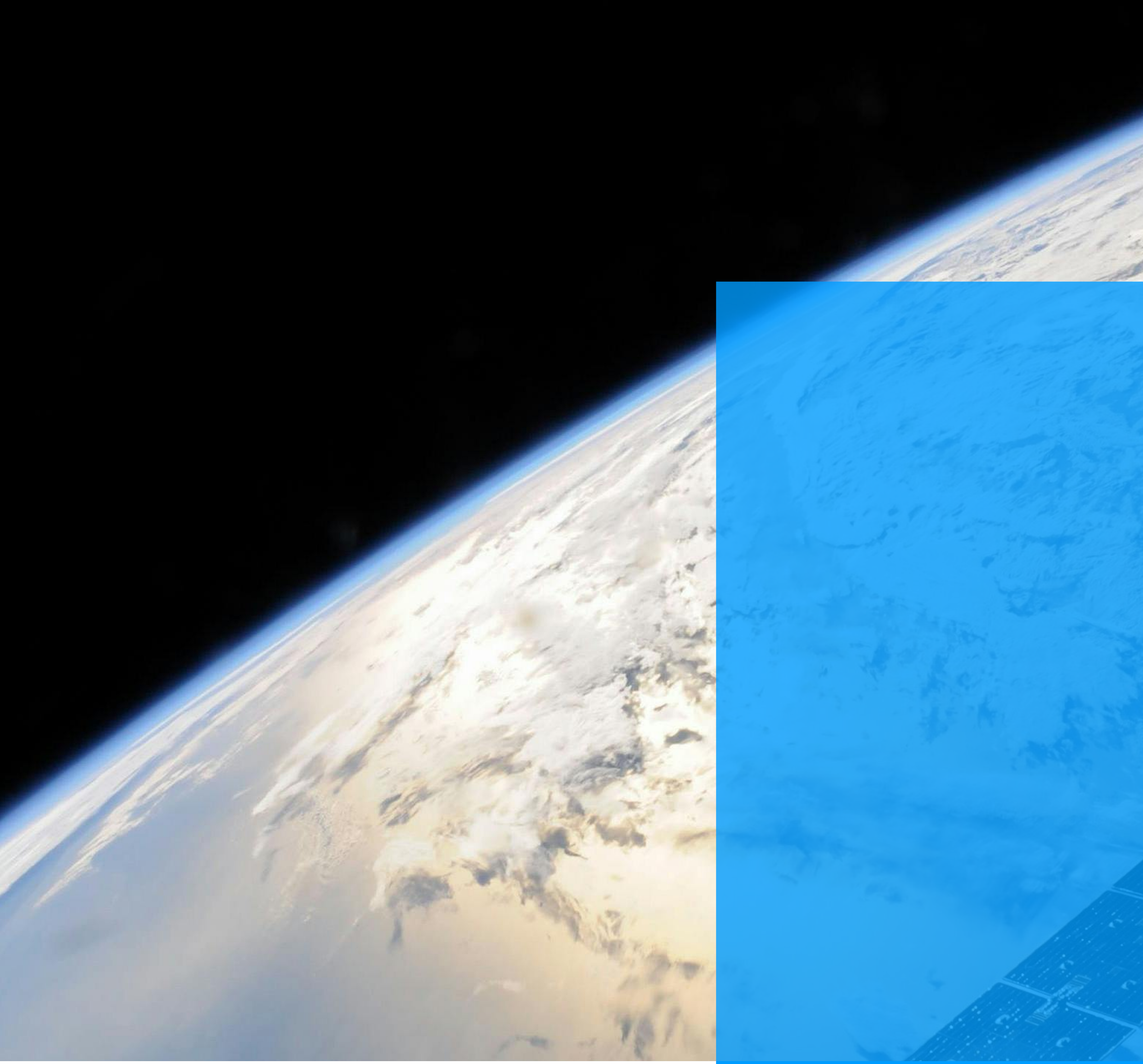

Go green. Help protect the environment.

The journal is available in

Hardbound printed edition, interactive PDF, EPUB, XML, Markdown, JATS and Flipbook.

Online ISSN 2631-8504

journalspress.com

THIS JOURNAL SUPPORT AUGMENTED REALITY APPS AND SOFTWARES